92-01208/

HEAVY OIL RECOVERY ENHANCEMENT BY IMPROVING FOAM PROPAGATION IN RESERVOIR ROCKS

Part of Energy, Mines and Resources Cost Shared Energy Conversion Program, and Part of the Program of the Federal Panel on Energy R&D (PERD)

Final Report
by

Karin Mannhardt, Monty J. Hans, Laurie A. Hodgins, and Jerry J. Novosad

Petroleum Recovery Institute
3512-33rd Street N.W.
Calgary, Alberta T2L 2A6

Work on the project was conducted under the auspices of the Canada Centre for Mineral and Energy Technology, Energy, Mines and Resources Canada

DSS File Number 006SQ.23440-8-9223
DSS Contract Serial Number 23440-8-9223/01-SQ
CANMET Scientific Authority: Dr. Kamal Jha

MICROMEDIA
112 pp

December 1990

EXECUTIVE SUMMARY

OBJECTIVE

Enhanced oil recovery processes that employ steam or gas injection tend to suffer from poor sweep efficiency caused by gravity override or the formation of preferential flow paths through high permeability or previously swept zones. These problems may be alleviated through the use of mobility control foams.

One of the more important factors that affect foam propagation is adsorption of surfactant at the solid/liquid interface. This work deals with adsorption of surfactants used for mobility control foams in steam flooding. The aim was to develop a better understanding of the adsorption behavior and/or adsorption mechanisms of surfactants of different chemical structures, with the ultimate goal of minimizing surfactant loss by adsorption. Injected fluids in steam-foam applications encounter salinity and temperature gradients, and knowledge of the dependence of adsorption on both parameters is thus crucial to successful foam applications.

HIGHLIGHTS

The results of this study contribute to our understanding of the adsorption behavior of different surfactant types and its dependence on salinity and temperature, and thus facilitate optimal surfactant selection. The possibility of reducing surfactant adsorption by mixing surfactants is demonstrated. Microcalorimetry appears to be a promising tool for screening of surfactants in terms of their interaction with solid surfaces.

SUMMARY

A solubility study was performed in order to select low molecular weight representatives of steam-foamers such that complete solubility at ambient to moderate temperatures was ensured. Four surfactants were chosen: an alpha olefin sulfonate (AOS), an internal olefin sulfonate (IOS), a linear xylene sulfonate (LXS), and a betaine. Adsorption of these surfactants on Berea sandstone was measured as a function of temperature or salinity through core flood experiments. Microcalorimetry was used to measure enthalpies of

adsorption and the intensity of surfactant/solid interactions. Surface tensions were measured as a function of surfactant concentration for all systems. This allowed determination of the critical micelle concentration and other parameters required as input to the surface excess model for flow through porous media. The core floods were simulated with this model, and the parameters of the model allowed calculation of adsorption isotherms for the various surfactant/brine systems.

CONCLUSIONS

Both the AOS and IOS did not adsorb at 23°C from 0.5% NaCl, but adsorption of these surfactants increased with increasing salinity and divalent ion concentration of the brine. Adsorption of the LXS from 0.5% NaCl decreased with increasing temperature. This surfactant was the least soluble of the four surfactants, and at 23°C precipitation of the surfactant in the core was caused by ion-exchanged calcium from the rock even when the rock had been pre-equilibrated with the brine. This leads to higher surfactant loss and alteration of the flow paths of surfactant and tracer in the core. No precipitation was observed at 75°C, and surfactant loss was substantially lower. The betaine is more tolerant to high salinity brines than any of the anionics, but adsorbed at substantially higher levels. Its adsorption was not strongly dependent on temperature. Adsorption of this surfactant could be reduced significantly by mixing it with one of the anionics (IOS). Results of the microcalorimetric measurements were found to correlate with the adsorption measurements.

RECOMMENDATIONS

The adsorption study of this work should be extended to higher molecular weight surfactants used in steam flooding. Further development of correlations between microcalorimetric measurements of surfactant-solid interactions and adsorption should be pursued. Minimizing adsorption by using surfactant mixtures is a promising approach to improving the economics of foam flooding and should be extended to a larger variety of surfactants to determine optimal mixtures.

SOMMAIRE EXÉCUTIF

BUT

Les procédés de récupération assistée du pétrole par injection de vapeur ou de gaz ont tendance à souffrir d'une mauvaise efficacité de balayage causée par une dominance de la gravité ou par la formation de chemins d'écoulement préférentiels dans les zones de haute perméabilité ou préalablement balayées. Ces problèmes peuvent être allégés par l'utilisation de mousses contrôlant la mobilité.

Un des facteurs très importants affectant la propagation de la mousse est l'adsorption du surfactant à l'interface solide/liquide. Ce travail traite de l'adsorption de surfactants utilisés pour les mousses contrôlant la mobilité lors des déplacements à la vapeur. Le but était de développer une meilleure compréhension du comportement de l'adsorption et/ou des mécanismes d'adsorption des surfactants à structures chimiques différentes, le but principal étant de minimiser la perte de surfactant par adsorption. Les fluides injectés dans les applications vapeur-mousse rencontrent des gradients de salinité et de température et il est donc important de connaître la dépendance de l'adsorption au niveau des deux paramètres afin de réussir les applications de mousses.

POINTS MARQUANTS

Les résultats de cette étude contribuent à notre connaissance du comportement de l'adsorption de types différents de surfactants et de sa dépendance de la salinité et de la température, et de ce fait, facilitent la sélection optimale des surfactants. Cette étude démontre également la possibilité de réduire l'adsorption du surfactant en mélangeant des surfactants. La microcalorimétrie semble être un outil prometteur pour la

sélection de surfactants vis-à-vis leur interaction avec les surfaces solides.

SOMMAIRE

Une étude de solubilité fut conduite afin de sélectionner des échantillons représentatifs de moussants à la vapeur de poids moléculaire bas afin d'assurer une solubilité complète à des températures ambiantes ou modérées. Nous avons choisi quatre surfactants: un sulfonate d'oléfine alpha (SOA), un sulfonate d'oléfine interne (SOI), un sulfonate de xylène linéaire (SXL), et un bêtaine. L'adsorption de ces surfactants sur du grès de Berea a été mesurée comme une fonction de la température ou de la salinité par des essais d'injection en carottage. Les enthalpies de l'adsorption et l'intensité des interactions entre les surfactants et les solides ont été mesurées par microcalorimétrie. Les tensions superficielles ont été mesurées comme une fonction de concentration de surfactant pour tous les systèmes. Ceci a permis la détermination de la concentration critique de micelles et d'autre paramètres requis comme données au modèle de l'excès de surface pour l'écoulement à travers des média poreux. Les injections en carottage ont été simulées avec ce modèle et les paramètres du modèle ont permis le calcul des isothermes d'adsorption pour les divers systèmes de surfactant/saumure.

CONCLUSIONS

À 23°C, il n'y eu pas d'adsorption du SOA ni du SOI d'une solution de 0.5% de NaCl, cependant, l'adsorption de ces surfactants augmenta avec une hausse de salinité et une concentration d'ions divalente de la saumure. L'adsorption du SXL d'une solution de 0.5% de NaCl diminua avec une hausse de température. Ce surfactant s'est avéré le moins soluble des quatre surfactants et à 23°C, la précipitation du surfactant dans la carotte a été causée par le calcium échangeur d'ions de la roche bien que la roche fut préalablement équilibrée avec la saumure. Ceci mène à une perte de surfactant plus élevée et à un changement des chemins d'écoulement du surfactant et du traceur

dans la carotte. Aucune précipitation ne s'est produite à 75°C, et la perte de surfactant fut substantiellement plus basse. Le bêtaine tolère les saumures très salées mieux que n'importe quel autre des anioniques, mais est adsorbé à des niveaux substantiellement plus élevés. Son adsorption n'a pas été fortement influencée par la température. L'adsorption de ce surfactant pourrait être réduite de façon significative en le mélangeant avec un des anioniques (SOI). Les résultats des mesures microcalorimétriques ont correspondu au mesures de l'adsorption.

RECOMMANDATIONS

L'étude d'adsorption de ce travail devrait s'étendre vers des surfactants à poids moléculaire plus élevé employés dans les injections de vapeur. Des développements plus approfondis de la corrélation entre les mesures calorimétriques des interactions surfactant/solides et de l'adsorption devraient être poursuivis. La minimalisation de l'adsorption par l'usage de mélanges de surfactants est une approche prometteuse en ce qui concerne la réduction des coûts d'injection de mousse et devrait s'étendre vers une plus grande variété de surfactants afin de déterminer les mélanges optimaux.

TABLE OF CONTENTS

Executive Summary	ii
Sommaire Exécutif	iv
Table of Contents	vii
List of Tables	viii
List of Figures	ix
Introduction	1
Literature Review: Steam-Foams	3
1. Thermal Stability	3
2. Laboratory Testing of Steam-Foams	4
3. Steam-Foam Field Application	6
4. Solubility and Phase Behavior	7
5. Adsorption Studies	8
Outline and Objectives	12
Experimental Methods	14
1. Materials	14
2. Surfactant Solubility Measurements	14
3. Core Floods	15
4. Surface Tension Measurement	17
5. Microcalorimetry	17
Adsorption Model and History Matching	19
Results and Discussion	23
1. Surfactant Solubilities	23
2. Critical Micelle Concentrations	25
3. Adsorption of Single Surfactants	28
4. Adsorption of a Surfactant Mixture	35
5. Microcalorimetry	38
Summary and Conclusions	39
Acknowledgements	41
References	42
Tables	
Figures	
Appendix A: Two-Phase Titration of an Anionic/Amphoteric Surfactant Mixture	
Appendix B: Surface Tension Data	

LIST OF TABLES

Table 1. Core and displacement data.

Table 2(a). Properties of brines used in core floods.

Table 2(b). Composition of mixed brines used in surfactant solubility tests.

Table 3. Surfactants.

Table 4. Surfactant solubility as a function of NaCl concentration.

Table 5. Surfactant solubility as a function of surfactant concentration.

Table 6. Effect of calcium ion on solubility of IOS 1518 and AOS 1416.

Table 7. Data from surface tension measurements, 23°C.

Table 8. Adsorption data from material balance calculations and flow model parameters.

Table 9. Enthalpy of surfactant adsorption on Berea sandstone. Surfactant concentration 0.5%, 0.5% NaCl, 25°C.

LIST OF FIGURES

Figure 1. Thermal activity monitor.

Figure 2. The heat flow principle.

Figure 3. Schematic of experimental setup for microcalorimetry.

Figure 4. Power output from microcalorimeter during adsorption of 0.5% AOS 1416 on Berea sandstone. 0.5% NaCl, 25°C.

Figure 5. Power output from microcalorimeter during adsorption of 0.5% LXS 810 on Berea sandstone. 0.5% NaCl, 25°C.

Figure 6. Power output from microcalorimeter during adsorption of 0.5% Stepanflo 60 on Berea sandstone. 0.5% NaCl, 25°C.

Figure 7. Enthalpy of adsorption of 0.5% AOS 1416 on Berea sandstone, 0.5% NaCl, 25°C.

Figure 8. Enthalpy of adsorption of 0.5% LXS 810 on Berea sandstone, 0.5% NaCl, 25°C.

Figure 9. Enthalpy of adsorption of 0.5% Stepanflo 60 on Berea sandstone, 0.5% NaCl, 25°C.

Figure 10. Surfactant solubility as a function of salinity, surfactant concentration: 1%.

Figure 11. Surfactant solubility as a function of surfactant concentration, brine: 0.5% NaCl.

Figure 12. Surface tension, Enordet AOS 1416 in 0.5% NaCl, 23°C.

Figure 13. Surface tension, Enordet AOS 1416 in 2.32% NaCl, 23°C.

Figure 14. Surface tension, Enordet AOS 1416 in 2.27% TDS brine, 23°C.

Figure 15. Surface tension, Enordet IOS 1518 in 0.5% NaCl, 23°C.

Figure 16. Surface tension, Enordet IOS 1518 in 2.32% NaCl, 23°C.

Figure 17. Surface tension, Enordet IOS 1518 in 2.27% TDS brine, 23°C.

Figure 18. Surface tension, Enordet LXS 810 in 0.5% NaCl, 23°C.

Figure 19. Surface tension, Stepanflo 60 in 0.5% NaCl, 23°C.

Figure 20. Surface tension, Stepanflo 60 in 0.5% NaCl at 23°C by Du Nouy ring and spinning bubble methods.

Figure 21. Surface tension, 0.72:0.30 (w:w) Enordet IOS 1518 : Stepanflo 60 in 0.5% NaCl, 23°C.

Figure 22. Core CM-2 effluent profiles. 10 g/l Enordet AOS 1416 in 0.5% NaCl, 23°C.

Figure 23. Core CM-9 effluent profiles. 10 g/l Enordet AOS 1416 in 2.32% NaCl, 23°C.

Figure 24. Core CM-12 effluent profiles. 10 g/l Enordet AOS 1416 in 2.27% TDS brine, 23°C.

Figure 25. Core CM-3 effluent profiles. 10 g/l Enordet IOS 1518 in 0.5% NaCl, 23°C.

Figure 26. Core CM-10 effluent profiles. 10 g/l Enordet IOS 1518 in 2.32% NaCl, 23°C.

Figure 27. Core CM-11 effluent profiles. 10 g/l Enordet IOS 1518 in 2.27% TDS brine, 23°C.

Figure 28. Adsorption isotherms from flow model parameters, Enordet AOS 1416 and Enordet IOS 1518 at 23°C in different brines.

Figure 29. Core CM-4 effluent profiles. 10 g/l Enordet LXS 810 in 0.5% NaCl, 23°C.

Figure 30. Core CM-13 effluent profiles. 10 g/l Enordet LXS 810 in 0.5% NaCl, 23°C (repeat).

Figure 31. Core CM-8 effluent profiles. 10 g/l Enordet LXS 810 in 0.5% NaCl, 75°C.

Figure 32. Core CM-6 effluent profiles. 10 g/l Stepanflo 60 in 0.5% NaCl, 23°C.

Figure 33. Core CM-7 effluent profiles. 10 g/l Stepanflo 60 in 0.5% NaCl, 75°C.

Figure 34. Adsorption isotherms from flow model parameters, Enordet LXS 810 and Stepanflo 60 in 0.5% NaCl at different temperatures.

Figure 35. Core CM-14 effluent profiles. Surfactant mixture in 0.5% NaCl, 23°C (3 g/l Stepanflo 60 and 7 g/l Enordet IOS 1518).

Figure 36. Core CM-14 effluent profiles. Surfactant mixture in 0.5% NaCl, 23°C (3 g/l Stepanflo 60 and 7 g/l Enordet IOS 1518).

Figure 37. Enthalpy of adsorption. 0.5% surfactant in 0.5% NaCl, Berea sandstone, 25°C.

Figure 38. Summary of adsorption data: Plotted are the maximum adsorption levels from the adsorption isotherms, except in the case of the mixture. Values for the mixture were obtained from material balance calculations.

INTRODUCTION

Steam injection has been the most successful enhanced oil recovery (EOR) technique in heavy oil reservoirs. More than 70% of the tertiary oil produced in the United States has been recovered through steam flooding. While Canada's EOR projects for conventional oil have been dominated by hydrocarbon miscible flooding, there is also much interest in the application of steam to heavy oil reservoirs.

The adverse mobility ratio caused by the low density and viscosity of the injected steam may lead to gravity override or to the formation of preferential flow paths of the steam through high permeability or swept zones, hence to poor sweep efficiency. These problems may be alleviated by adding a small amount of surfactant solution to the steam to form a mobility control foam. Interest in this technology has surged over the past decade, and a large amount of literature on the laboratory and field testing of foams for mobility control in gas flooding operations is available. Marsden (1986) has reviewed the development of EOR foam technology from 1956 to 1985.

The injection of a chemical into a reservoir is always associated with additional costs, and it is therefore essential to optimize a foam process before applying it in the field. For a foam to be effective as a mobility control or blocking agent, it has to propagate into the reservoir from the injection well. The assessment of foam propagation in porous media, particularly on the reservoir scale, is of major concern in the design of a foam project, but is poorly understood at present. Foam propagation depends on factors such as pore structure, fluid velocity, surfactant solution properties, reservoir fluids and surfactant adsorption, precipitation, partitioning, or chemical degradation. While the mechanisms of lamella generation and collapse are crucial to foam performance and propagation, the maximum distance a foam will travel is dictated by surfactant losses in the reservoir. While surfactants that are chemically stable at steam flood conditions have been identified, and the relative solubility of these surfactants at different salinities has been investigated, their adsorption behavior has not been studied extensively or systematically. The objective

of this study was to determine the adsorption of representatives of different classes of steam flood surfactants. The ultimate goal of gaining a better understanding of the adsorption of these surfactants is to minimize surfactant loss through adsorption.

LITERATURE REVIEW: STEAM-FOAMS

In this section, different aspects relevant to the application of steam-foams that have been addressed in the literature will be briefly reviewed.

1. THERMAL STABILITY

A prime requirement for the applicability of a surfactant to steam flooding is its chemical stability at steam flood temperatures. The lowest temperature at which a steam flood might be expected to operate is approximately 180°C (Handy et al., 1982a). This limits the surfactants that can be used for steam-foam applications to only a few chemical classes. Alkyl aromatic sulfonates have been found to be the most thermally stable foamers (Owete et al., 1980; Al-Khafaji et al., 1982; Angstad and Tsao, 1987; Muijs et al., 1988). The stability of a number of surfactants in this chemical class has been compared by Muijs et al. (1988). One member of this class, Suntech IV, has been studied quite extensively, and has been found to be very stable up to 300°C at a pH of 5 or higher (Owete et al., 1980; Al-Khafaji et al., 1982; Angstad and Tsao, 1987). By comparison, alpha olefin sulfonates (AOS's) are more tolerant to moderate salt concentrations than alkyl aryl sulfonates, but their thermal stability is lower (Scharer et al., 1985; Angstad and Tsao, 1987; Muijs et al., 1988). Ethoxylated alcohols are more salt-tolerant still, but are not stable enough to be used as steam flood additives (Handy et al., 1982a; Scharer et al., 1985). Handy et al. (1982a) have compared the thermal stability of sodium dodecyl benzene sulfonate, a diphenyletherdisulfonate, a nonionic nonyl phenoxy polyethanol, and several petroleum sulfonates. While none of these surfactants was found to be stable enough for steam flooding, the authors suggest that they might be applied to micellar flooding at temperatures higher than those usually encountered in micellar flooding. Marriott et al. (1982) have tested the thermal stability of diphenyletherdisulfonates, manufactured by Dow Chemical under the trade name Dowfax, and found them stable to 270°C when the pH was buffered to near neutral.

A comparative study by Scharer et al. (1985) indicates the following trend in surfactant thermal stability: alkyl aryl sulfonates > olefin sulfonates > petroleum sulfonates > ethoxylated alcohols and ethoxylated sulfates.

Thermal degradation of aromatic sulfonates is believed to take place by desulfonation of the benzene ring, which is accompanied by the formation of sulfuric acid:

$$ArSO_3^- + 2\ H_2O \longrightarrow ArH + SO_4^{2-} + H_3O^+$$
$$ArSO_3^- + H_3O^+ \longrightarrow ArH + SO_4^{2-} + 2\ H^+$$

There has been some discussion regarding the order of this reaction and the mechanism by which it proceeds (Handy et al., 1982a,b; Clark, 1982; Marriott et al., 1982; Isaacs et al., 1982; Angstad and Tsao, 1987), but there is general agreement that it is catalyzed by acid. High initial pH, the presence of sodium chloride, and a high surfactant concentration (> cmc) can have a stabilizing effect on the surfactant (Handy et al., 1982a; Marriott et al., 1982; Isaacs et al., 1982; Angstad and Tsao, 1987; Muijs et al., 1988). The presence of sand provides some pH buffering capacity and has been found to retard surfactant degradation, while the presence of calcium chloride may promote degradation in addition to causing precipitation of the surfactant (Al-Khafaji et al., 1982). Bavière et al. (1988) suggest that degradation of alpha olefin sulfonates may also proceed by oxidation in the presence of air at temperatures as low as 77°C, and that this degradation may be inhibited by high pH and the presence of an alcohol.

2. LABORATORY TESTING OF STEAM FOAMS

Extensive laboratory testing has been performed with foam-forming surfactants for steam flood applications. This work has included papers by Dilgren et al. (1982), Duerksen (1984), Maini and Ma (1984, 1986), Strycker et al. (1987), Muijs et al. (1988), Green and Isaacs (1988), Isaacs et al. (1988), Lau and Borchardt (1989), Hamida et al. (1990), and Djabbarah et al. (1990), as well as a large number of papers on foams for other gas flood processes and on fundamental aspects of foam behavior. The stability of a

foam and its effectiveness in reducing gas mobility are usually measured either in bulk foam tests or in porous media through core floods, both in the absence and in the presence of oil. In bulk foam experiments, foaming capability or foam stability are determined by measurements of maximum foam volume, or the half life of foam volume or liquid drainage. In a core flood, the effectiveness of a foam is assessed by comparing the pressure drop generated across a core during foam flow to the pressure drop when gas (steam) and brine are flowing in the absence of any surfactant. Although some investigators have been able to correlate bulk foam behavior with performance in porous media (Maini and Ma, 1984; Strycker et al., 1987), no general correlation between the two types of test has been found.

Surfactant classes most frequently tested for mobility control in steam flooding are those believed to be chemically stable at steam flood conditions and have included alpha olefin sulfonates, internal olefin sulfonates, alkyl aromatic sulfonates, Chevron proprietary sulfonates, and petroleum sulfonates. The laboratory testing of foams discussed in above-mentioned papers has included measurement of the effects on foam performance of surfactant type and concentration, salt, steam quality, foam liquid volume fraction, temperature, flow rate, and the presence of a noncondensible gas.

In general, foam performance has been found to deteriorate with increasing temperature. Foam strength increases with increasing length of the surfactant's hydrocarbon chain, particularly at high temperatures. Muijs et al. (1988) have found that the maximum pressure drop generated in core floods shifts to higher temperatures with increasing alkyl chain length of the surfactant. A surfactant that performs well at moderate temperatures may thus not be suitable at high temperatures and vice versa. The presence of salt can be both beneficial and detrimental to foam, while the presence of small amounts of a noncondensible gas improves foam performance.

The effect of oil on foam performance has been studied by several investigators (Maini, 1986; Nikolov et al., 1986; Lau and O'Brien, 1988a; Manlowe and Radke, 1988; Raterman, 1989; Novosad et al., 1989; Schramm and Novosad, 1990; Schramm et al., 1990). Most foams are destabilized by crude

oil. However, in some cases foam performance has been found to improve in the presence of oil (Maini, 1986), and some surfactants generate foams that are completely unaffected by oil (Novosad et al., 1989; Robin and Demay, 1989). Criteria for determining the degree of oil sensitivity of foams formed with different surfactants have been developed by Schramm and Novosad (1990) and Schramm et al. (1990).

3. STEAM-FOAM FIELD APPLICATIONS

Several field pilots have shown that the application of foams in steam flooding can provide substantial benefits over injection of steam alone. Reviews by Castanier and Brigham (1988) and Hirasaki (1989) indicate that many of the field pilots reported in the literature have been promising both technically and economically. In the field, the performance of a steam-foam process can be assessed from increases in injection pressure, changes in injection profile, reduced steam production, improved vertical sweep, improved temperature profile, and increased oil production and oil/steam ratio (Hirasaki, 1989). The development of field application technology of steam-foams over the past two decades has been reviewed by Eson and Cooke (1989).

The selection of surfactants for field application is usually based on extensive laboratory testing, and surfactant behavior in the field is often consistent with results obtained in the laboratory (Dilgren et el., 1982; Castanier and Brigham, 1988; Djabbarah et al., 1990). Surfactants that have been used for steam-foam applications in the field are alpha olefin sulfonates, alkyl benzene sulfonates, alkyl toluene sulfonates, and Chevron proprietary sulfonates. Examples of positive response to foam injection have been obtained with all these surfactant types (Castanier and Brigham, 1988; Eson and Cooke, 1989; Hirasaki, 1989; Djabbarah et al., 1990).

4. SOLUBILITY AND PHASE BEHAVIOR

Most surfactants considered for steam flood applications have limited solubility in water and a relatively low tolerance to salt solutions (Al-Khafaji et al., 1982; Scharer et al., 1985; Bavière et al., 1988). Incomplete dissolution can lead to complex phase behavior in aqueous surfactant systems (Miller and Neogi, 1985). Changing solution conditions, such as surfactant and salt concentrations or temperature, may lead to precipitation of a solid phase or to the formation of liquid crystalline phases of different morphologies. For example, the formation of two distinct liquid phases was observed with one of the surfactants investigated in this study when the salinity was increased. Franses et al. (1979) have investigated the solubility of a pure alkyl benzene sulfonate in detail by spectroturbidimetry, conductimetry, ultrafiltration, ultracentrifugation, vapor sorption, polarizing microscopy, and nuclear magnetic resonance (nmr) spectroscopy, and found that this surfactant can exhibit complex phase behavior even in very dilute solution. These authors pointed out the difficulties in measuring the solubility of a surfactant, and found that more than one method was required to completely determine solubility. ^{13}C nmr spectroscopy was used to detect a finely dispersed liquid crystalline phase in visually clear solutions.

Scharer et al. (1985) have compared the salinity tolerance of several surfactant classes and have found the following general trend: ethoxylated alcohols or sulfates > olefin sulfonates > petroleum sulfonates ≅ alkyl aryl sulfonates. Within each class of surfactant, solubility decreases with increasing molecular weight of the hydrophobe. Surfactants that form effective foams at steam flood temperatures are usually of relatively high molecular weight (C_{14} to C_{24} hydrocarbon chain) and are not soluble at ambient conditions, which makes laboratory studies with these surfactants and handling in the field more difficult than with lower molecular weight homologues. Foam performance depends both on the surfactant's molecular weight and on temperature, higher molecular weights being required at higher temperatures (Muijs et al., 1988; Hamida et al., 1990).

A surfactant system that does not suffer from low tolerance to salt

solutions and has been suggested for mobility control at steam flood conditions has been described by Lim (1985). This formulation is a blend of a diphenyletherdisulfonate (Dowfax) and an alpha olefin sulfonate, and is soluble in near-saturated brines. Diaryl sulfonated surfactants, by themselves or in mixtures, have been suggested by Angstadt (1987) for improved salt tolerance of steam-foam formulations.

Somasundaran et al. (1984a) have studied the precipitation/redissolution and adsorption behavior of alkyl aryl sulfonates in the presence of mono- and multivalent ions. The surfactant was found to precipitate when the surfactant and/or salt concentrations were increased, but redissolved upon further increasing the surfactant concentration, possibly because of micelle formation. The work of Somasundaran and Hanna (1985) points out some of the difficulties involved in measuring adsorption in systems of limited solubility. The surfactant losses measured by these authors are a combination of adsorption and precipitation, termed "abstraction," and do not constitute a true measure of adsorption. The purpose of this work was to measure surfactant loss by adsorption alone, and systems were chosen such that complete solubility was ensured.

5. ADSORPTION STUDIES

Loss of surfactant by adsorption affects both the economics and the effectiveness of a foam process. The measurement of adsorption is therefore an important part of evaluating surfactants for foam applications. While surfactant adsorption has been studied quite extensively at sub-steam temperatures, only limited data on adsorption at steam flood conditions are available. The injection of steam into a reservoir may result in large temperature and salinity gradients, and complete evaluation of a foaming surfactant should thus include the effects of temperature and salinity on adsorption.

Physical adsorption is an exothermic process and should therefore decrease with increasing temperature. Several authors have verified that some anionic steam flood surfactants follow this trend: alkylbenzene sulfonate on Berea

sandstone (Ziegler and Handy, 1981) and Kern River reservoir rock (Dilgren and Owens, 1982), alkyl toluene sulfonate and alpha olefin sulfonate on silica sand (Novosad et al., 1986), and alpha olefin sulfonate dimer (Chevron Chaser SD 1000) on Berea sandstone (Friedmann et al., 1988). Of these studies, only those by Novosad et al. (1986) and Friedmann et al. (1988) have included measurements at temperatures exceeding 100°C. Novosad et al. (1986), Bavière et al. (1988) and Lau and O'Brien (1988b) have investigated the effect of salinity on alpha olefin sulfonate or alkyl toluene sulfonate adsorption on silica sand, kaolinite, and reservoir sands. Methods of improving surfactant propagation in steam-foam formulations have been studied by Lau and Borchardt (1989). These authors found that addition of alkali to a C_{16-18} alpha olefin sulfonate, use of a high molecular weight disulfonated AOS, or use of a high molecular weight monosulfonated AOS in combination with sodium sulfate reduce surfactant loss below that observed with the C_{16-18} AOS alone.

One purpose of this work was to determine and compare adsorption levels of different classes of commercial surfactants used in steam flooding. A systematic study of the effect of surfactant structure on adsorption has been conducted by Somasundaran et al. (1984b) and Somasundaran (1988, 1989) with pure, well-defined surfactants and solids. Using sulfonate surfactants and alumina, the effects of the following structural features of the surfactant molecule on adsorption were investigated: alkyl chain length, addition of an aryl group, branching of the alkyl group, addition of a second alkyl group to the aromatic ring of alkyl aryl sulfonates, ethylene oxide addition, addition of an ether linkage to form a diphenyletherdisulfonate, and the position of the alkyl groups in a dialkyl benzene sulfonate. Adsorption was found to be related to the relative hydrophobicity or "effective chain length" of the surfactants, as determined from HPLC retention times, the hydrophobicity, in turn, depending on surfactant structure. Different structural features in the surfactant molecule were found to affect adsorption in different regions of the isotherm, since adsorption in different regions of the isotherm can be determined by different factors such as electrostatic attraction or repulsion, solvent power of the aqueous medium for the surfactant, Van der Waals interaction between surfactant hydrophobes, electrostatic repulsion

between surfactant polar groups in the adsorbed phase, and packing density or steric hindrance in the adsorbed layer.

A goal of measuring the adsorption of different types of steam flood surfactants in this study was to investigate the possibility of formulating surfactant mixtures so as to reduce adsorption. Several papers and numerous patents discuss surfactant blends that display properties desirable in EOR, such as improved salinity tolerance, foaming capacity, or interfacial tension lowering. The possibility of lowering adsorption by blending surfactants has also been noted in the literature (Trogus et al., 1979; Scamehorn et al., 1982a,b; Byth and Thompson, 1983; Balzer, 1987; Mannhardt and Novosad, 1991a), but only limited experimental data on the behavior of surfactant mixtures in porous media are available (Scamehorn et al., 1982a,b; Harwell et al., 1985; Somasundaran, 1989; Mannhardt and Novosad, 1991b). Surfactant blends designed specifically for steam flood applications have been described in the patent literature: a diphenyletherdisulfonate/alpha olefin sulfonate blend (Lim, 1985), a mixture of alkyl aryl sulfonate or olefin sulfonate with polyalkoxylated sulfonate (Dilgren and Owens, 1989), and mixtures of diarylsulfonated surfactants and co-surfactants (Angstadt, 1987). All these mixtures were designed to improve the salinity tolerance of the formulation. In the first two, a surfactant that is itself not a good foamer but is soluble at high salinities, is added to the foaming surfactant. Problems that might arise from thermal degradation of polyalkoxylated surfactants at steam flood temperatures are not addressed by Dilgren and Owens. Dawe and Oswald (1989) have measured adsorption of the diphenyletherdisulfonate/alpha olefin sulfonate blend on sand and found that adsorption of the foaming component (AOS) is significantly reduced in the mixture. Adsorption of this surfactant mixture has also been measured quite extensively by Mannhardt and Novosad (1988) and Mannhardt et al. (1990). None of the measurements were carried out at steam flood temperatures, however. Djabbarah (1987) has suggested the use of surfactant/lignosulfonate mixtures in foams to reduce surfactant adsorption.

From the available literature it is evident that no systematic study on adsorption of steam-foamers as a function of surfactant type, salinity, and temperature is available. Because of the difficulties involved in performing

experiments at steam flood temperatures, most studies have been restricted to sub-steam temperatures and have involved measurements at a single temperature only. Adsorption of the high molecular weight surfactants that may be required to form effective mobility control foams at high temperatures has not been measured, a possible reason being experimental problems arising from their low solubility at sub-steam temperatures and the more difficult nature of experiments at high temperatures.

OUTLINE AND OBJECTIVES

In this work, we have attempted to gain some insight into the effects of surfactant type, salinity, and temperature on adsorption of steam-foamers. As a starting point in developing an understanding of the temperature dependence of adsorption, the measurements were limited to sub-steam temperatures. It was hoped that the functional dependence of adsorption on temperature would lead to a better understanding of the mechanisms involved and allow extrapolation to higher temperatures. In order to ensure complete solubility of the surfactants, low molecular weight representatives of different classes of steam-foamers were used. The adsorption measurements were complemented with measurements of the heats of adsorption in order to determine whether a correlation exists between surface excess and enthalpy of adsorption.

Enthalpy changes accompanying an adsorption process are possible measures of the intensity of solid-surfactant interactions. Firstly, experimentally determined enthalpies of adsorption could be used to assess the temperature dependence of adsorption. Secondly, the plateau of the adsorption isotherm could be estimated directly from the enthalpy changes during the adsorption process (Sircar et al., 1972). Since it should be faster to measure the enthalpy of adsorption microcalorimetrically than to determine the complete adsorption isotherm, such a relationship could be useful in screening large numbers of surfactants.

Our original purpose was to test both of these ideas. However, difficulties with the initial experiments and a breakdown of the instrument that occurred on October 8, 1990 (manufacturer was not able to resolve the problem as of this writing) have given us a chance to evaluate only the second idea.

The following experiments were performed toward the objectives of this project:

1. The solubilities of surfactants in different chemical classes were determined. Based on these measurements, surfactants that were completely soluble at the lowest temperature used in the adsorption experiments and

that are representative of surfactant types described in the literature for steam flood applications were selected for further study.

2. Core floods were run in order to measure adsorption of four surfactants (three anionics and one amphoteric) on Berea sandstone from a low salinity sodium chloride brine at 23°C.

3. Two of these surfactants adsorbed on the sandstone at these conditions. Adsorption of these surfactants was then measured at 75°C.

4. The other two surfactants did not adsorb measurably. Since adsorption was expected to be even lower at higher temperature, adsorption of these two surfactants was not measured at elevated temperature. The brine salinity and hardness were increased in order to determine the dependence of adsorption of the two surfactants at 23°C on these factors.

5. One of the surfactants (the amphoteric) adsorbed very strongly. This surfactant was mixed with one of the anionics to determine if its adsorption could be lowered in this way.

6. The critical micelle concentration (cmc) of all systems was determined through surface tension measurements. The cmc of a surfactant critically affects adsorption and is required as input into the adsorption model.

7. The coreflood data were simulated using the surface excess model of adsorption in flow through porous media. The model parameters allowed calculation of the equilibrium adsorption isotherm for each system, and also yielded information on the kinetics of adsorption and desorption.

8. Enthalpies of adsorption were measured by microcalorimetry for three surfactants in 0.5% NaCl brine.

EXPERIMENTAL METHODS

1. MATERIALS

Cores: Berea sandstone cores were supplied by Cleveland Quarries (Amherst, Ohio). Properties of the cores used in the adsorption floods are listed in Table 1.

Brines: Three different brines were used in core floods: 0.5% w/w NaCl, 2.32% w/w NaCl, and 2.274% w/w TDS brine containing 2.192 % w/w NaCl and 0.082 % w/w $CaCl_2$. The 2.32% NaCl and the 2.274% TDS brines have the same ionic strength. Properties of the brines are listed in Table 2(a). For the surfactant solubility measurements, brines containing 0.2 to 5% w/w NaCl and brines containing NaCl and $CaCl_2$ at different ratios and constant total ionic strength were used (Table 2(b)).

Surfactants: Six anionic surfactants and one amphoteric were used (Table 3). The anionics (Enordets) were supplied by the Shell Chemical Company, and the amphoteric (Stepanflo 60) by Stepan Company. Some properties of the surfactants are listed in Table 3.

2. SURFACTANT SOLUBILITY MEASUREMENTS

In order to ensure complete solubility of the surfactants that were to be used in core floods, the solubility of the surfactants listed in Table 3 was measured as a function of salinity and surfactant concentration by doing a salinity scan at constant surfactant concentration and a surfactant concentration scan at constant salinity.

To test solubility as a function of NaCl concentration, samples of about 10 ml volume were prepared in test tubes. The amounts of surfactant required to give 1% w/w (active) surfactant solutions were weighed into the test tubes and brines ranging from 0 to 5% w/w NaCl concentration were added. The solubility was determined by visual inspection of the appearance of the sample. Samples showing any turbidity or precipitate were denoted incompletely soluble. These samples were heated slowly to 85°C in a waterbath. The temperature at which the samples cleared was taken as the

minimum solubility temperature. Some samples that were not soluble up to 85°C were heated further to 135°C in an oven.

A similar set of experiments was run to determine solubility as a function of surfactant concentration. Surfactant solutions were prepared at surfactant concentrations ranging from 0.01 to 5% w/w (active), keeping the brine salinity constant at 0.5% w/w NaCl. Again, the minimum solubility temperature was determined by heating the samples that were not soluble at room temperature.

The calcium tolerance of two surfactants (AOS 1416 and IOS 1518) was determined at 23°C by testing their solubilities in brines of the same ionic strength as the 2.32% NaCl, but containing NaCl and $CaCl_2$ at different ratios. The compositions of these brines are listed in Table 2(b).

3. CORE FLOODS

Adsorption of four surfactants that were selected on the basis of the solubility measurements (AOS 1416, IOS 1518, LXS 810, Stepanflo 60) on Berea sandstone was measured by performing single-phase displacement tests. Cylindrical cores 3.8 cm in diameter and 10 cm long were used. After cutting a core to size it was dried at about 110°C for several hours. It was then mounted in a lead sleeve inside a stainless steel, high pressure core holder, and an overburden pressure of 1000 psi was applied. The pore volume was determined using gas expansion and Boyle's law, and the absolute permeability to air was measured. The core was filled with CO_2 and saturated with brine by flooding with approximately 15 pore volumes (PV) of brine against a back pressure of 30 psi. The absolute permeability to brine was measured.

A total of 12 core floods was run using four surfactants, three brines, and two temperatures. One of these core floods was run with a surfactant mixture containing an anionic and an amphoteric surfactant (IOS 1518 and Stepanflo 60) at a 7:3 mass ratio. All floods were run at atmospheric pressure. Detailed core and displacement data are shown in Table 1.

A measured volume of surfactant solution (approximately 2 PV, 10 g/l active concentration) was injected into the brine saturated core at a constant flow rate of 2 ml/h, which corresponds to an apparent linear velocity of about 20 cm/day. A non-adsorbing tracer (tritiated water) was injected with the surfactant solution, and served as a check on the material balance. The relative positions of the tracer and surfactant effluent profiles also give a direct visual indication of adsorption. The chemical slug was followed by brine injection until the tracer and surfactant concentrations at the core outlet dropped to near zero. The pressure drop across the core was measured in all floods in order to detect possible core plugging by surfactant precipitation. This allowed additional assessment of whether we were measuring surfactant loss by adsorption alone or by a combination of adsorption and precipitation.

Effluent fractions from the core were collected at intervals and analyzed for surfactant and tracer concentrations. The anionic surfactants were determined by two-phase titration with Hyamine (Reid et al., 1967), and the amphoteric by back titration with Hyamine (Schramm et al., 1989), both in chloroform/water with mixed indicator at pH 2. The unknown core effluent concentrations were determined from calibration curves constructed by titrating a set of standards prepared with each surfactant used in core floods. Chemical analysis of each component in the surfactant mixture (anionic/amphoteric) required the development of a special technique, which involved titrating each sample twice, once at pH 2 and once at pH 10. The concentrations of total anionic surfactant, free excess anionic or amphoteric, and anionic-amphoteric complex could then be determined with the help of three different calibration curves, and this allowed calculation of the concentrations of anionic and amphoteric surfactant in the mixture. Details of this method are given in Appendix A. The tracer was analyzed with a scintillation counter. Since adsorption is a function of pH through the surface charges on the solid, the pH of each sample was also measured. Effluent concentrations of Ca^{2+} and Mg^{2+} were measured by atomic absorption spectroscopy in one flood (core CM-13).

4. SURFACE TENSION MEASUREMENTS

Surface tensions were determined as a function of surfactant concentration at ambient conditions for all surfactant/brine systems used in core flooding. This allowed determination of the critical micelle concentration (cmc) of each system and the packing density in a monolayer at the gas/liquid interface. The latter number allowed calculation of the molecular area of the surfactant molecules. Surface tensions were measured with a Fisher Model 20 Du Nouy ring tensiometer.

5. MICROCALORIMETRY

Enthalpy changes accompanying surfactant adsorption were measured using a Thermometric 2277 Thermal Activity Monitor (TAM) equipped with an adsorption cell. A schematic drawing of the calorimeter is shown in Figure 1.

This type of calorimeter is based on heat flow and heat leakage principles, "where any heat produced in a thermally-defined vessel flows away in an effort to establish thermal equilibrium with its surroundings" (ThermoMetric 2277 Thermal Activity Monitor Instruction Manual, 1988). A schematic drawing of the heat flow principle is shown in Figure 2. The heat produced or consumed in a measuring calorimetric cell is compared to the heat changes in a reference cell and the difference is ascribed to the heat produced in the measuring cell. Such a differential measurement, in principle, eliminates experimental noise that might be generated by fluctuations in the temperature of the surroundings of the cells.

The Thermometric TAM utilizes a dual water thermostat maintaining constant temperatures between 5 and 80^{o}C within 0.0002^{o}C. Such a precise temperature control allows determination of a power output from the measuring cell in the range of few microwatts. However, such extreme sensitivity eliminates certain experimental sequences that would be advantageous in adsorption measurements. For example, batch injection of surfactant solution into the measuring cell disrupts the adsorption measurements as the hydrodynamic friction during flow overwhelms the enthalpy changes due to adsorption. This

limited the options in designing the adsorption experiments as it was practically impossible to stop or to restart injection of the surfactant solution into the measuring cell without overwhelming the adsorption measurements.

Inability of adding adsorbing surfactant solutions to the measuring cell in batch mode necessitated modifications to the adsorption experiments. In order to maintain constant hydrodynamic friction throughout the whole experiment, the surfactant solutions were injected continuously into the measuring cell containing the Berea sandstone immersed in a brine.

The final experimental arrangement is shown in Figure 3. The measuring cell was filled completely with a crushed adsorbent (1 mm chunks of Berea sandstone) and with 0.5% NaCl brine. The inlet and outlet flow lines were then connected and brine injection commenced at a constant flow rate. The heat produced from the hydrodynamic friction within the cell was thus monitored by the microcalorimeter prior to all adsorption experiments, and the power output from the cell was taken as a baseline for the adsorption measurements. When the baseline stabilized, the injected brine was replaced with a 0.5% surfactant solution that was pumped at the same rate. As the surfactant solution reached the adsorption cell, the combined heat of micellization and adsorption was continuously monitored by the microcalorimeter. When adsorption equilibrium was established, the power output resulting from the hydrodynamic friction returned approximately to the baseline level in most experiments. To correct for the heat generated by the micellization, blank experiments with no adsorbent in the measuring cell were conducted prior to adsorption measurements. The total enthalpy change resulting from surfactant adsorption was then determined by integrating the areas under the power output curves. The original calorimetric data are shown in Figures 4 to 6 and the integrated enthalpies can be seen in Figures 7 to 9.

ADSORPTION MODEL AND HISTORY MATCHING

In order to evaluate surfactant adsorption isotherms from core floods, the surface excess model of adsorption, developed at PRI, was used to match surfactant effluent concentrations. We have used this procedure quite extensively in the determination of adsorption of foam-forming surfactants at different conditions of temperature and salinity, and several versions of the model have been described (Mannhardt and Novosad, 1988; 1991a,b; Mannhardt et al. 1990). The model that was used in this work has been described in detail by Mannhardt and Novosad (1991a,b).

At the heart of the model is a one-dimensional transport equation for flow of adsorbing chemicals in porous media. The term that takes into account adsorption is written in terms of the surface excess, and adsorption is based on surfactant monomer rather than overall concentrations. This last point is based on the observation made by many investigators and described repeatedly in the literature that surfactant adsorption takes place from the monomer phase, but not from the micelles. The model thus determines the surfactant monomer concentration at any given total surfactant concentration, and then calculates adsorption based on the monomer concentration.

At surfactant concentrations below the critical micelle concentration, the monomer concentration is equal to the total surfactant concentration, since no micelles have yet been formed. In a solution containing a single pure surfactant above the cmc, the monomer concentration remains constant when the surfactant concentration is increased, since any surfactant added will form micelles. In such a system, adsorption will therefore also remain constant at its plateau value at any surfactant concentration above the cmc. The adsorption isotherm generated by this kind of model rises steeply at very low surfactant concentrations and becomes constant when the concentration reaches the cmc. In surfactant mixtures, both the composition of the monomer phase and the overall monomer concentration change even above the cmc, and a monomer-micelle model is required to calculate monomer concentrations. Since monomer concentrations change above the cmc, so do the

adsorption isotherms in the mixture.

In the work to be described in this report, the commercial surfactant samples were treated as single-surfactant systems. This is, of course, an approximation, since essentially all commercial surfactants are mixtures, often of complex composition. Even if the composition of these mixtures was known precisely, models that accurately describe monomer-micelle behavior and adsorption of such complex systems are not yet available. While the assumption of constant monomer concentration above the cmc is therefore not strictly true for these surfactants, we have found in our previous work that the shape of the adsorption isotherm (a steeply rising isotherm) obtained using this assumption is more realistic than an isotherm obtained by basing adsorption on overall concentrations, i.e. ignoring monomer-micelle equilibrium and treating the surfactant like any other non-aggregating chemical. In this work, the model was used for floods carried out with single surfactants only. The following discussion therefore refers to single-surfactant systems.

Input to the model includes core properties, details of the displacement experiment, the cmc of the surfactant solution, and the model parameters. The latter are as follows:

S = selectivity

m_1 = monolayer coverage of surfactant (mmol/g)

m_2 = monolayer coverage of water (mmol/g)

k_1 = rate constant of adsorption (h^{-1})

k_2 = rate constant of desorption (h^{-1})

λ = dispersion parameter (cm) ($D = \lambda v$, where D is the dispersion coefficient and v frontal velocity)

The selectivity is essentially a measure of the affinity of the surfactant for the solid. A high selectivity indicates large attractive forces between the surfactant and the solid. Selectivity is defined as

$$S = \frac{x_1'/x_2'}{x_1/x_2} \qquad (1)$$

where

x_1' = surfactant mole fraction in the adsorbed phase
x_2' = solvent (brine) mole fraction in the adsorbed phase
x_1 = surfactant mole fraction in the bulk phase
x_2 = solvent (brine) mole fraction in the bulk phase

S>1 indicates a solid that attracts the solute (surfactant) preferentially, S<1 a solid that prefers the solvent over the solute, and S=1 a solid that shows no preference for either component.

Experimental data on the kinetics of surfactant adsorption are not readily available in the literature. In the model used in this work, the kinetics of adsorption and desorption were assumed to be first order.

The monolayer coverages represent the number of molecules that will fit on the solid surface in a tightly packed monolayer and are taken to be the maximum adsorptive capacity of the rock. They are calculated independently from the molecular area of the surfactant and water molecules and the specific surface area of the solid. The molecular area of a surfactant molecule in a monolayer can be determined from surface tension measurements and the Gibbs adsorption equation, as has been described in detail by Rosen (1978) and Chattoraj and Birdi (1984) and the references cited by these authors. An average value for the molecular area of water was taken from the literature, and is 12.5 Å^2 (McClellan and Harnsberger, 1967). The model thus contains four adjustable parameters: S, k_1, k_2, and λ.

Simulated effluent concentrations are matched to experimental ones by changing the parameters of the model and observing the effect on the shape and position of the effluent profile. The best fit is chosen by visually comparing experimental and simulated effluent profiles. Once a match has been obtained, the model parameters can be used to calculate the adsorption isotherm of the particular system through the following equation:

$$n_1^e = \frac{m_1 x_{1d} x_{2d} (S-1)}{S x_{1d} + (m_1/m_2) x_{2d}} \qquad (2)$$

where n_1^e is the surface excess adsorption in mmol/g, x_{1d} is the mole

fraction of surfactant in the monomer (dispersed) phase, x_{2d} is the mole fraction of water in the monomer phase, and the other variables are as previously defined.

Equation (2) requires the monomer mole fractions of surfactant. In a system containing a single surfactant below the cmc, the monomer mole fraction is equal to the overall surfactant mole fraction. Above the cmc, the monomer concentration is constant and equal to the cmc.

The adsorption model that was used in this work was written in molar units, since it is based on thermodynamic quantities and derivations which are always expressed in terms of moles rather than grams of material. Equation (2) is therefore also written in molar units. Since it is more common to use units of mass in petroleum engineering, adsorption was calculated in molar units using Equation (2) and was then converted to mass units using the molecular weights specified in Table 3.

The evaluation of adsorption thus involved history matching of experimental core effluent concentrations, followed by calculation of adsorption isotherms using Equation (2). This allowed comparison of adsorption levels in the various systems studied.

RESULTS AND DISCUSSION

1. SURFACTANT SOLUBILITIES

In order to select completely soluble surfactants for the adsorption measurements, the solubility of a number of surfactants was measured as a function of salinity and surfactant concentration. Surfactants were chosen from those chemical classes that have been discussed in the literature in connection with steam flooding, as described in the literature review above. The anionic surfactants used in this study were alpha olefin sulfonates (AOS), an internal olefin sulfonate (IOS), a linear toluene sulfonate (LTS), and linear xylene sulfonates (LXS). To the authors' knowledge, the amphoteric surfactant (Stepanflo 60) has not been used in steam flooding, but is listed as a possible steam flood additive in the 1989 EOR Chemicals Overview in Petroleum Engineer International. According to the manufacturer this surfactant is chemically stable at steam flood temperatures (Stepan Company, personal communication). Also, we chose to test only surfactants of known chemical structure. Surfactants that are used in steam flooding but whose chemical composition is proprietary were not used.

The results of a salinity scan are shown in Table 4 and Figure 10. Surfactant solutions at a concentration of approximately 1% w/w were prepared in brines of increasing sodium chloride concentration at room temperature (23^{o}C). Samples that appeared visually clear were denoted soluble at this temperature. Samples that were cloudy or formed a precipitate were heated, and the temperatures at which these samples became clear were denoted solubility temperature and are listed in Table 4 and plotted in Figure 10. Those samples that did not dissolve on heating are denoted "ns" (not soluble) next to the highest temperature tested, and are marked with an arrow in Figure 10. Note that samples that were soluble at room temperature were given a solubility temperature of 23^{o}C. They were not cooled, and the points at 23^{o}C in Table 4 and Figure 10 thus have a true solubility temperature lower than 23^{o}C. Similar data for solubility as a function of surfactant concentration at a constant salinity of 0.5% NaCl are shown in Table 5 and Figure 11. The estimated error for the listed temperatures is ±3^{o}C.

Of the surfactants tested, those containing a phenyl group were the least salt tolerant. At room temperature, LXS 1314 and LTS 1618 were soluble only in deionized water. A lower molecular weight LXS (LXS 810) was soluble at room temperature up to 0.5% NaCl, but not at higher salt concentrations. Even at low surfactant concentrations (0.01% in 0.5% NaCl) LXS 1314 and LTS 1618 required substantially elevated temperatures to dissolve (Table 5, Figure 11). The IOS, both AOS's, and Stepanflo 60 were relatively more soluble. AOS 1618 and IOS 1518 required slightly elevated temperatures to dissolve at the higher salt concentrations, while a lower molecular weight AOS (AOS 1416) and the amphoteric surfactant (Stepanflo 60) dissolved at 23°C up to the highest tested salt and surfactant concentrations.

Based on the information in Tables 4 and 5 and Figures 10 and 11, the surfactants can be assigned an approximate ranking according to their solubility (numbers in parentheses are average molecular weights):

AOS 1416 (325) / Step 60 (400) > AOS 1618 (356) / IOS 1518 (339) > LXS 810 (334) > LXS 1314 (397) / LTS 1618 (422)

Increasing the molecular weight of the hydrophobe within a chemical class decreases the surfactant's solubility. Addition of a phenyl group to the molecule also significantly decreases solubility. The amphoteric surfactant is very soluble, although its average molecular weight is higher than that of most of the other tested surfactants.

Four surfactants that were soluble at 23°C in 0.5% NaCl and are members of different chemical classes were chosen for adsorption testing:

AOS 1416
IOS 1518
LXS 810
Stepanflo 60

While the three anionic surfactants are lower in molecular weight than would be used in steam flooding, they were chosen as representatives of surfactant types used in steam flooding for a comparative adsorption study.

Some observations made in this solubility study were as follows. Some

samples appeared soluble at room temperature initially, but formed a precipitate after standing overnight. Conversely, some samples that required heating to dissolve seemed to stay in solution when they were allowed to cool to room temperature. The LXS 1314 exhibited interesting phase behavior. When the solubility of this surfactant increased, for example by increasing the temperature or decreasing the salt concentration, it went through the following phase changes:

solid precipitate → two liquid phases → milky liquid → clear liquid

In the two-phase system, the lower phase was oily in appearance and was most likely a surfactant-rich phase containing some form of large surfactant aggregate. When relatively dilute solutions (0.068% and 0.12% in 0.5% NaCl) of this surfactant were heated to 135°C they changed from a milky liquid to a clear liquid with suspended needle-like crystals. As has been mentioned previously, surfactants can exhibit complex phase behavior (Miller and Neogi, 1985).

Adsorption of all four surfactants listed above was measured from 0.5% NaCl brine. Adsorption of AOS 1416 and IOS 1518 was also measured from two higher salinity brines: 2.32% w/w NaCl and 2.27% w/w TDS brine. The former was chosen because we have used it in previous adsorption studies with different surfactants (Mannhardt et al., 1990). The latter has the same ionic strength as the 2.32% NaCl, but contains both NaCl and $CaCl_2$. Its composition was chosen on the basis of a simple solubility test. In order to test the calcium tolerance of the two surfactants, 1% w/w surfactant solutions were prepared in a series of mixed brines of constant ionic strength containing NaCl and $CaCl_2$ at different ratios (Table 2(b)). The results are shown in Table 6. Both surfactants were soluble in the 2.27% w/w TDS mixed brine, but IOS 1518 was probably very close to its solubility limit. This brine was chosen for adsorption experiments.

2. CRITICAL MICELLE CONCENTRATIONS

The critical micelle concentration (cmc) is a characteristic property of a surfactant solution. It determines the concentration of surfactant monomer.

In the adsorption model outlined above, adsorption depends on surfactant monomer concentration, and the cmc is required as input into the model. There are numerous methods to determine the cmc experimentally (Shinoda, 1963; Mukerjee and Mysels, 1970). Surface tension measurements were used for this purpose in this study.

Surface tensions were measured as a function of surfactant concentration for all surfactant/brine systems used in core floods. These systems are listed in Table 7 together with information obtained from the surface tension curves shown in Figures 12 to 21. All surface tension values are listed in Appendix B.

Cmc's were determined from Figures 12 to 21 from the intersection of two straight lines as indicated in the figures. The results are tabulated in Table 7. The cmc's of AOS 1416 and IOS 1518 decrease with increasing NaCl concentration, consistent with the observations of previous investigators (Shinoda, 1963; Rosen, 1978). The cmc of IOS 1518 is affected more strongly by calcium ion, and this may reflect the higher sensitivity of this surfactant to calcium (Table 6). The cmc of LXS 810 is higher than those of the other surfactants by an order of magnitude. This surfactant has a smaller alkyl group than the AOS 1416 and IOS 1518. Even when one takes into account the fact that adding a benzene group is equivalent to adding 3.5 methylene groups (Shinoda, 1963), the LXS still has a smaller hydrophobe than the other two anionics, and this may account for its higher cmc. In general, the addition of one methylene group to a surfactant's hydrophobe has been found to lower the cmc by one third (Shinoda, 1963).

In addition to the cmc, the molecular area of a surfactant molecule in a monolayer can be determined from the surface tension curves. The slope of a curve of surface tension versus logarithm of surfactant concentration is related to the surface excess of surfactant at the gas/liquid interface through the Gibbs adsorption equation (Rosen, 1978; Chattoraj and Birdi, 1984):

$$\Gamma = \frac{-1}{2.303mRT} \frac{d\gamma}{d\ \log(C)} \qquad (3)$$

where Γ is the surface excess (in moles per unit surface area), R the universal gas constant, T absolute temperature, γ surface tension, and C surfactant concentration. The value of m depends on the salt concentration. In the presence of excess salt, m=1. From the slope just below the cmc the packing density of surfactant molecules in a monolayer can be calculated, and this gives the surface area occupied by a molecule in a monolayer. The surface excess and molecular area for each system used in this work are listed in Table 7. The molecular areas for the anionic surfactants are similar to those listed by Rosen (1978), and the molecular area of the amphoteric is similar to those we have previously measured for other surfactants of this type (Mannhardt et al., 1990; Mannhardt and Novosad, 1991b).

Two of the parameters of the adsorption model are the monolayer coverages of surfactant and water on the rock surface. Using the molecular areas from Table 7 and a specific surface area for Berea sandstone of 0.91 m^2/g (Donaldson et al., 1975; Mannhardt et al., 1990), the monolayer coverage for each surfactant/brine system can be calculated (Table 8). The molecular area of water was taken as 12.5 $Å^2$ (McClellan and Harnsberger, 1967), giving a monolayer coverage of 0.0121 mmol/g for water.

Surface tensions were measured for one surfactant mixture that was used in one of the adsorption experiments (IOS 1518 : Stepanflo 60, 0.72:0.30 w/w). The results are shown in Figure 21. The cmc and average molecular area of the mixture fall between those of the pure components (Table 7).

Average surface tensions above the cmc are also listed in Table 7, and are very similar for all systems.

The dependence of the cmc on temperature is complex (Rosen, 1978). The cmc of anionic surfactants has been found to go through a minimum around 25°C, while limited measurements carried out with zwitterionic surfactants indicate a decrease in cmc with increasing temperature.

Two of the core floods described in the next section were run at 75°C. With the Du Nouy ring tensiometer used in this work, surface tensions cannot be

measured at elevated temperature. An attempt was made to use a University of Texas spinning drop tensiometer for this purpose. Bubbles of 2 to 4 μl in the surfactant solution of interest were used. In order to test the method and compare it to the ring method, surface tensions were measured at 23°C for one of the systems that had already been measured by the ring method. Figure 20 compares surface tensions obtained by both methods. The spinning bubble resulted in more scatter than the ring method. The reason for this is not clear at this point. Also, the cmc as determined from the spinning bubble method is lower than that from the ring method by a factor of 4. We have previously measured cmc's of different surfactants by both methods and obtained similar trends. Since cmc's determined by the two different methods are not comparable, no attempt was made to determine the cmc's at 75°C by the spinning bubble method, and for the purpose of modelling the two 75°C floods the cmc's measured at 23°C were used.

3. ADSORPTION OF SINGLE SURFACTANTS

Results of all core floods are summarized in Table 8 and shown in Figures 22 to 34. The columns in Table 8 and the figures have been ordered by surfactant.

The data in Table 8 include the average effluent pH for each core flood, material balance calculations for surfactant and tracer, the flow model parameters that gave the best fit to experimental data, and the plateau adsorption values taken from the adsorption isotherms calculated from the flow model parameters. The model parameters listed are for surfactant unless otherwise stated.

The average pH was calculated from the pH's of all effluent samples of each core flood. These are included in the table for reference only, since adsorption can be a strong function of pH through the surface charges on the solid. The pH was fairly constant, with some fluctuation around the average, in all floods. Also, the average effluent pH fell between 7.3 and 8.4 in all floods, although the pH's of the injected surfactant solutions were quite different from each other (Table 3). AOS 1416 was near neutral, IOS 1518 and

LXS 810 slightly basic, and Stepanflo 60 quite acidic. The Berea rock seems to buffer the injected solutions to about the same pH.

From the amounts of tracer injected in the surfactant slug and tracer produced in the effluent, the tracer balance was calculated for all floods. As can be seen from Table 8, the tracer balance is closed to within a few percent in all cases. The tracer balance provides a check on the quality of the data and indicates that we were properly accounting for injected and produced fluids.

Effluent profiles for AOS 1416 in 0.5% NaCl at 23°C are shown in Figure 22. The tracer and surfactant curves coincide within the accuracy of the measurements, indicating that there is essentially no adsorption in this system. The material balance calculation shown in Table 8 (core CM-2) confirms this: All the injected surfactant is recovered during chase brine injection. (Some of the material balance calculations in Table 8 resulted in a small negative number for the amount of surfactant lost. However, this number was never more than a few milligrams and is well within the accuracy of the experiment. Negative values were set to zero in Table 8.) Since adsorption was zero in this flood, the data were not modelled.

As has been mentioned, physical adsorption decreases with increasing temperature. Since AOS 1416 did not adsorb from 0.5% NaCl at 23°C, we did not expect it to adsorb at higher temperatures either, and no core floods were therefore performed with this system at elevated temperature. Instead, the salinity was changed by first increasing the NaCl concentration to 2.32% and then adding $CaCl_2$ but keeping the total ionic strength constant (2.27% TDS with the composition in Table 2(b)). Effluent profiles for these two floods are shown in Figures 23 and 24, and material balance calculations are in Table 8 (cores CM-9 and CM-12). The separation between the tracer and surfactant curves indicate that adsorption is increased both by increasing salinity and by increasing divalent ion content.

Both floods with AOS 1416 in the higher salinity brines were modelled, and the fitted effluent profiles are shown in Figures 23 and 24. The best-fit parameters are listed in Table 8 (cores CM-9 and CM-12). Note that the

monolayer coverages were not treated as adjustable parameters, but were calculated independently from the molecular areas of the surfactant molecules and the specific surface area of Berea sandstone, as described in the previous section. The other parameters were adjusted until a fit with the experimental data was obtained. To fit the tracer, adsorption was set to zero by letting S=1. The only adjustable parameter for the tracer profile is thus the dispersion parameter λ. A good fit was obtained for all effluent profiles.

From the model parameters in Table 8 adsorption isotherms were calculated using Equation (2), and these are shown in Figure 28. Adsorption increases with increasing surfactant concentration up to the cmc, and then levels off at a plateau, since the monomer concentration, and therefore adsorption, is assumed to remain constant beyond the cmc. The concentration at which plateau adsorption commences is much lower than concentrations of practical interest in EOR, and adsorption levels in the different systems can therefore conveniently be compared by comparing the plateau adsorption levels. These have been listed in different sets of units in Table 8. In general, the calculated plateau adsorption levels agree very well with the material balance adsorption levels for all systems investigated in this work.

Figure 28 and Table 8 indicate that adsorption of AOS 1416 from 0.5% NaCl at $23^{o}C$ on Berea sandstone is negligible, but increases with increasing salinity and divalent ion content of the brine. This trend is reflected in the material balance numbers, the plateau adsorption levels, and the selectivities.

The trends in adsorption behavior observed with IOS 1518 are quite similar to AOS 1416. Effluent profiles for this surfactant in three different brines are shown in Figures 25 to 27, and adsorption levels from material balance calculations and calculated adsorption isotherms are summarized in Table 8 (cores CM-3, CM-10, and CM-11). Adsorption isotherms are shown in Figure 28 together with those of AOS 1416. There is no adsorption from 0.5% NaCl, and this core flood was therefore not modelled. Adsorption increases at higher salinity and in the presence of divalent ions. Adsorption of this surfactant

seems to be less strongly affected by calcium ions than AOS 1416 even though its solubility in the mixed brine is lower that that of AOS (Table 6).

Effluent profiles for LXS 810 in 0.5% NaCl at 23°C (core CM-4) are shown in Figure 29. Several points of interest can be noted from this figure. Loss of this surfactant from the low salinity brine is significantly higher than in the case of AOS 1416 and IOS 1518 (Figures 22 and 25), as indicated by the separation of tracer and surfactant profiles. The leading edge of the tracer profile exhibits the typical symmetrical S-shape of the error function solution to the dispersion equation, while there is a shoulder in the surfactant profile's leading edge. Chase brine injection into this core was started after two pore volumes of surfactant solution had been injected. Since this brine has to travel through the core before appearing at the outlet, one would expect the tracer and surfactant concentrations to decrease at a total throughput of about 3 PV, or slightly less because of dispersion. However, in this flood both tracer and surfactant concentrations decrease early and show an unusually long tail. (In other floods, such as those in Figures 22 to 27, the tracer profile would follow the dashed line predicted by the model.) These effluent profiles thus show some unusual features that cannot be attributed to convection-dispersion and adsorption alone. Since it was not known if this behavior was caused by the surfactant or possibly by problems with this particular core, such as a fracture that formed a preferential flow path through the core, this flood was repeated in a fresh core.

The results of the repeat flood with LXS 810 in 0.5% NaCl at 23°C (core CM-13) are shown in Figure 30. Clearly, the effluent profiles exhibit the same unusual features as in the previous flood, and these were therefore attributed to the surfactant itself. The LXS 810 is relatively less soluble than the other surfactants, and surfactant precipitation was suspected. While the solubility study discussed above indicates that this surfactant was soluble in 0.5% NaCl at 23°C, and while no precipitate was evident in the core effluent, the pressure drop in this and the previous flood increased very slightly during surfactant injection and then decreased during chase brine injection.

The trailing edges of the profiles in Figures 29 and 30 indicate that the surfactant changed the flow path of both the surfactant and the tracer through the core. The shape of the profiles in this region is typical of a system with capacitance and slow mass transfer between the flowing and stagnant fractions of the pore volume (Coats and Smith, 1964). Precipitated surfactant may have blocked some of the pore space, and slow diffusion of tracer from the blocked to the flowing pore volume may have caused tailing in the tracer profile. This effect is absent at the leading edge because the tracer moves ahead of the surfactant and is thus unaffected by precipitating surfactant. The same effect combined with dissolution of precipitated surfactant on chase brine injection may have caused the long tail in the surfactant profile.

In order to investigate possible causes for surfactant precipitation, the concentrations of calcium and magnesium ions in the effluent of the second flood with LXS 810 at 23°C were measured. The results are shown in Figure 30. At the start of surfactant injection the core had been flooded with 14 PV of 0.5% NaCl, and ion exchange with the clays would thus have been complete, i.e. the rock was in equilibrium with the injected brine at this point. However, it has been shown by Novosad (1981) and Hirasaki (1982) that a system in which the brine preflush, surfactant slug, and chase brine all have the same electrolyte concentration can exhibit an increase in divalent ion concentration in the surfactant bank. Micelles of ionic surfactants bind calcium in preference to sodium (Hirasaki and Lawson, 1982). The micelles form a medium that exchanges calcium with the clays or binds calcium that dissolves from the rock. Berea sandstone contains clays, mostly kaolinite, and also a small amount of calcite that may provide a source of dissolved calcium ion. Figure 30 indicates that the "baseline" calcium produced at the start of the flood (i.e. when the in-situ brine was being flushed from the core) is about 20 ppm. The calcium concentration increases simultaneously with the surfactant concentration, indicating that calcium is being carried by the surfactant bank, most likely bound to the surfactant micelles. The calcium reaches a peak at the shoulder in the surfactant profile. This shoulder could be caused by surfactant precipitation, which causes surfactant to be produced at a concentration lower than in the absence of precipitation. At this point ion exchange between the clays and the micelles

has probably reached equilibrium. The calcium concentration decreases, surfactant precipitation thus ceases, and the surfactant effluent concentration rises to the injected value. The calcium concentration decreases to a level that is lower than ahead of the surfactant bank, since the overall calcium content of the system is now lower. The magnesium concentration in the effluent is lower than the calcium concentration, but shows the same general trend.

Since the shapes of the effluent profiles in Figures 29 and 30 were not determined by convection-dispersion and adsorption alone, they could not be modelled very well. The fit of simulated and experimental effluent profiles shown in Figures 29 and 30 is thus not as good as in previous data sets for the reasons explained above. The "retention isotherms" for LXS 810 at 23^{o}C in Figure 34 thus include other phanomena in addition to adsorption at the solid/liquid interface. The adsorption levels in Table 8 (core CM-4 and CM-13) represent a combination of adsorption and precipitation. Also note that the adsorption levels and isotherms for the duplicate floods are not the same. The poor reproducibility may be due to differences between the two cores, which may affect the amount of Ca^{2+} in the core and may cause different amounts of surfactant to precipitate in the two floods.

The next core flood (core CM-8) was performed with the same surfactant/brine system at elevated temperature (75^{o}C). From the effluent profiles in Figure 31 and the results in Table 8 it is evident that surfactant loss has been greatly reduced at this temperature. Also, the effluent profiles no longer exhibit the features of those obtained at the lower temperature. The higher temperature increases the solubility of the surfactant sufficiently for it to tolerate the ion-exchanged or dissolved calcium from the rock. A very slight turbidity was noted in the effluent samples of this flood. The presence of calcium thus did not cause the surfactant to precipitate inside the core at 75^{o}C, but caused some surfactant to precipitate in the sample tubes which were kept at room temperature. In this particular flood, the reduction in surfactant loss at elevated temperture can be attributed to a combination of lower adsorption and the absence of precipitation. Almost all the injected surfactant is recovered in this flood.

Effluent profiles for Stepanflo 60 in 0.5% NaCl at 23°C and 75°C are shown in Figures 32 and 33. In contrast to the anionics, this surfactant adsorbs very strongly on sandstone, consistent with our previous results with amphoteric surfactants (Mannhardt and Novosad, 1988; Mannhardt et al., 1990). The material balance calculations in Table 8 (cores CM-6 and CM-7) indicate that increasing the temperature decreases adsorption slightly. The adsorption isotherms obtained from history matching are the same for both floods (Figure 34, Table 8). However, the fit of the 23°C flood (Figure 32) is poor, and the model overpredicts the amount of surfactant produced. It can be concluded that adsorption of Stepanflo 60 decreases slightly with increasing temperature, but the dependence is not a strong one. Again this is consistent with previous measurements with amphoteric surfactants (Mannhardt and Novosad, 1988).

Adsorption isotherms for LXS 810 and Stepanflo 60 at two different temperatures are shown in Figure 34. As has been pointed out above, the isotherms for LXS 810 at 23°C probably overestimate adsorption, since surfactant precipitation contributed to loss of this surfactant.

It has been pointed out in the previous section that both 75°C floods were modelled using cmc's measured at 23°C. The cmc determines the concentration at which plateau adsorption begins (Figure 34). Had the cmc at 75°C been measured and used in the model, the break point in the adsorption isotherms would likely be at a different concentration, but the plateau adsorption level would not be affected appreciably, i.e. the maximum adsorption levels would be the same.

Surfactant adsorption is often correlated to surfactant solubility, low solubility driving the surfactant to the solid/liquid interface and resulting in higher adsorption levels. Clearly, this trend is not observed with the amphoteric surfactant. It is more soluble in concentrated brines than the anionics, yet it adsorbs very strongly. Adsorption of this surfactant may proceed by a different mechanism than adsorption of the anionics (Mannhardt et al., 1990).

Some general comments on the model parameters in Table 8 may be made. The

kinetics of adsorption are higher than the kinetics of desorption in all floods, consistent with previous observations (Mannhardt and Novosad, 1988; Mannhardt et al., 1990). In fact, the surfactants studied do not desorb appreciably on the time scale of the experiments. The dispersion parameters for the tracer are of the same order for all floods. Tracer dispersion is generally small, resulting in a piston-like displacement. Fitting the surfactant profile required a dispersion parameter that is slightly higher than that for the tracer in most cases. Cores CM-4 and CM-13 required significantly higher dispersion coefficients for tracer than for surfactant. However, these effluent profiles were poorly represented by the model because of surfactant precipitation. Both floods with Stepanflo 60 (cores CM-6 and CM-7) also required high dispersion coefficients for the surfactant.

4. ADSORPTION OF A SURFACTANT MIXTURE

One of the surfactants investigated in this work, Stepanflo 60, adsorbed strongly. While its high adsorption level severely restricts its application in sandstone reservoirs, an advantage of this surfactant over the anionics is its complete solubility in near-saturated salt solutions. In order to test the possibility of reducing adsorption of this surfactant, it was mixed with one of the surfactants that did not adsorb from 0.5% NaCl at 23^{o}C, IOS 1518. A core flood was run at 23^{o}C with a mixture containing 3 g/l Stepanflo 60 and 7 g/l IOS 1518 in 0.5% NaCl. The overall surfactant concentration was thus the same as in the floods of the previous section.

Effluent profiles for total surfactant and tracer are shown in Figure 35, while those for each component and the tracer are shown in Figure 36. As is pointed out in Appendix A, chemical analysis of this surfactant mixture is difficult, and this is the reason for the large amount of scatter in the effluent concentrations of Stepanflo 60. Analysis of IOS 1518 in the mixture is relatively straightforward and involves a single two-phase titration. The effluent curve for IOS 1518 is thus smooth and very similar in shape to those described in the previous section. However, determination of the amphoteric surfactant, and therefore also of total surfactant, requires

taking the difference of the results of two titrations, and a large error can be introduced by doing this.

Although large errors in individual sample analyses are associated with the effluent profiles of Stepanflo 60, the overall trend in surfactant effluent concentration is well defined. The following observations can be made from Figures 35 and 36 and Table 8 (core CM-14). The separation between the surfactant and tracer curves in Figure 35 indicates low overall adsorption of surfactant from the mixture. IOS does not adsorb from the single-surfactant solution at the conditions of this flood (Figure 25), but seems to adsorb slightly from the mixture (Figure 36). The material balance for IOS (Table 8) also indicates that adsorption of IOS from the mixture is small. The more interesting conclusions can be reached regarding Stepanflo 60. The material balance calculations in Table 8 give an adsorption level of 1.7 mg/g for this surfactant from the single-surfactant solution (core CM-6). In the mixture, the adsorption level is reduced to 0.16 mg/g (core CM-14). The effluent profiles for Stepanflo 60 in Figures 32 and 36 are also markedly different. The surfactant peak is significantly larger in Figure 36, and this is so in spite of the fact that the injected Stepanflo concentration in this flood was much lower than that in Figure 32 (3 g/l as compared to 10 g/l). This implies that less of the injected surfactant is being retained in the core from the mixture than from the single-surfactant system. It can therefore be concluded that adsorption of Stepanflo 60 has been reduced by blending it with IOS 1518.

This core flood was not modelled because our model cannot yet handle surfactant mixtures with non-ideal mixing in the micelles. Ideal mixing in the micelles implies that interactions between unlike molecules in the micelles are similar to interactions between like molecules. The mixture studied here almost certainly forms non-ideal mixed micelles, since the two surfactants have a tendency to complex to each other through electrostatic interaction between the anionic surfactant and the positive charge on the amphoteric. (The titration procedure for chemical analysis of these surfactants is, in fact, based on this; see Appendix A.) To study mixed micelle behavior and to model it requires measuring cmc's as a function of mixture composition. With the surface tensiometer available to us, we have

not yet been able to measure cmc's accurately enough to ascertain the type of mixed micelle behavior, and this is another reason that the core flood with the mixture was not modelled. Further studies on this topic are in progress.

The mechanism of adsorption reduction in mixed surfactant systems can be attributed to micelle formation. Both the micelles and the adsorbed phase compete for molecules from the monomer phase. If mixed micelle formation causes a surfactant to prefer the micelles over the adsorbed phase, then adsorption of this surfactant can be reduced by surfactant mixing. Another factor that may contribute to lower adsorption of the amphoteric in the mixture studied in this work may be complex formation between the two surfactants. The surfactant with the lower tendency to adsorb (IOS 1518) may bind to the amphoteric, thereby keeping it in solution.

Amphoteric surfactants have been found to be very good foamers in high salinity and hardness conditions (Novosad and Ionescu, 1987). However, their extremely high adsorption level on sandstones make their application to sandstone reservoirs economically unattractive. The results of this study indicate that the restrictions placed on the use of this surfactant type by its high adsorption levels may be alleviated by mixing it with an anionic surfactant. While only one experiment has been run with a surfactant mixture and the data are thus preliminary, the results are encouraging.

The solubility study discussed above has indicated that Stepanflo 60 is more tolerant to salt solutions than IOS 1518. In order to determine if the solubility of the IOS can be improved by mixing it with Stepanflo 60, a simple solubility study was carried out. A 3:7 w/w Stepanflo 60 : IOS 1518 mixture was prepared in brines containing from 2 to 10% w/w NaCl. The surfactant mixture was soluble only up to 2% NaCl. Reversing the mixture composition to 7:3 w/w Stepanflo 60 : IOS 1518 gave the same results. Comparison of these results with Table 4 indicates that the solubility of the mixture seems to be determined by the solubility of IOS 1518.

5. MICROCALORIMETRY

Enthalpy of adsorption was measured for three surfactants, Stepanflo 60, AOS 1416, and LXS 810 dissolved in 0.5% NaCl brine at 25°C. The enthalpies accompanying adsorption of these surfactants on Berea sandstone expressed in units of energy per unit mass of the adsorbent (mJ/g) are shown in Table 9 and in Figure 37. Adsorption of these surfactants is an exothermic process.

It can be seen from Figure 37 that the enthalpy change is minimal for AOS 1416 and LXS 810 surfactants while the enthalpy change accompanying adsorption of the Stepanflo 60 is almost four times larger. The order of these enthalpy changes is consistent with the relative adsorption of these surfactants as the Stepanflo 60 adsorbs more than the other two surfactants.

SUMMARY AND CONCLUSIONS

On the basis of a solubility study, four surfactants of the type used in steam-foam applications were selected for adsorption testing: Enordet AOS 1416, Enordet IOS 1518, Enordet LXS 810, and Stepanflo 60. The first three are anionic and are low molecular weight representatives of surfactant types used in steam flooding, while the fourth one is an amphoteric that has also been suggested for steam-foam applications.

Adsorption was measured dynamically as a function of temperature or salinity by performing single-phase displacement experiments in Berea sandstone. Effluent profiles of surfactant and tracer were modelled with the surface excess model for flow of adsorbing chemicals in porous media, which allowed calculation of adsorption isotherms from the model parameters. The results of the adsorption study are summarized in Figure 38. The main conclusions are as follows:

1. AOS 1416 and IOS 1518 do not adsorb from a low salinity (0.5% NaCl) brine at 23°C, but adsorption of both surfactants increases with increasing salinity and increasing divalent ion content of the brine.

2. At 23°C, LXS 810 at a concentration of 10 g/l (1%) in 0.5% NaCl is very close to its solubility limit. Ion exchange of calcium between the clays and surfactant micelles and/or dissolution of small amounts of calcite from Berea rock cause this surfactant to precipitate during core flooding. The measured surfactant loss is thus a combination of adsorption and precipitaion. The flow pattern through the rock is changed by the precipitated surfactant. At 75°C, precipitation is eliminated. Surfactant loss is due to adsorption alone, and is low.

3. The amphoteric surfactant, Stepanflo 60, adsorbs much more strongly on sandstone than the anionics. Its adsorption is weakly dependent on temperature. While this surfactant is extremely tolerant to high salinity brines, its high adsorption level puts severe economic restrictions on its application in sandstone reservoirs.

4. Adsorption of Stepanflo 60 can be reduced significantly by mixing it with IOS 1518, making foam applications with amphoteric surfactants in sandstone reservoirs economically more attractive.

5. Data such as those in Figure 38 can be used in selecting a surfactant for a specific reservoir. The injected fluids in a steam-foam application may encounter both salinity and temperature gradients, and the dependence of surfactant adsorption on both must be taken into account.

6. Enthalpy of adsorption determined microcalorimetrically trends consistently with the maxima in adsorption isotherms for three types of surfactants studied.

The following recommendations can be made for further studies in the area of enhancement of surfactant propagation in steam-foam applications. In this work, adsorption of low molecular weight representatives of classes of surfactants that have been suggested for steam flooding has been measured and compared. The study should be extended to higher molecular weight surfactants of the same chemical classes, since these are more likely to be used in steam flooding. The limited solubility of the higher molecular weight surfactants would require the use of high temperatures normally encountered in steam flooding.

A direct measurement of solid/surfactant solution interactions through microcalorimetric measurements of adsorption enthalpies seems to be a promising method for screening of surfactants in terms of their adsorption at the solid/liquid interface. This technique should be further pursued.

The potential of reducing surfactant adsorption by formulating surfactant mixtures has been demonstrated in this study. Further studies in this area, using not only steam-foamers but foam-forming surfactants in general, may prove useful both from a scientific and an economic point of view.

ACKNOWLEDGEMENTS

The following persons are thanked for their valuable contributions to this work: Roy Woo for writing the data acquisition program for the microcalorimeter, Audrey Cameron, Paul Stanislav, and Hisham Nasr-El-Din for their help with the atomic absorption analyses, and Mary Chan for her assistance in developing the analytical technique in Appendix A.

REFERENCES

Al-Khafaji, A.H., Wang, P.-T. F., Castanier, L.M., Brigham, W.E., Steam Surfactant Systems at Reservoir Conditions, SPE #10777, California Regional Meeting of the Society of Petroleum Engineers, San Francisco, CA, March 24-26 (1982).

Angstadt, H.P., Salt-Tolerant Alkyl Aryl Sulfonate Compositions for Use in Enhanced Oil Recovery Processes, United States Patent 4,699,214 (1987).

Angstadt, H.P., Tsao, H., Kinetic Study of the Decomposition of Surfactants for EOR, SPE Reservoir Engineering 2(4), 613-618 (1987).

Balzer, D., Phase Behaviour, Core Flooding and Retention Studies of Caboxymethylated Ethoxylates Blended with Sulfonates, Proc. 4th European Symposium on Enhanced Oil Recovery, p.155-169, Hamburg, West Germany, Oct. 27-29 (1987).

Bavière, M., Bazin, B., Noïk, C., Surfactants for EOR: Olefin Sulfonate Behavior at High Temperature and Hardness, SPE Reservoir Engineering 3(2), 597-603 (1988).

Byth, N.J., Thompson, J.L., Surfactant Compositions Useful in Enhanced Oil Recovery Processes, Canadian Patent 1 146 834 (1983).

Castanier, L.M., Brigham, W.E., An Evaluation of Field Projects of Steam with Additives, SPE #17633, SPE International Meeting on Petroleum Engineering, Tianjin, China, Nov. 1-4 (1988).

Chattoraj, D.K., Birdi, K.S., Adsorption and the Gibbs Surface Excess, Plenum Press, New York (1984).

Clark, P.E., Discussion of Thermal Stability of Surfactants for Reservoir Application, Soc. Petrol. Eng. J. 22(6), 905-908 (1982).

Coats, K.H., Smith, B.D., Dead-End Pore Volume and Dispersion in Porous Media, Soc. Petrol. Eng. J. 4(1), 73-84 (1964).

Dawe, B., Oswald, T., Reduced Adsorption and Separation of Blended Surfactants on Sand and Clay, CIM Paper #89-40-28, 40th Annual Technical Meeting of the Petroleum Society of CIM, Banff, Alberta, May 28-31 (1989).

Dilgren, R.E., Deemer, A.R., Owens, K.B., The Laboratory Development and Field Testing of Steam/Noncondensible Gas Foams for Mobility Control in Heavy Oil Recovery, SPE #10774, California Regional Meeting of the Society of Petroleum Engineers, San Francisco, CA, March 24-26 (1982).

Dilgren, R.E., Owens, K.B., Surfactant-Enhanced Steam Drives for Heavy Oil Recovery, J. Amer. Oil Chem. Soc. 59(10), 818A-822A (1982).

Dilgren, R.E., Owens, K.B., Steam-Foaming Surfactant Mixtures which are Tolerant of Divalent Ions, Canadian Patent 1 259 475 (1989).

Djabbarah, N.F., Sweep Improvement in Enhanced Oil Recovery, Canadian Patent 1 221 305 (1987).

Djabbarah, N.F., Weber, S.L., Freeman, D.C., Muscatello, J.A., Ashbaugh, J.P., Covington, T.E., Laboratory Design and Field Demonstration of Steam Diversion with Foam, SPE #20067, 60th SPE California Regional Meeting, Ventura, CA, April 4-6 (1990).

Donaldson, E.C., Kendall, R.F., Baker, B.A., Manning, F.S., Surface Area Measurement of Geologic Materials, Soc. Petrol. Eng. J. 15(2), 111-116 (1975).

Duerksen, J.H., Laboratory Study of Foaming Surfactants as Steam-Diverting Additives, SPE #12785, SPE California Regional Meeting, Long Beach, CA, April 11-13 (1984).

EOR Chemicals Overview: Wide Variety of Chemicals Available for Enhanced Recovery, Petroleum Engineer International 61(5), 42-48 (May 1989).

Eson, R.L., Cooke, R.W., A Comprehensive Analysis of Steam Foam Diverters and Application Methods, SPE #18785, SPE California Regional Meeting, Bakersfield, CA, April 5-7 (1989).

Franses, E.I., Davis, H.T., Miller, W.G., Scriven, L.E., Phase Behavior of a Pure Alkyl Aryl Sulfonate Surfactant, Chemistry of Oil Recovery, R.T. Johansen, R.L. Berg (Eds.), ACS Symposium Series No. 91, p. 35-74, American Chemical Society (1979).

Friedmann, F., Chen, W.H., Gauglitz, P.A., Experimental and Simulation Study of High-Temperature Foam Displacement in Porous Media, SPE/DOE #17357, SPE/DOE Enhanced Oil Recovery Symposium, Tulsa, OK, April 17-20 (1988).

Green, M.K., Isaacs, E.E., Laboratory Investigation of the Use of Foam-Forming Surfactants during Steam Injection, AOSTRA Journal of Research 4, 133-142 (1988).

Hamida, F.M., Demiral, B.M.R., Shallcross, D.C., Castanier, L.M., Brigham, W.E., Further Characterization of Surfactants as Steamflood Additives, SPE #20065, 60th SPE California Regional Meeting, Ventura, CA, April 4-6 (1990).

Handy, L.L., Amaefule, J.O., Ziegler, V.M., Ershaghi, I., Thermal Stability of Surfactants for Reservoir Application, Soc. Petrol. Eng. J. 22(5), 722-730 (1982a).

Handy, L.L., Amaefule, J.O., Ziegler, V.M., Ershagi, I., Authors' Reply to Discussion of Thermal Stability of Surfactants for Reservoir Application, Soc. Petrol. Eng. J. 22(6), 909-909 (1982b).

Harwell, J.H., Schechter, R.S., Wade, W.H., Surfactant Chromatographic Movement: An Experimental Study, AIChE J. 31(3), 415-427 (1985).

Hirasaki, G.J., Ion Exchange with Clays in the Presence of Surfactant, Soc. Petrol. Eng. J. 22(2), 181-192 (1982).

Hirasaki, G.J., Lawson, J.B., An Electrostatic Approach to the Association of Sodium and Calcium with Surfactant Micelles, SPE #10921, 57th Annual Fall

Technical Conference and Exhibition of the Society of Petroleum Engineers of AIME, New Orleans, LA, Sept. 26-29 (1982).

Hirasaki, G.J., The Steam-Foam Process, J. Petrol. Tech. 41(5), 449-456 (1989).

Isaacs, E.E., McCarthy, C., Smolek, K.F., Application of Surfactants at High Temperatures to the Recovery of Bitumen from Oil Sands, Proc. 2nd European Symposium on Enhanced Oil Recovery, p. 549-563, Paris, France, Nov. 8-10 (1982).

Isaacs, E.E., McCarthy, F.C., Maunder, J.D., Investigation of Foam Stability in Porous Media at Elevated Temperatures, SPE Reservoir Engineering 3(2), 565-572 (1988).

Lau, H.C., O'Brien, S.M., Effects of Spreading and Nonspreading Oils on Foam Propagation through Porous Media, SPE Reservoir Engineering 3(3), 893-896 (1988a).

Lau, H.C., O'Brien, S.M., Surfactant Transport through Porous Media in Steam Foam Processes, SPE Reservoir Engineering 3(4), 1177-1185 (1988b).

Lau, H.C., Borchardt, J.K., Improved Steam Foam Formulations: Concepts and Laboratory Results, SPE #18783, SPE California Regional Meeting, Bakersfield, CA, April 5-7 (1989).

Lim, T., Surfactant Compositions for Steamfloods, World Patent WO 85/05146 (1985).

Maini, B.B., Ma, V., Relationship between Foam Stability Measured in Static Tests and Flow Behavior of Foams in Porous Media, SPE #13073, 59th Annual Technical Conference and Exhibition of the Society of Petroleum Engineers, Houston, TX, Sept. 16-19 (1984).

Maini, B.B., Laboratory Evaluation of Foaming Agents for High Temperature Applications - III. Effect of Residual Oil on Mobility Reduction Performance, CIM Paper #86-37-01, 37th Annual Technical Meeting of the Petroleum Society of CIM, Calgary, Alberta, June 8-11 (1986).

Maini, B.B., Ma, V., Laboratory Evaluation of Foaming Agents for High-Temperature Applications - I. Measurements of Foam Stability at Elevated Temperatures and Pressures, J. Can. Petrol. Tech. 25(6), 65-69 (1986).

Manlowe, D.J., Radke, C.J., A Pore Level Investigation of Foam/Oil Interactions in Porous Media, SPE #18069, 63rd Annual Technical Conference and Exhibition of the Society of Petroleum Engineers, Houston, TX, Oct. 2-5 (1988).

Mannhardt, K., Novosad, J.J., Modelling Adsorption of Foam-Forming Surfactants, Rev. Inst. Français Pétrole 43(5), 659-671 (1988).

Mannhardt, K., Schramm, L.L., Novosad, J.J., Effect of Rock Type and Brine Composition on Adsorption of Two Foam-Forming Surfactants, SPE #20463, 65th Annual Technical Conference and Exhibition of the Society of Petroleum Engineers, New Orleans, LA, Sept. 23-26 (1990).

Mannhardt, K., Novosad, J.J. Chromatographic Movemant of Surfactant Mixtures in Porous Media, Chem. Eng. Sci. 46(1), 75-83 (1991a).

Mannhardt, K., Novosad, J.J., Chromatographic Effects in Flow of a Surfactant Mixture in a Porous Sandstone, in press, J. Petrol. Sci. Eng. (1991b).

Marriott, R.C., Kao, C.I., Kristal, F.W., Kinetic Study of Desulfonation of Disulfonated Alkyl Diphenyloxide Surfactants, Soc. Petrol. Eng. J. 22(6), 993-997 (1982).

Marsden, S.S., Foams in Porous Media, U.S. Dept. of Energy DOE/SF/11564-15, (DE86 000290) (1986).

McClellan, A.L., Harnsberger, H.F., Cross-Sectional Areas of Molecules Adsorbed on Solid Surfaces, J. Colloid Interface Science 23, 577-599 (1967).

Miller, C.A., Neogi, P., Surfactants, Interfacial Phenomena, Equilibrium and Dynamic Effects, Ch. 4, p.140-183, Marcel Dekker, New York (1985).

Muijs, H.M., Keijzer, P.P.M., Wiersma, R.J., Surfactants for Mobility Control in High-Temperature Steam-Foam Applications, SPE/DOE #17361, SPE/DOE Enhanced Oil Recovery Symposium, Tulsa, OK, April 17-20 (1988).

Mukerjee, P., Mysels, K.J., Critical Micelle Concentrations of Aqueous Surfactant Systems, U.S. Dept. of Commerce, National Bureau of Standards NSRDS-NBS 36 (1970).

Nikolov, A.D., Wasan, D.T, Huang, D.W., Edwards, D.A., The Effect of Oil on Foam Stability: Mechanisms and Implications for Oil Displacement by Foam in Porous Media, SPE #15443, 61st Annual Technical Conference and Exhibition of the Society of Petroleum Engineers, New Orleans, LA, Oct. 5-8 (1986).

Novosad, J., Experimental Study and Interpretation of Surfactant Retention in Porous Media, Proceedings, European Symposium on Enhanced Oil Recovery, p. 101-121, Bournemouth, England, September 21-23 (1981).

Novosad, J., Maini, B.B., Huang, A., Retention of Foam-Forming Surfactants at Elevated Temperatures, J. Can. Petrol. Tech. 25(3), 42-46 (1986).

Novosad, J.J., Ionescu, E.F., Foam Forming Surfactants for Beaverhill Lake Carbonates and Gilwood Sands Reservoirs, CIM Paper #87-38-80, 38th Annual Technical Meeting of the Petroleum Society of CIM, Calgary, Alberta, June 7-10 (1987).

Novosad, J.J., Mannhardt, K., Rendall, A., The Interaction between Foam and Crude Oils, CIM Paper #89-40-29, 40th Annual Technical Meeting of the Petroleum Society of CIM, Banff, Alberta, May 28-31 (1989).

Owete, O.S., Al-Khafaji, A., Sanyal, S.K., Castanier, L., Brigham, W.E., Foam as a Mobility Control Agent in Steam Injection Processes - Temperature Stability of Foaming Agents: Application to Improved Steam Injection, SPE #8912-B, 50th Annual California Regional Meeting of the Society of Petroleum Engineers of AIME, Los Angeles, CA, April 9-11 (1980).

Raterman, K.T., An Investigation of Oil Destabilization of Nitrogen Foams in Porous Media, SPE #19692, 64th Annual Technical Conference and Exhibition of the Society of Petroleum Engineers, San Antonio, TX, Oct. 8-11 (1989).

Reid, V.W., Longman, G.F., Heinerth, E., Determination of Anionic-Active Detergents by Two-Phase Titration, Tenside 4(9), 292-304 (1967).

Robin, M., Demay, C., Process for Improving the Gas Sweeping of an Oil Formation, Using Foams Mainly Containing Surfactants with Perfluoric Groups, U.S. Patent 4,836,281 (1989).

Rosen, M.J., Surfactants and Interfacial Phenomena, John Wiley & Sons, New York (1978).

Scamehorn, J.F., Schechter, R.S., Wade, W.H., Adsorption of Surfactants on Mineral Oxide Surfaces from Aqueous Solutions. II. Binary Mixtures of Anionic Surfactants, J. Colloid Interface Science 85(2), 479-493 (1982a).

Scamehorn, J.F., Schechter, R.S., Wade, W.H., Adsorption of Surfactants on Mineral Oxide Surfaces from Aqueous Solutions. III. Binary Mixtures of Anionic and Nonionic Surfactants, J. Colloid Interface Science 85(2), 494-501 (1982b).

Scharer, D.H., Bright, D.B., Merrill, C.L., Shankar, P.K., Bolsman, T.A.B.M., Olefin Sulfonates in Crude Oil Production, Amer. Oil Chemists' Soc. 76th Annual Meeting (Symposium on Olefin Sulfonates - Versatile Surfactants for Household and Industry), Philadelphia, PA, May 8 (1985).

Schramm, L.L., Hodgins, L., Mannhardt, K., An Analytical Method for Amphoteric Betaine Surfactants, Petroleum Recovery Institute Internal Document (1989).

Schramm, L.L., Novosad, J.J., Micro-Visualization of Foam Interactions with a Crude Oil, Colloids & Surfaces 46, 21-43 (1990).

Schramm, L.L., Turta, A.T., Novosad, J.J., Microvisual and Coreflood Studies of Foam Interactions with a Light Crude Oil, SPE/DOE #20197, SPE/DOE 7th Symposium on Enhanced Oil Recovery, Tulsa, OK, April 22-25 (1990).

Shinoda, K., The Formation of Micelles, Colloidal Surfactants, K. Shinoda, T. Nakagawa, B.-I. Tamamushi, T. Isemura (Eds.), Ch. 1, p. 1-96, Academic Press, New York (1963).

Sircar, S., Novosad, J., Myers, A.L., Adsorption from Liquid Mixtures on Solids: Thermodynamics of Excess Properties and their Temperature Coefficients, Ind. Eng. Chem. Fundam. 11, 249-254 (1972).

Somasundaran, P., Celik, M., Goyal, A., Manev, E., The Role of Surfactant Precipitation and Redissolution in the Adsorption of Sulfonate on Minerals, Soc. Petrol. Eng. J. 24(2), 233-239 (1984a).

Somasundaran, P., Middleton, R., Viswanathan, K.V., Relationship between Surfactant Structure and Adsorption, Structure/Performance Relationships in Surfactants, M.J. Rosen (Ed.), ACS Symposium Series 253, American Chemical Society, Washington, D.C. (1984b).

Somasundaran, P., Hanna, H.S., Adsorption/Desorption of Sulfonates by Reservoir Rock Minerals in Solutions of Varying Sulfonate Concentrations, Soc. Petrol. Eng. J. 25(3), 343-350 (1985).

Somasundaran, P., Adsorption from Flooding Solutions in Porous Media, U.S. Dept. of Energy DOE/BC/10848-10 (DE88 001217) (1988).

Somasundaran, P., Adsorption from Flooding Solutions in Porous Media. A Study of Interactions of Surfactants and Polymers with Reservoir Minerals, U.S. Dept. of Energy DOE/BC/10848-15 (DE98000733) (1989).

Strycker, A.R., Madden, M.P., Sarathi, P., Effectiveness of Screening Tests as Predictive Models for Steamflood Additives, SPE Reservoir Engineering 2(4), 543-548 (1987).

Trogus, F.J., Schechter, R.S., Wade, W.H., A New Interpretation of Adsorption Maxima and Minima, J. Colloid Interface Science 70(2), 293-305 (1979).

Ziegler, V.M., Handy, L.L., Effect of Temperature on Surfactant Adsorption in Porous Media, Soc. Petrol. Eng. J. 21(2), 218-228 (1981).

TABLE 1. Core and displacement data.

Core ID	CM-2	CM-9	CM-12	CM-3	CM-10	CM-11	CM-4	CM-13	CM-8	CM-6	CM-7	CM-14
Surfactant	AOS 1416	AOS 1416	AOS 1416	IOS 1518	IOS 1518	IOS 1518	LXS 810	LXS 810	LXS 810	Step 60	Step 60	IOS 1518/ Step 60
Brine	0.5% NaCl	2.32% NaCl	2.27% TDS	0.5% NaCl	2.32% NaCl	2.27% TDS	0.5% NaCl	0.5% NaCl	0.5% NaCl	0.5% NaCl	0.5% NaCl	0.5% NaCl
Temp. (^{o}C)	23	23	23	23	23	23	23	23	75	23	75	23
Length (cm)	9.86	10.12	9.34	9.72	9.75	9.67	9.98	9.44	9.65	9.90	9.65	10.17
Cross-section (cm^2)	11.22	11.20	11.18	11.21	11.17	11.20	11.24	11.20	11.23	11.21	11.22	11.21
Pore vol. (ml)	24.9	25.9	24.4	26.5	23.6	23.6	25.1	24.2	25.1	26.1	23.6	24.8
Porosity (frac.)	0.225	0.228	0.234	0.243	0.216	0.218	0.224	0.229	0.232	0.235	0.218	0.218
Dry weight (g)	232.45	239.02	220.52	228.48	229.90	228.35	234.59	222.60	227.26	233.45	228.14	240.38
Abs. perm. (md)												
air	588	465	488	592	508	482	540	488	484	478	517	467
brine	220	188	245	251	237	199	223	188	183	177	219	190
Injected surfac. conc. (g/l)	10.015	10.009	10.045	10.432	10.105	10.010	10.025	10.017	10.016	10.005	10.011	10.024*
Slug vol. (ml)	50.2	49.4	48.5	52.4	49.8	45.6	50.9	47.9	50.0	49.8	47.6	49.5
(PV)	2.02	1.91	1.98	1.98	2.11	1.93	2.03	1.98	1.99	1.91	2.02	1.99
Flow rate (ml/h)	1.98	2.02	1.96	2.00	2.05	1.98	2.02	1.99	2.01	1.97	1.96	2.00

* 3.015 g/l Step 60, 7.009 g/l IOS 1518

TABLE 2(a). Properties of brines used in core floods.

	23°C		75°C		
	Density (g/ml)	Viscosity (cp)	Density (g/ml)	Viscosity (cp)	pH
0.50% w/w NaCl	1.002	0.952	0.979	0.385	7.0
2.32% w/w NaCl	1.015	0.964	—	—	7.0
2.274% w/w TDS (2.192% w/w NaCl, 0.082% w/w $CaCl_2$)	1.014	0.985	—	—	6.4

TABLE 2(b). Composition of mixed brines used in surfactant solubility tests. Ionic strength = 0.403 mol/l (= ionic strength of 2.32% NaCl)

NaCl (g/l)	$CaCl_2$ (g/l)	TDS (% w/v)	Ca^{2+} (mol/l)	Ca^{2+} (ppm)	Na^+ (mol/l)	Na^+ (ppm)	
20.040	2.220	2.226	0.0200	800	0.3429	7880	
21.793	1.110	2.290	0.0100	400	0.3729	8570	
22.232	0.832	2.306	0.0075	300	0.3804	8750	(*)
22.670	0.555	2.322	0.0050	200	0.3879	8920	

(*) This is the 2.274% w/w TDS brine in Table 2(a).

TABLE 3. Surfactants.

Trade Name	Chemical Class	Active conc. (%)	Molec. wt. (g/mol)	pH[3] (1% solution)
Enordet AOS 1416 (Shell Chemical)	C_{14-16} alpha olefin sulfonate	39.0	325[1]	7.1
Enordet AOS 1618 (Shell Chemical)	C_{16-18} alpha olefin sulfonate	29.5	356[1]	—
Enordet IOS 1518 (Shell Chemical)	C_{15-18} internal olefin sulfonate	25.2	339[1]	9.0
Enordet LTS 1618 (Shell Chemical)	C_{16-18} linear toluene sulfonate	15.2	422[1]	—
Enordet LXS 810 (Shell Chemical)	C_{8-10} linear xylene sulfonate	20.2	334[1]	9.4
Enordet LXS 1314 (Shell Chemical)	C_{13-14} linear xylene sulfonate	19.5	397[1]	—
Stepanflo 60 (Stepan Company)	Alkylamido-betaine of coconut oil	30.0	400[2]	3.5

(1) Specified by manufacturer.

(2) Estimated from synthetic route supplied by manufacturer.

(3) Average pH of solutions prepared for core floods.

TABLE 4. Surfactant solubility as a function of NaCl concentration. Surfactant concentration is about 1% w/w. The listed temperatures are the temperatures at which the surfactant dissolved.
ns = not soluble at indicated temperature.

(a) Enordet AOS 1618

NaCl (% w/w)	Surfactant conc. (% w/w)	Temp. (°C)
0.0	1.00	23
0.2	1.02	27
0.5	1.00	30
1.0	0.90	32
2.0	0.80	32
5.0	1.00	34

(b) Enordet AOS 1416

NaCl (% w/w)	Surfactant conc. (% w/w)	Temp. (°C)
0.0	0.99	23
0.2	1.01	23
0.5	1.02	23
1.0	1.01	23
2.0	1.02	23
5.0	1.04	23

(c) Enordet IOS 1518

NaCl (% w/w)	Surfactant conc. (% w/w)	Temp. (°C)
0.0	1.00	23
0.5	1.01	23
1.0	1.00	23
2.0	1.01	23
5.0	1.01	49

(d) Enordet LTS 1618

NaCl (% w/w)	Surfactant conc. (% w/w)	Temp. (°C)
0.0	1.00	49
0.5	1.01	83 ns
1.0	0.99	83 ns
2.0	1.00	83 ns
5.0	1.00	83 ns

(e) Enordet LXS 1314

NaCl (% w/w)	Surfactant conc. (% w/w)	Temp. (°C)
0.0	1.01	23
0.2	1.01	80
0.5	1.01	135 ns

(f) Enordet LXS 810

NaCl (% w/w)	Surfactant conc. (% w/w)	Temp. (°C)
0.0	0.95	23
0.2	1.03	23
0.5	1.03	23
1.0	1.03	52
2.0	0.93	83 ns
5.0	0.91	83 ns

(g) Stepanflo 60

NaCl (% w/w)	Surfactant conc. (% w/w)	Temp. (°C)
0.0	1.03	23
0.5	0.99	23
1.0	1.00	23
2.0	1.03	23
5.0	0.96	23

TABLE 5. Surfactant solubility as a function of surfactant concentration. Brine: 0.5% w/w NaCl. The listed temperatures are the temperatures at which the surfactant dissolved.
ns = not soluble at indicated temperature.

(a) Enordet AOS 1618

Surfactant conc. (% w/w)	Temp. (°C)
0.014	26
0.081	27
0.092	27
0.47	27
1.00	30
1.89	33
2.99	33
5.01	33

(b) Enordet AOS 1416

Surfactant conc. (% w/w)	Temp. (°C)
0.013	23
0.073	23
0.12	23
0.49	23
0.99	23
2.00	23
4.97	23

(c) Enordet IOS 1518

Surfactant conc. (% w/w)	Temp. (°C)
1.01	23
4.98	23

(d) Enordet LTS 1618

Surfactant conc. (% w/w)	Temp. (°C)
0.014	113
0.046	135 ns
0.11	135 ns

(e) Enordet LXS 1314

Surfactant conc. (% w/w)	Temp. (°C)
0.010	90
0.068	135 ns
0.12	135 ns

(f) Enordet LXS 810

Surfactant conc. (% w/w)	Temp. (°C)
0.014	23
0.041	23
0.11	23
0.51	23
1.00	23
2.03	27
5.02	41

(g) Stepanflo 60

Surfactant conc. (% w/w)	Temp. (°C)
0.99	23
4.98	23

TABLE 6. Effect of calcium ion on solubility of IOS 1518 and AOS 1416. Brines contain NaCl and $CaCl_2$ at different ratios but constant ionic strength. Surfactant concentration: 1% w/w, temperature: 23°C.

Ca^{2+} conc. (mol/l)	Na^{+} conc. (mol/l)	Ionic strength (mol/l)	TDS (% w/v)	Observations IOS	AOS
0.0200	0.3429	0.403	2.226	ns	ns
0.0100	0.3729	0.403	2.290	ns	s
0.0075(1)	0.3804	0.403	2.306	ns, s overnight(2)	s
0.0050	0.3879	0.403	2.322	s	s

ns = not soluble, cloudy
s = soluble, clear solution

(1) This brine is 2.27% w/w, and is the brine used in the adsorption experiments.

(2) IOS 1518 dissolved in this brine after standing overnight.

TABLE 7. Data from surface tension measurements, 23°C.

Surfactant	Brine	cmc (g/l)	Surface excess (10^{-10} mol/cm^2)	Molec. area (Å^2)	Avg. surface tension above cmc (dyne/cm)
AOS 1416	0.5% NaCl	0.044	3.96	42	30.7
AOS 1416	2.32% NaCl	0.028	4.16	40	28.5
AOS 1416	2.27% TDS	0.029	4.37	38	29.2
IOS 1518	0.5% NaCl	0.054	2.81	59	29.9
IOS 1518	2.32% NaCl	0.020	4.05	41	28.8
IOS 1518	2.27% TDS	0.016	4.09	41	28.8
LXS 810	0.5% NaCl	0.38	3.17	52	28.5
Step 60	0.5% NaCl	0.026	6.04	27	31.5
IOS 1518/ Step 60 0.72/0.30 w/w)	0.5% NaCl	0.050	4.57	36	29.2

TABLE 8. Adsorption data from material balance calculations and flow model parameters.

Core ID	CM-2	CM-9	CM-12	CM-3	CM-10	CM-11	CM-4	CM-13	CM-8	CM-6	CM-7	CM-14
Surfactant	AOS 1416	AOS 1416	AOS 1416	IOS 1518	IOS 1518	IOS 1518	LXS 810	LXS 810 (repeat)	LXS 810	Step 60	Step 60	IOS 1518/ Step 60 *
Brine	0.5% NaCl	2.32% NaCl	2.27% TDS	0.5% NaCl	2.32% NaCl	2.27% TDS	0.5% NaCl	0.5% NaCl	0.5% NaCl	0.5% NaCl	0.5% NaCl	0.5% NaCl
Temp. (^{o}C)	23	23	23	23	23	23	23	23	75	23	75	23
Avg. effluent pH	7.9	7.8	7.4	7.8	7.9	7.3	8.0	8.3	8.4	8.0	7.8	7.9
MATERIAL BALANCE												
% tracer lost	-0.3	1.5	0.6	0.5	3.5	-0.3	2.1	-1.0	0.6	2.2	-0.03	0.5
												IOS Step
Surfac. inj. (mg)	503.53	494.44	487.18	546.64	503.23	456.46	510.27	479.81	500.80	498.25	476.52	347.0 149.2
Surfac. rec. (mg)	510.83	472.73	440.05	556.12	471.09	419.19	416.16	456.64	507.09	95.36	121.62	350.7 111.1
Surfac. lost (mg)	0.0	21.72	47.13	0.0	32.14	37.27	94.11	23.17	0.0	402.89	354.91	0.0 38.1
(mg/g)	0.0	0.09	0.21	0.0	0.14	0.16	0.40	0.10	0.0	1.73	1.56	0.0 0.16
FLOW MODEL PARAMETERS												
S		22,000	45,000		33,000	48,000	8,000	3,500	500	1.0×10^{6}	1.0×10^{6}	
m_1 (mmol/g)		0.00378	0.00398		0.00369	0.00369	0.00291	0.00291	0.00291	0.00560	0.00560	
m_2 (mmol/g)		0.0121	0.0121		0.0121	0.0121	0.0121	0.0121	0.0121	0.0121	0.0121	
k_1 (h^{-1})		0.5	0.5		1.0	0.5	0.5	0.5	0.5	0.1	0.15	
k_2 (h^{-1})		0.001	0.001		0.001	0.001	0.001	0.001	0.001	0.001	0.001	
λ (cm), surfac.		0.4	0.35		0.3	0.35	3.0	1.0	0.1	3.0	3.0	
λ (cm), tracer		0.2	0.18		0.3	0.2	0.1	0.1	0.1	0.2	0.1	
ADSORPTION PLATEAU FROM FLOW MODEL PARAMETERS												
(10^{-6} mol/g)		0.372	0.718		0.380	0.436	1.18	0.668	0.119	4.01	4.01	
(10^{-6} mol/m^2)		0.409	0.789		0.418	0.479	1.30	0.734	0.131	4.41	4.41	
(mg/g)		0.121	0.233		0.129	0.148	0.394	0.223	0.040	1.61	1.61	

* 3.015 g/l Step 60, 7.009 g/l IOS 1518

Table 9. Enthalpy of surfactant adsorption on Berea sandstone, measured by microcalorimetry. Surfactant concentration 0.5%, 0.5% NaCl, 25°C.

Surfactant	Enthalpy (mJ/g)
AOS 1416	22
LXS 810	21
Stepanflo 60	72

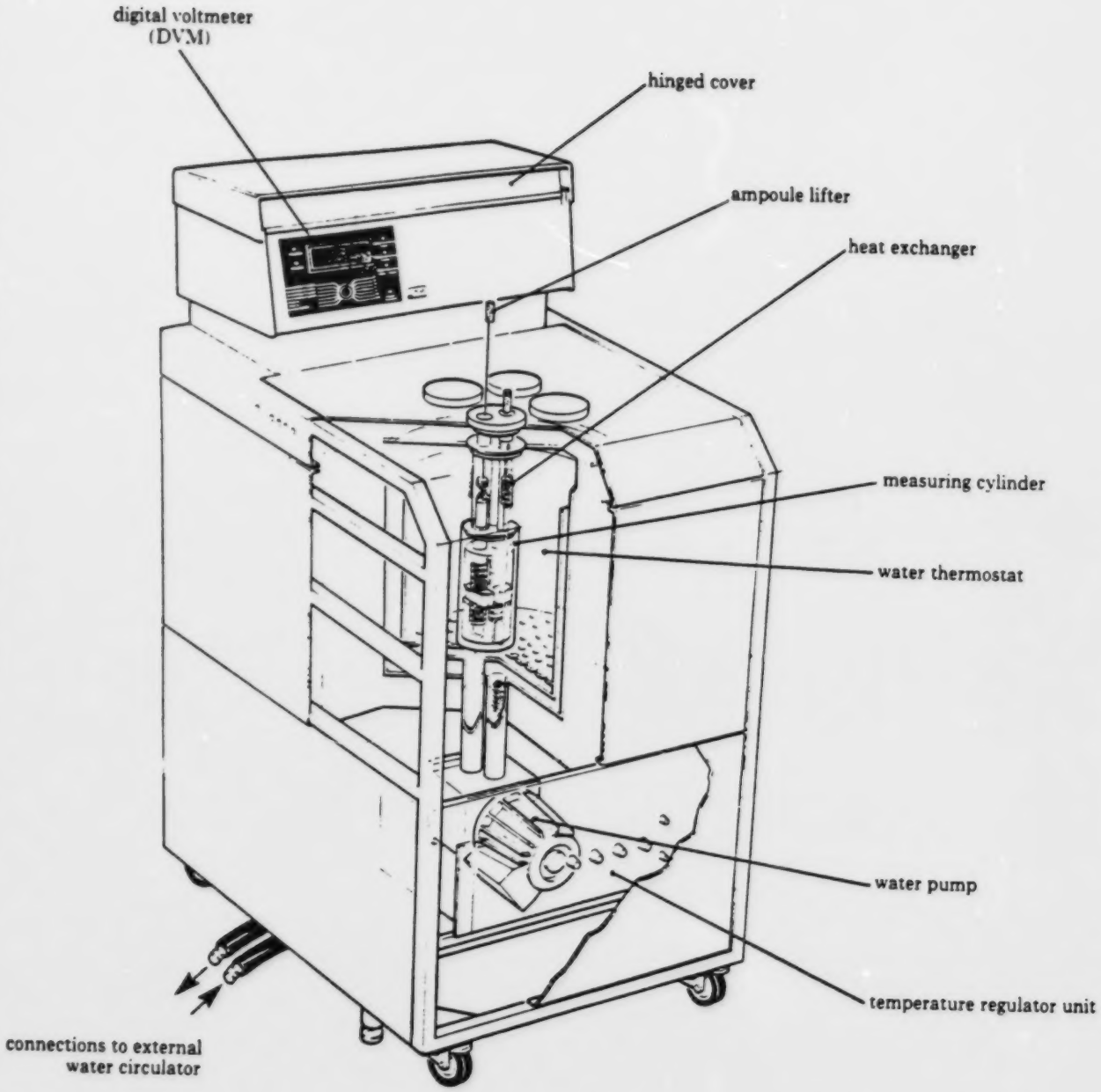

Figure 1.

Thermal activity monitor (from instrument manual).

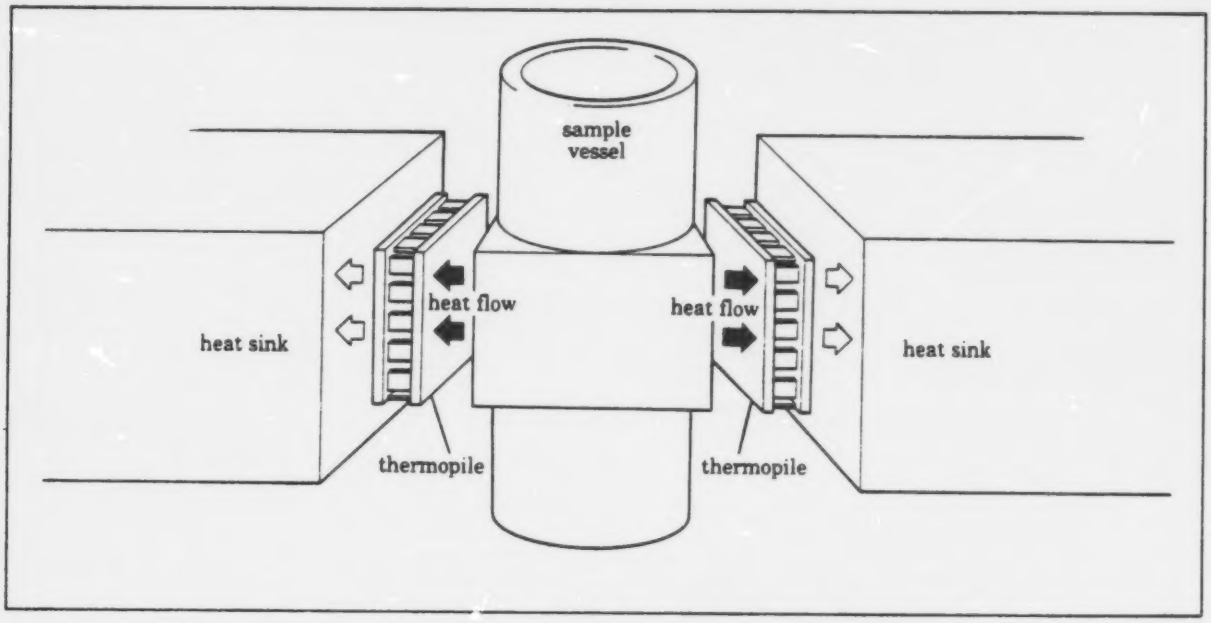

Figure 2.

The heat flow principle (from instrument manual).

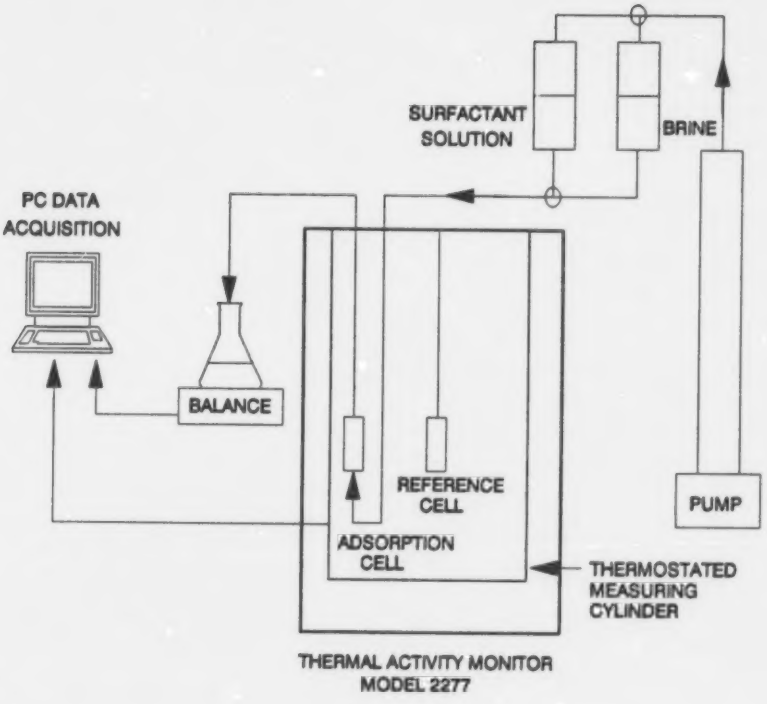

Figure 3.

Schematic of experimental setup for microcalorimetry.

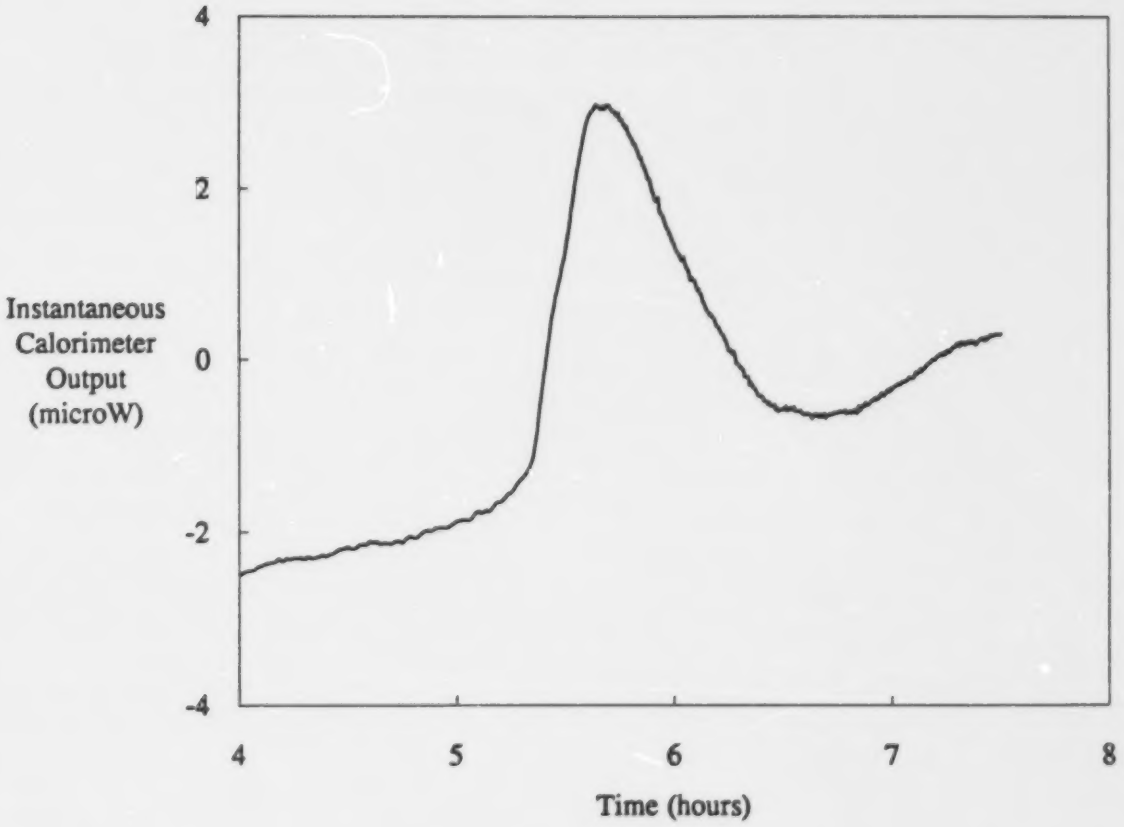

Figure 4.

Power output from microcalorimeter during adsorption of 0.5% AOS 1416 on Berea sandstone. 0.5% NaCl, 25 C.

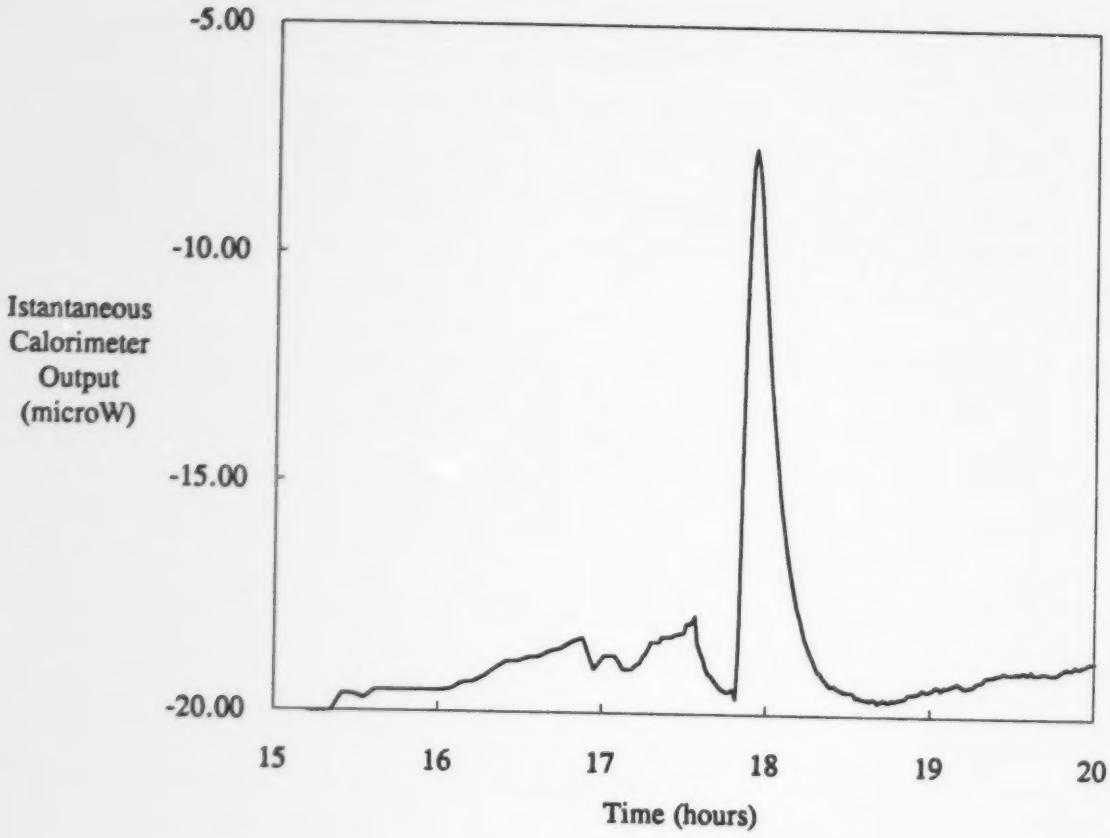

Figure 5.

Power output from microcalorimeter during adsorption of 0.5% LXS 810 on Berea sandstone. 0.5% NaCl, 25 C.

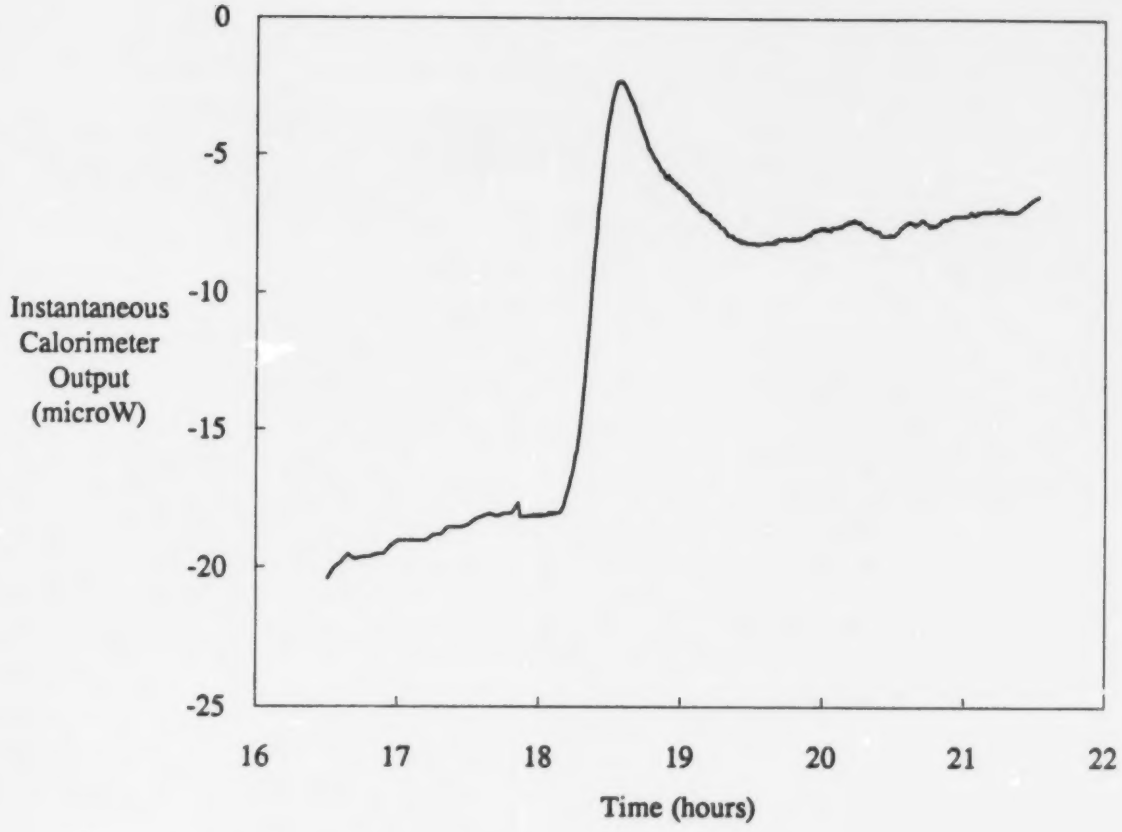

Figure 6.

Power output from microcalorimeter during adsorption of 0.5% Stepanflo 60 on Berea sandstone. 0.5% NaCl, 25 C.

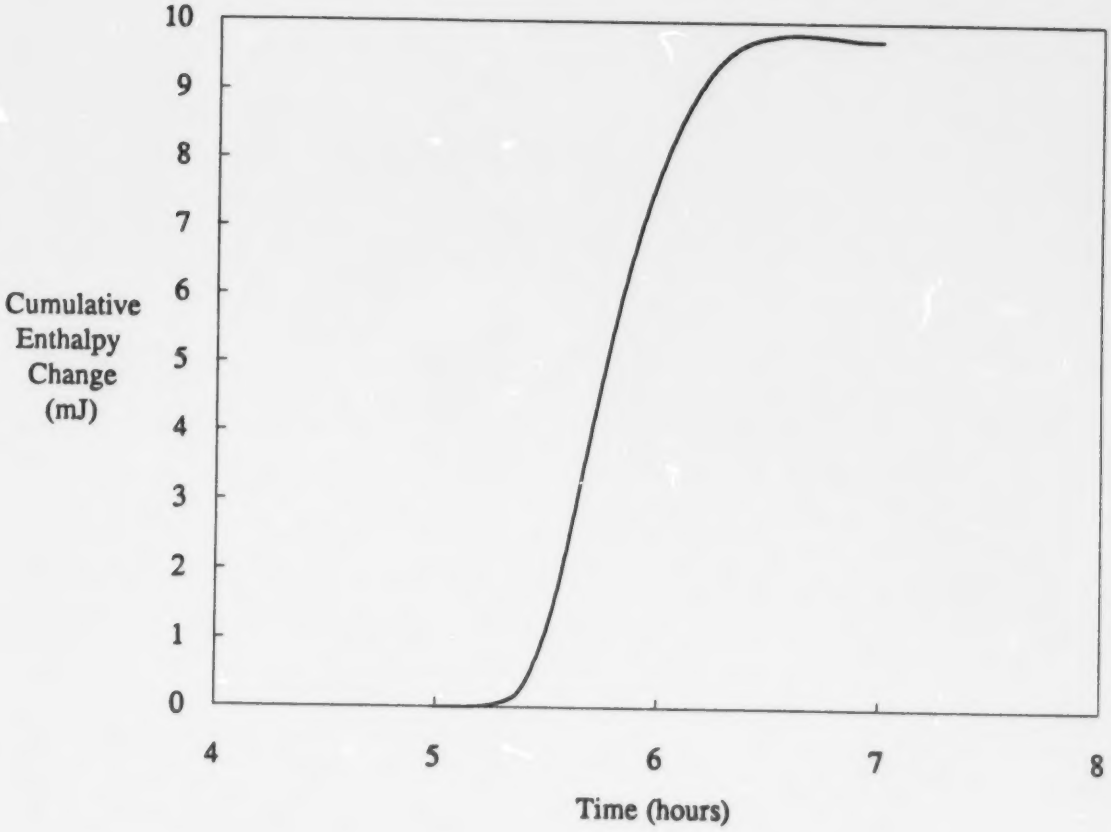

Figure 7.

Enthalpy of adsorption of 0.5% AOS 1416 on Berea sandstone, 0.5% NaCl, 25 C.

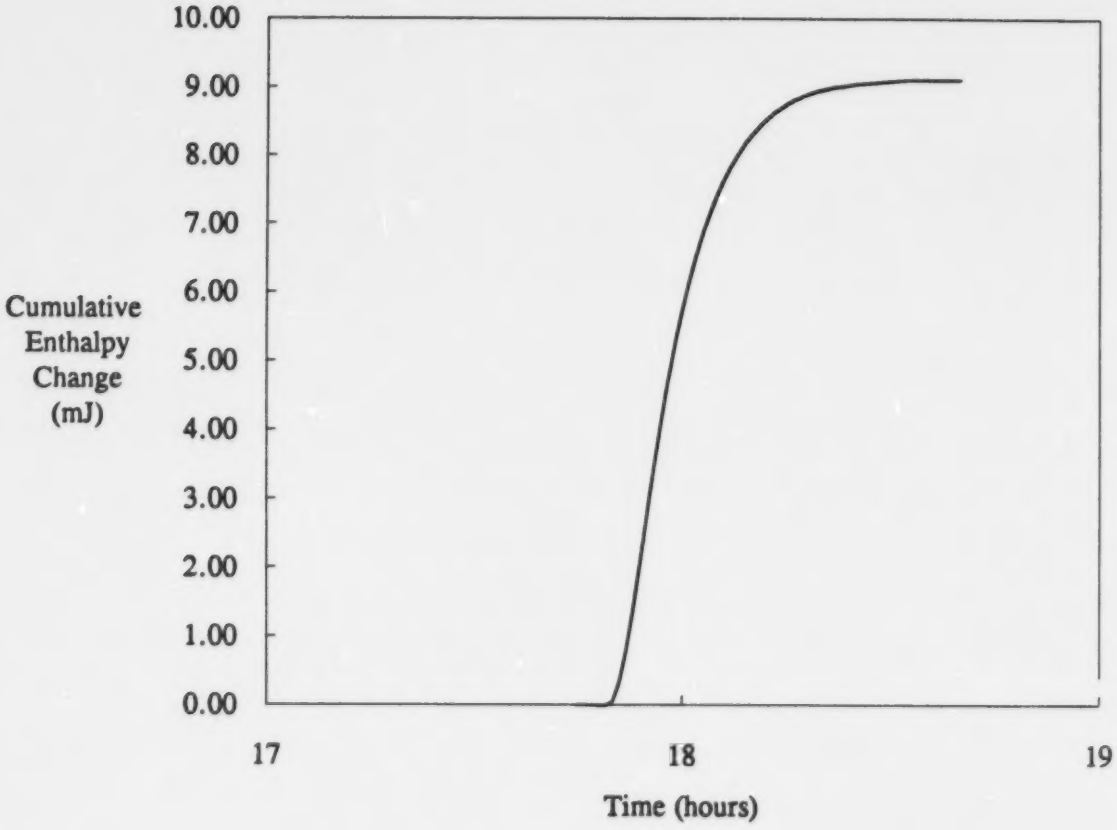

Figure 8.

Enthalpy of adsorption of 0.5% LXS 810 on Berea sandstone, 0.5% NaCl, 25 C.

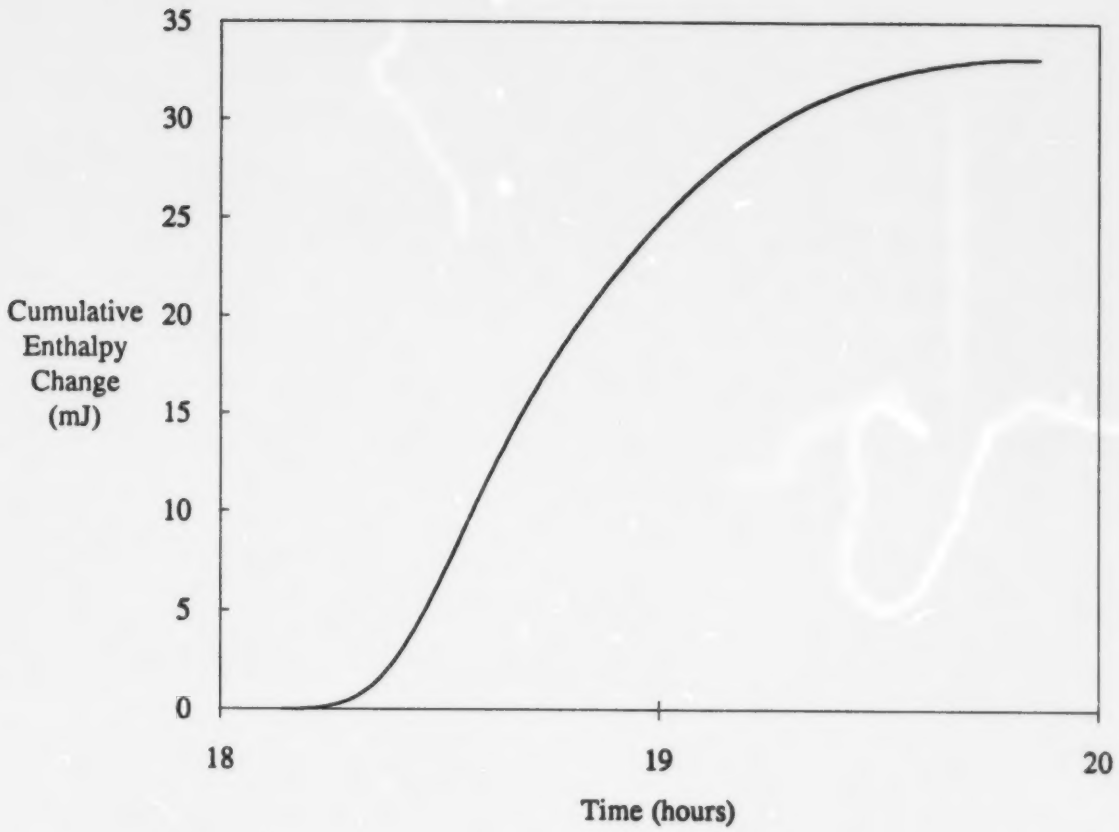

Figure 9.

Enthalpy of adsorption of 0.5% Stepanflo 60 on Berea sandstone, 0.5% NaCl, 25 C.

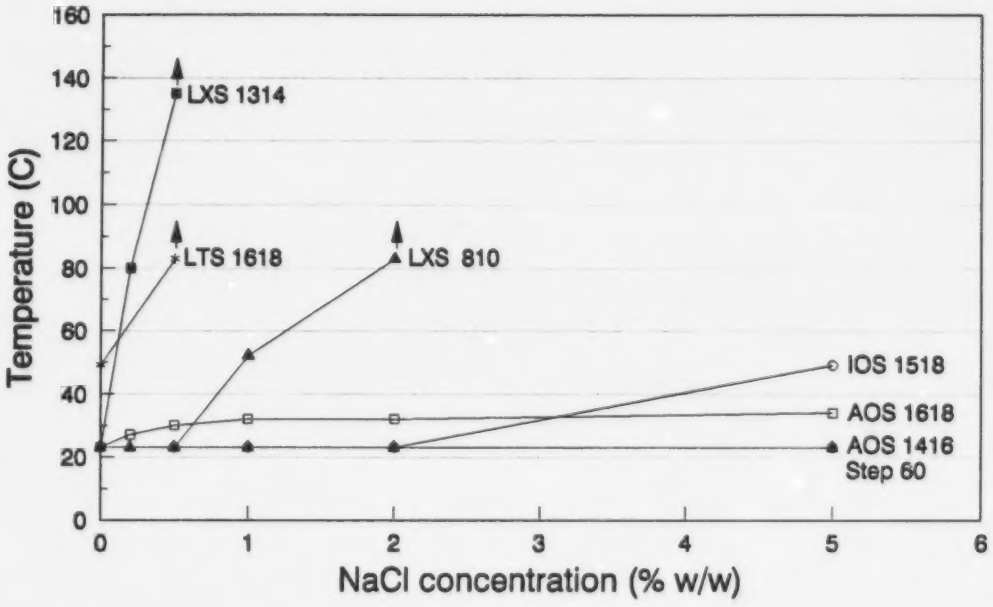

Figure 10.

Surfactant solubility as a function of salinity, surfactant concentration: 1%.

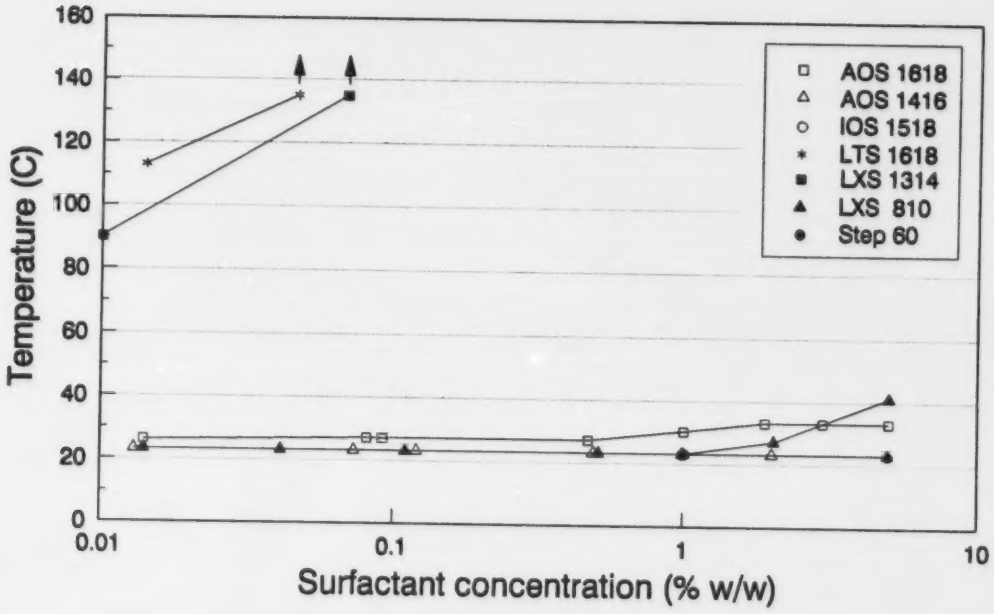

Figure 11.

Surfactant solubility as a function of surfactant concentration, brine: 0.5% NaCl.

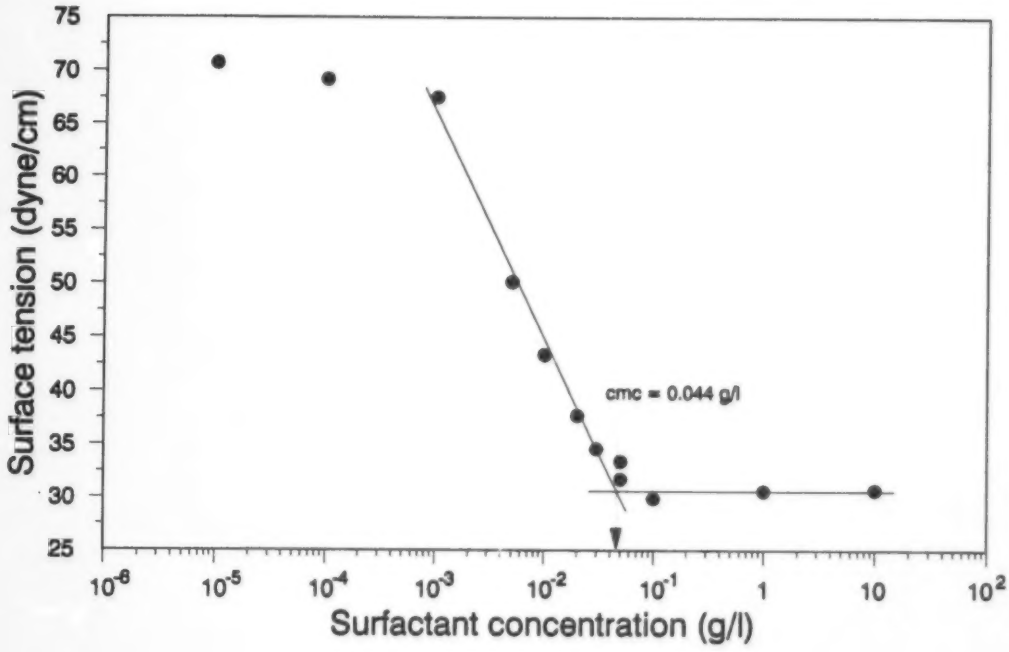

Figure 12.

Surface tension, Enordet AOS 1416 in 0.5% NaCl, 23 C.

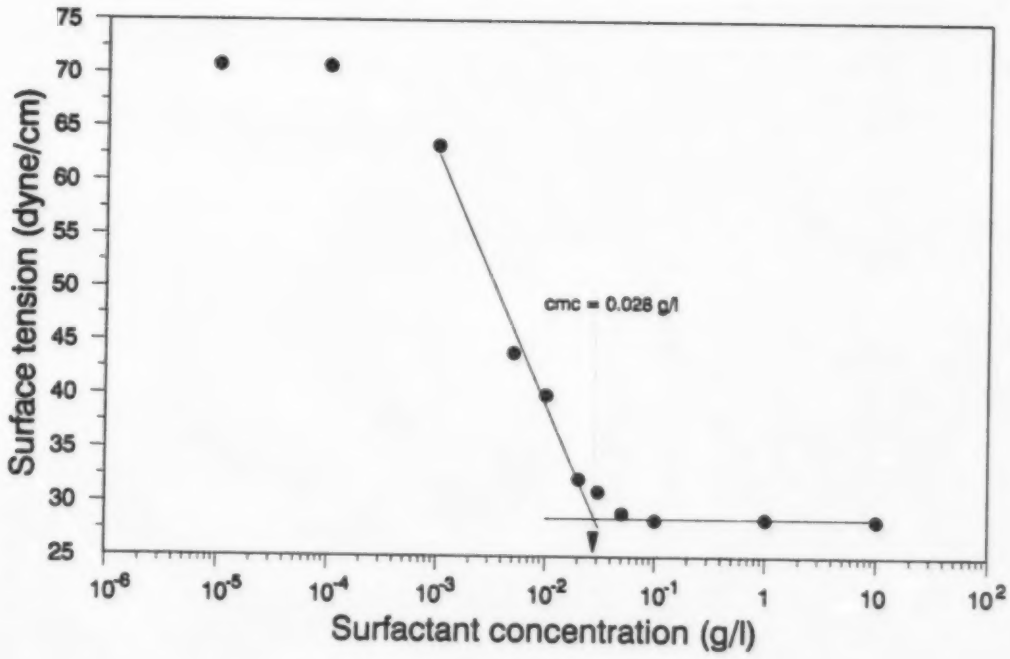

Figure 13.

Surface tension, Enordet AOS 1416 in 2.32% NaCl, 23 C.

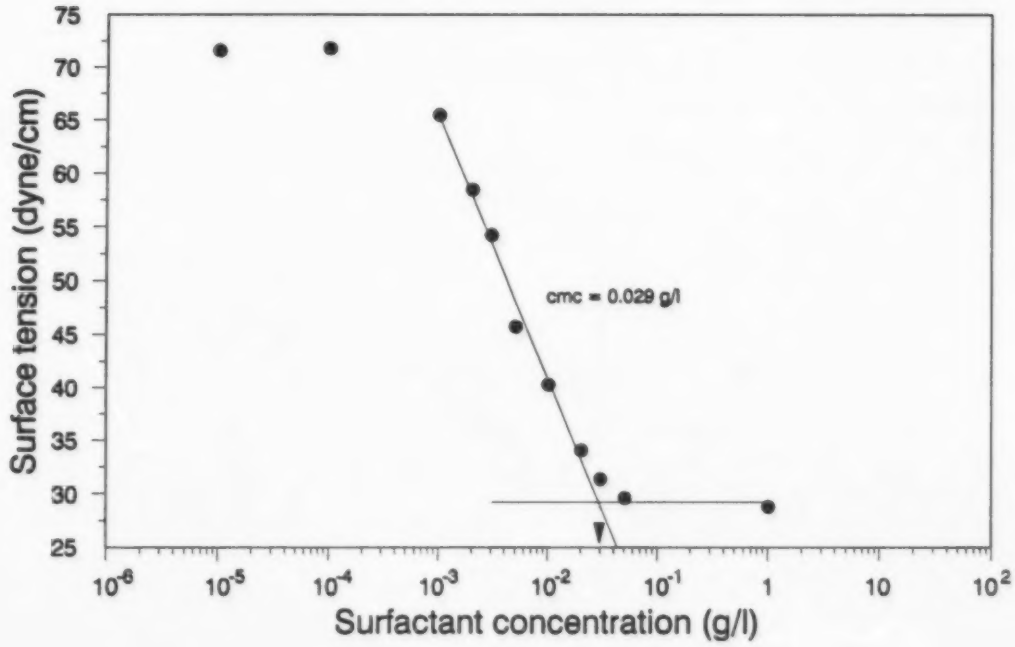

Figure 14.

Surface tension, Enordet AOS 1416 in 2.27% TDS Brine, 23 C.

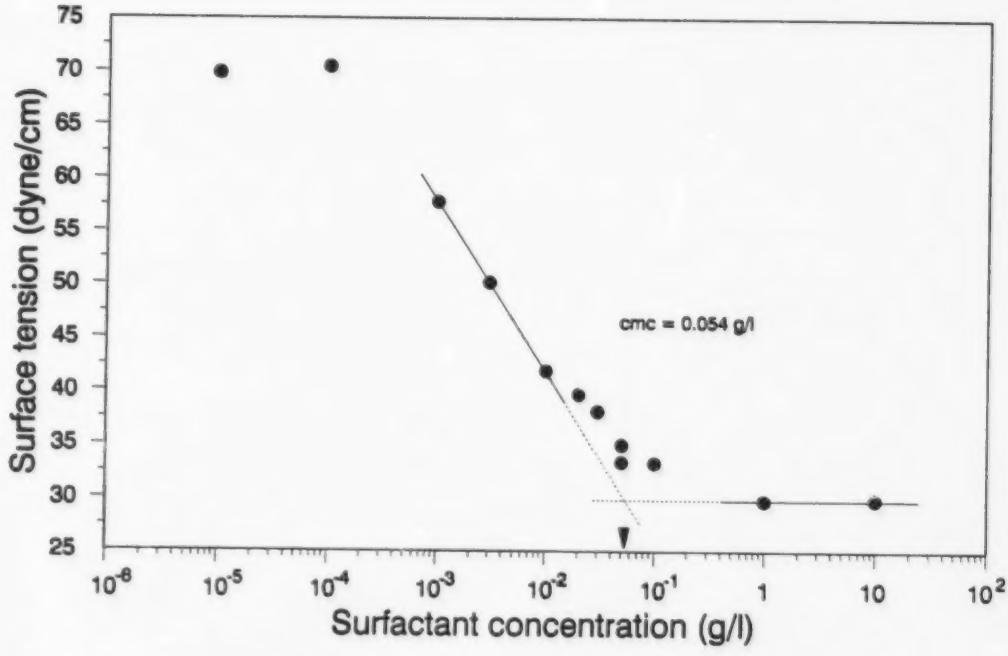

Figure 15.

Surface tension, Enordet IOS 1518 in 0.5% NaCl, 23 C.

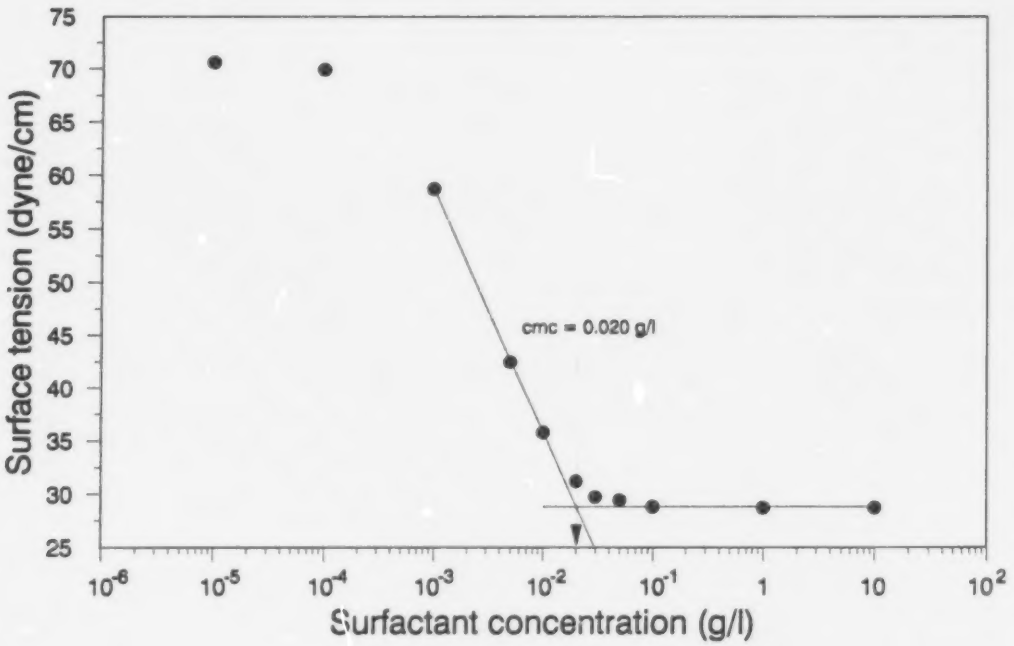

Figure 16.

Surface tension, Enordet IOS 1518 in 2.32% NaCl, 23 C.

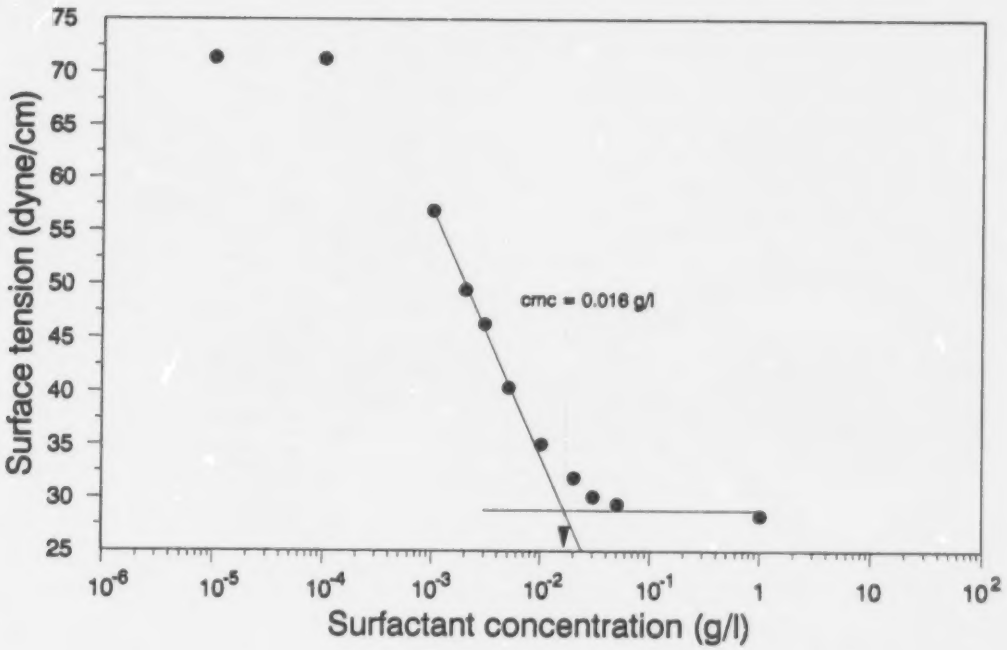

Figure 17.

Surface tension, Enordet IOS 1518 in 2.27% TDS Brine, 23 C.

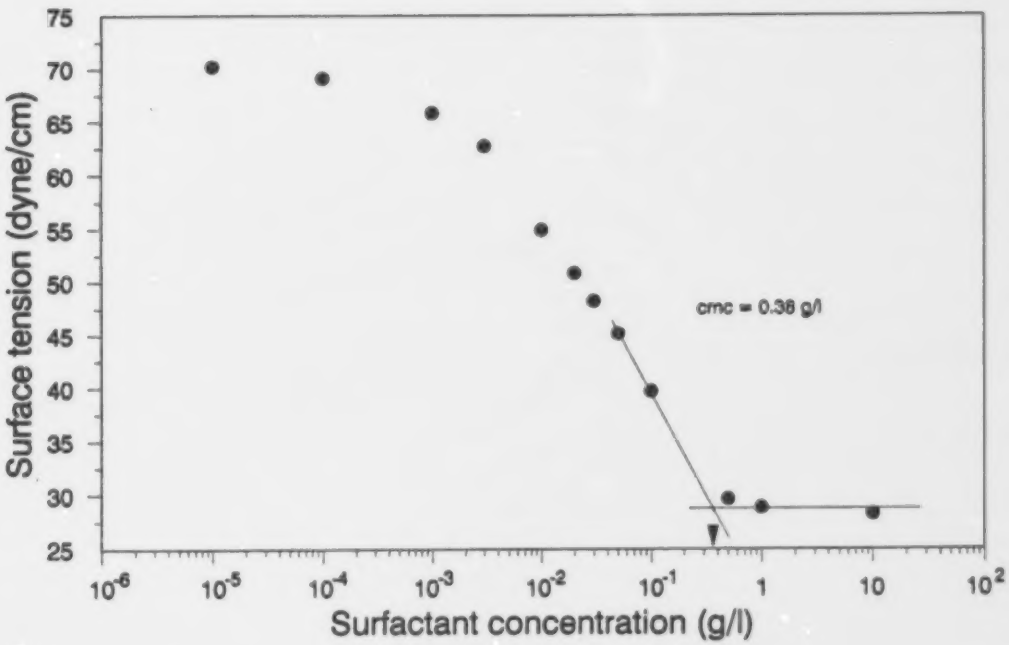

Figure 18.

Surface tension, Enordet LXS 810 in 0.5% NaCl, 23 C.

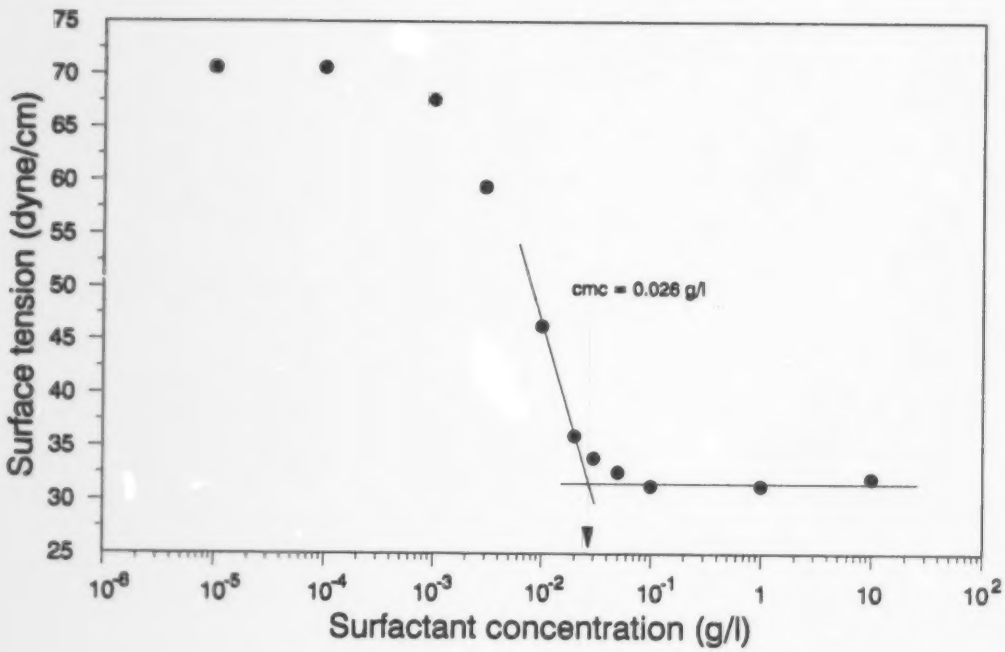

Figure 19.

Surface tension, Stepanflo 60 in 0.5% NaCl, 23 C.

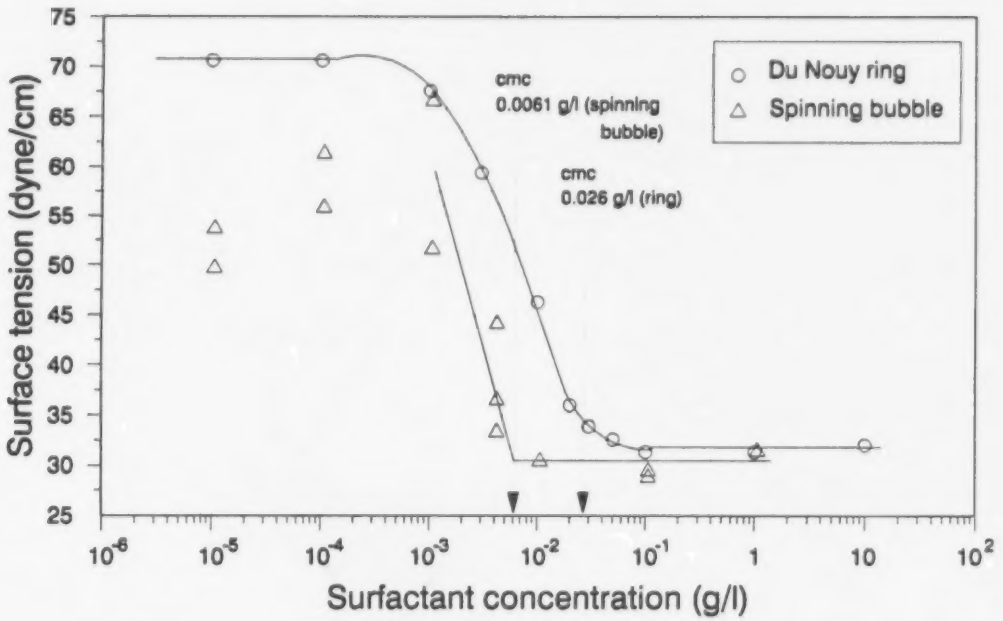

Figure 20.

Surface tension, Stepanflo 60 in 0.5% NaCl at 23 C
by Du Nouy ring and spinning bubble methods.

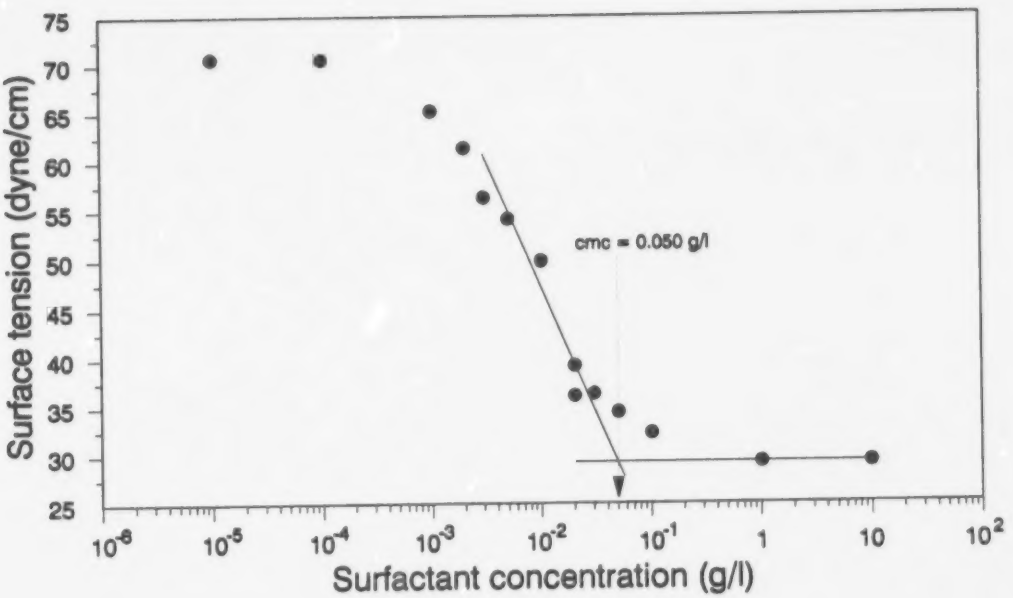

Figure 21.

Surface tension, 0.72:0.30 (w:w) Enordet IOS 1518 : Stepanflo 60 in 0.5% NaCl, 23 C

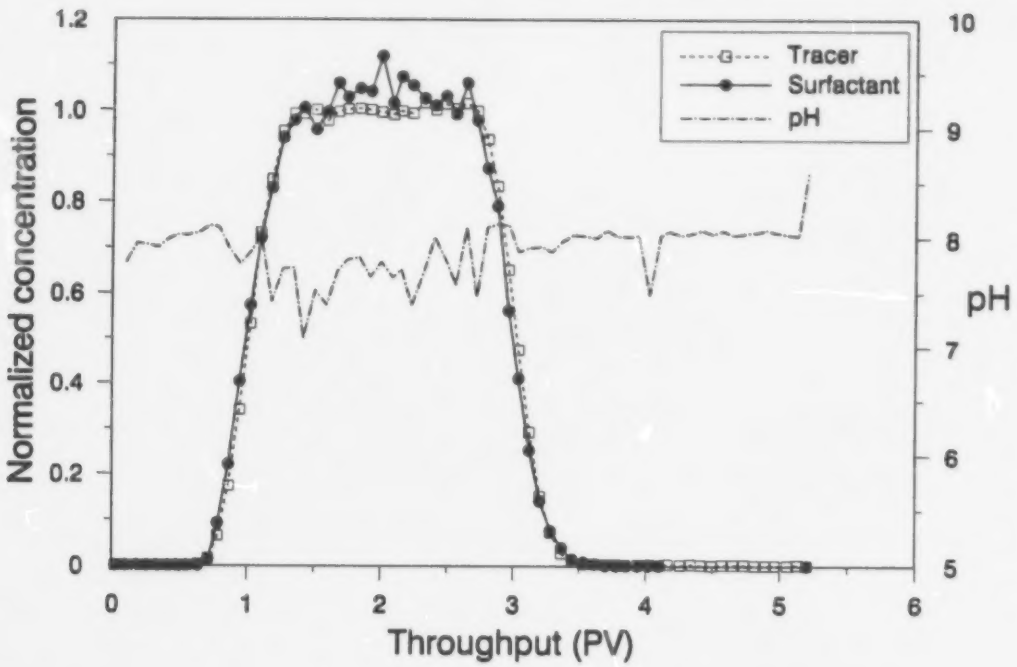

Figure 22.

Core CM-2 effluent profiles.
10 g/l Enordet AOS 1416 in 0.5% NaCl, 23 C.

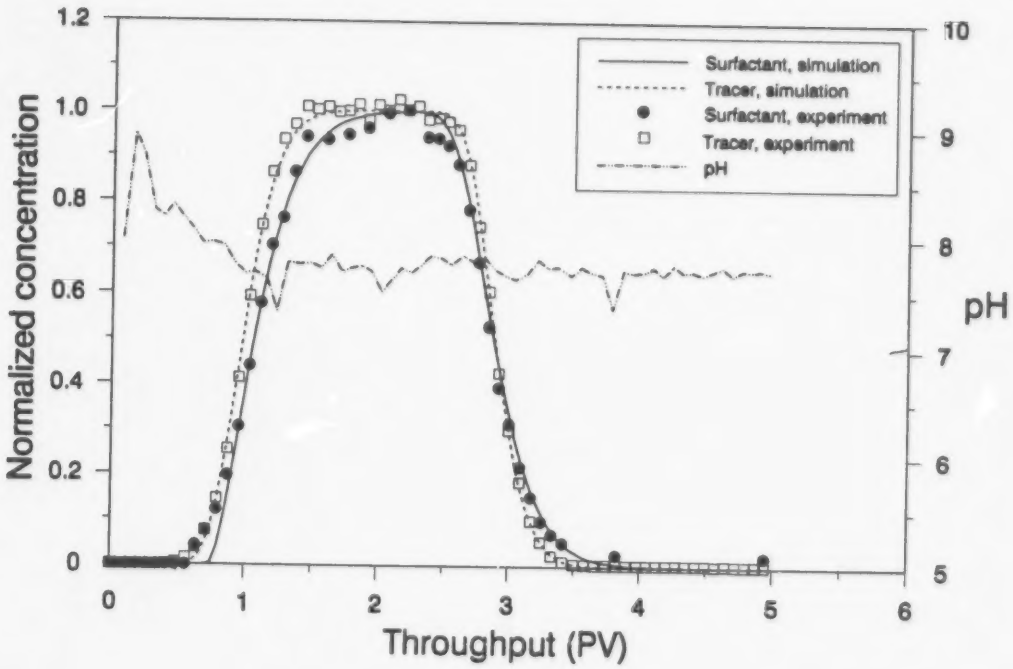

Figure 23.

Core CM-9 effluent profiles.
10 g/l Enordet AOS 1416 in 2.32% NaCl, 23 C.

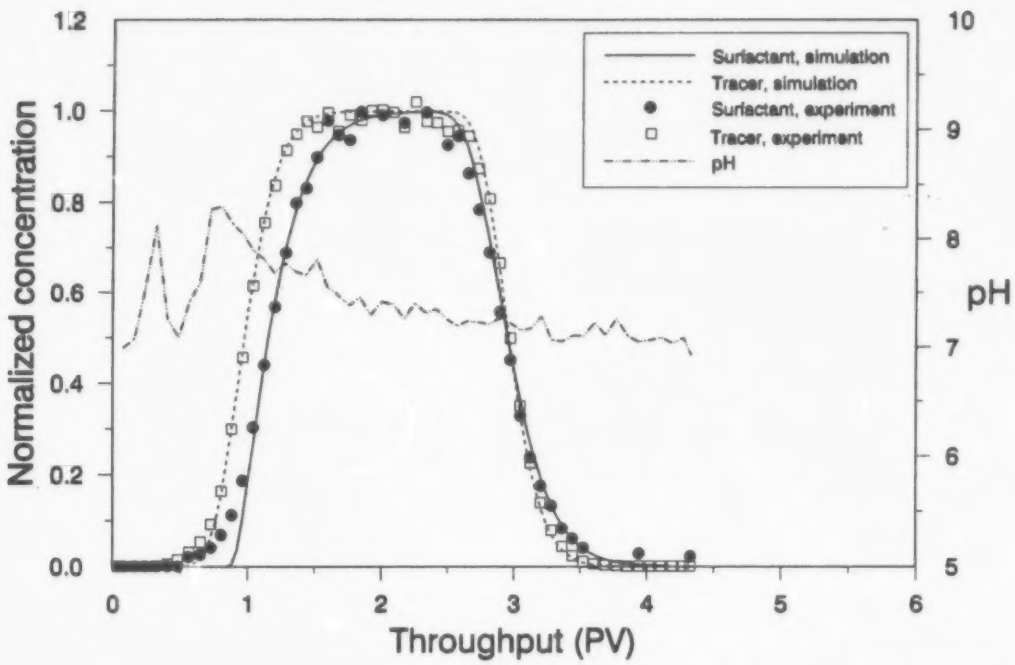

Figure 24.

Core CM-12 effluent profiles.
10 g/l Enordet AOS 1416 in 2.27% TDS Brine, 23 C.

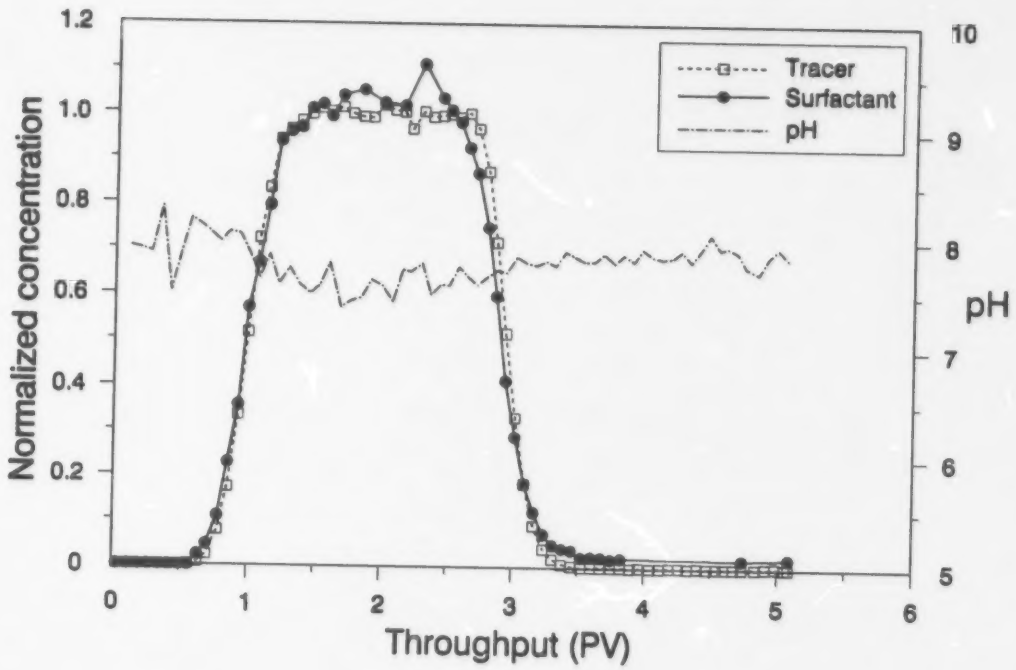

Figure 25.

Core CM-3 effluent profiles.
10 g/l Enordet IOS 1518 in 0.5% NaCl, 23 C.

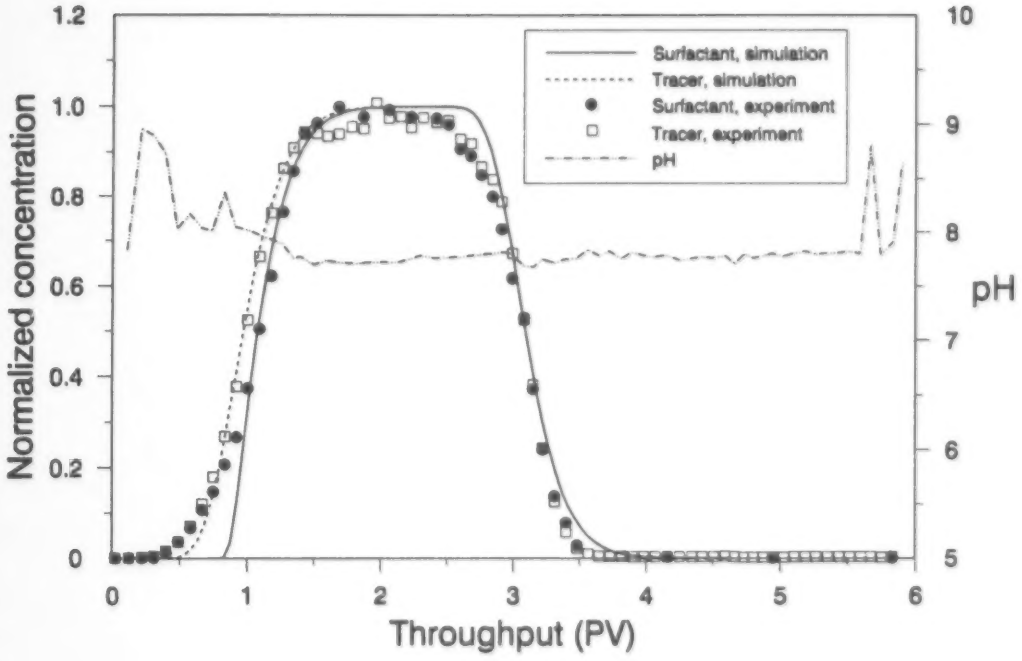

Figure 26.

Core CM-10 effluent profiles.
10 g/l Enordet IOS 1518 in 2.32% NaCl, 23 C.

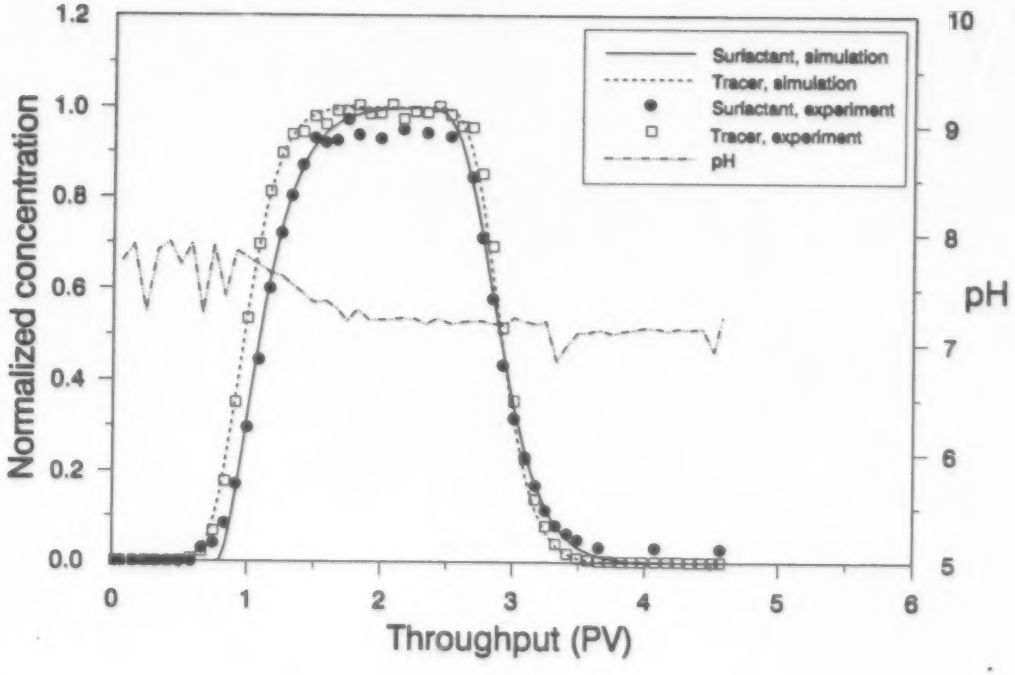

Figure 27.

Core CM-11 effluent profiles.
10 g/l Enordet IOS 1518 in 2.27% TDS Brine, 23 C.

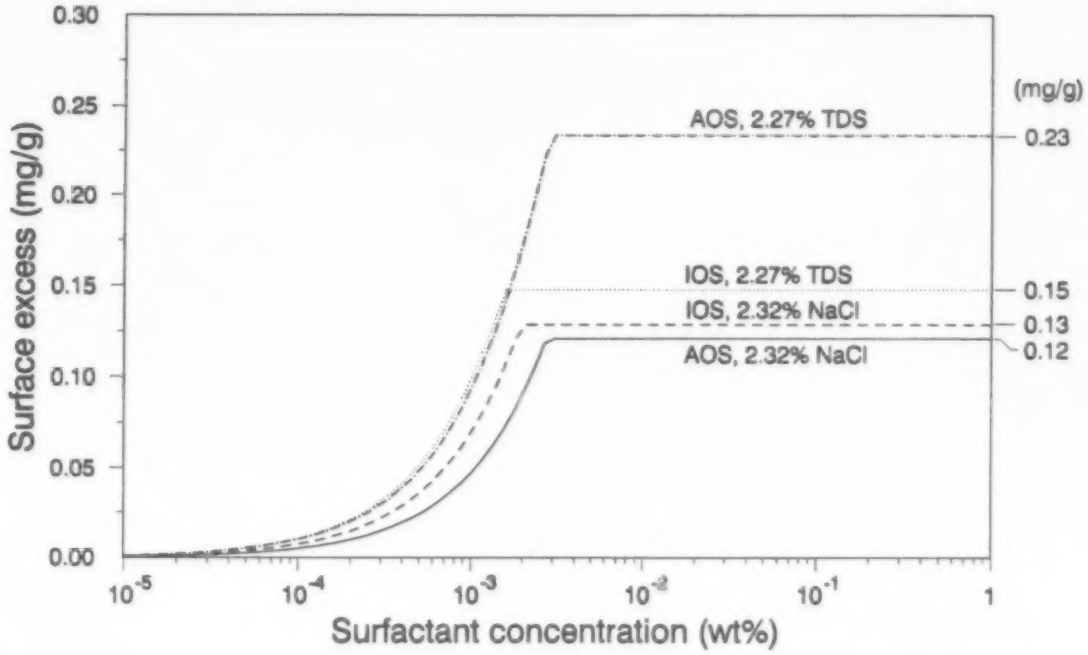

Figure 28.

Adsorption isotherms from flow model parameters, Enordet AOS 1416 and Enordet IOS 1518 at 23 C in different brines.

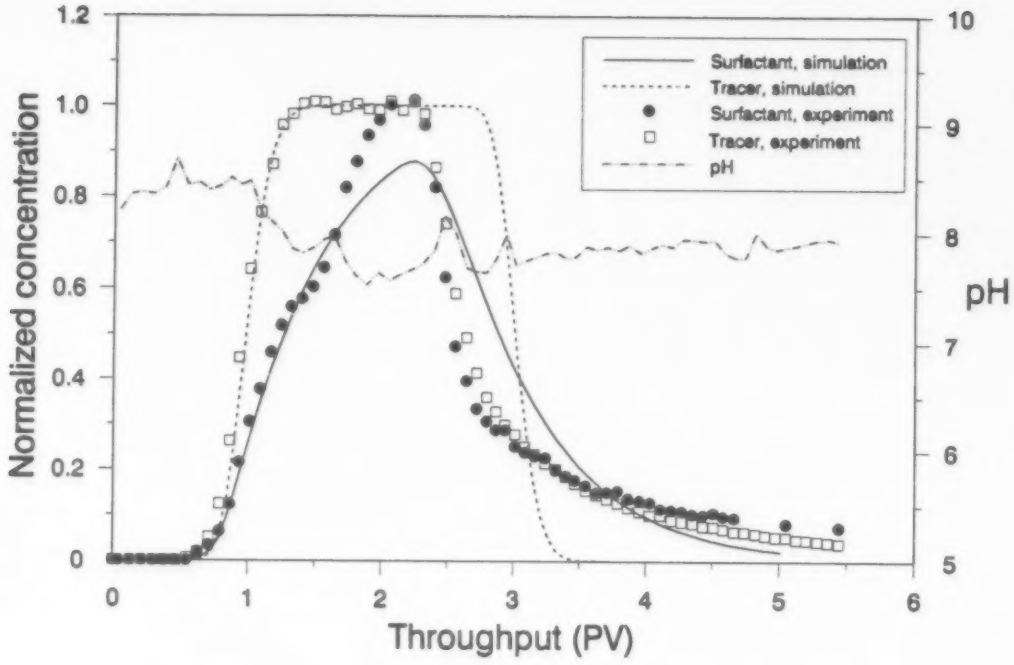

Figure 29.

Core CM-4 effluent profiles.
10 g/l Enordet LXS 810 in 0.5% NaCl, 23 C.

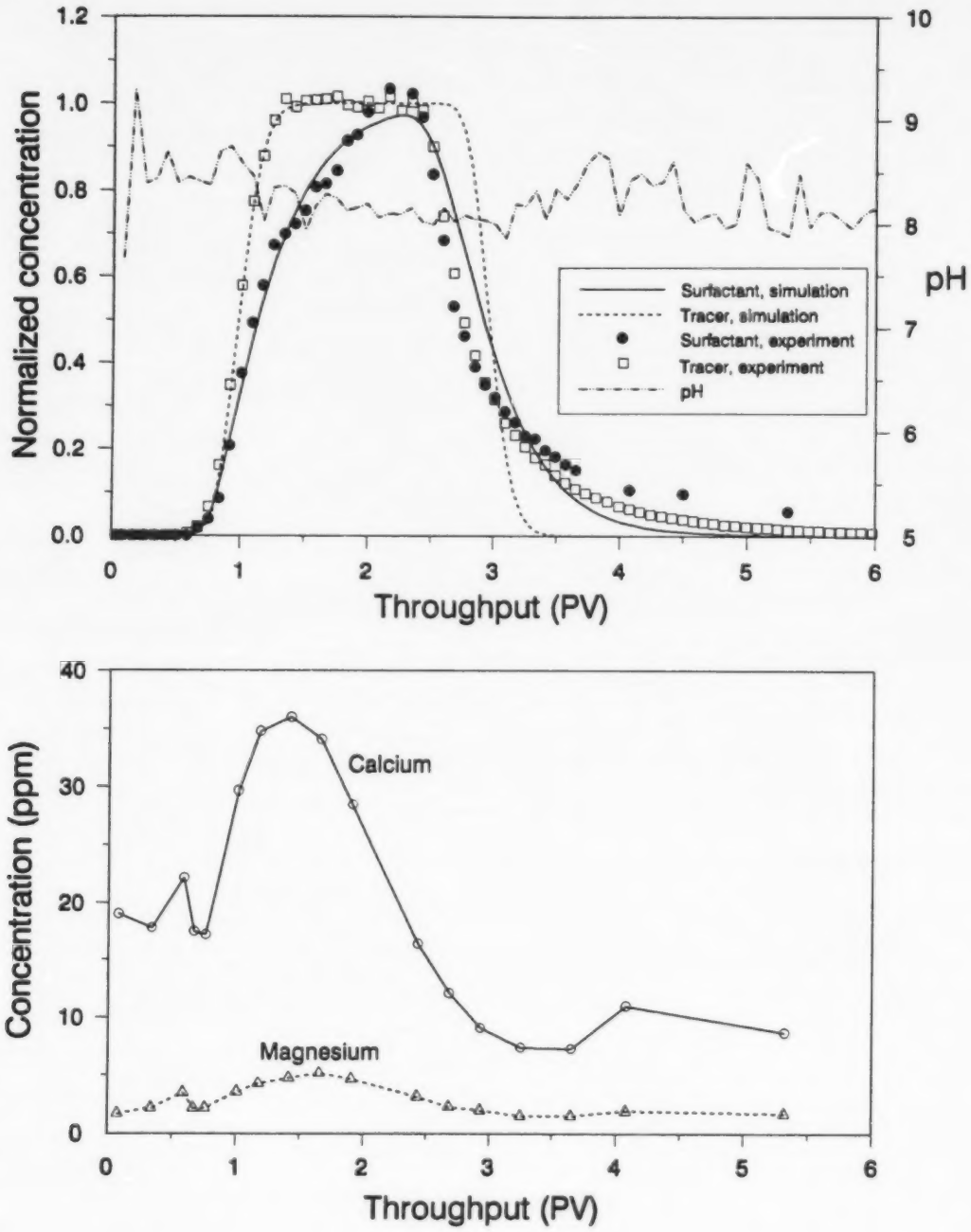

Figure 30.

Core CM-13 effluent profiles.
10 g/l Enordet LXS 810 in 0.5% NaCl, 23 C (repeat).

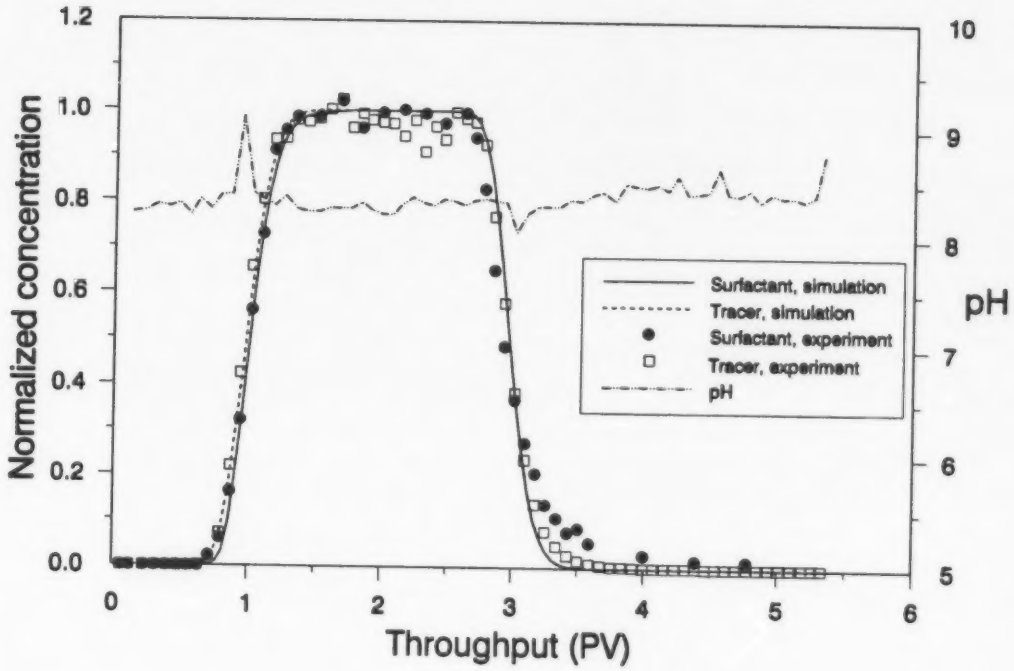

Figure 31.

Core CM-8 effluent profiles.
10 g/l Enordet LXS 810 in 0.5% NaCl, 75 C.

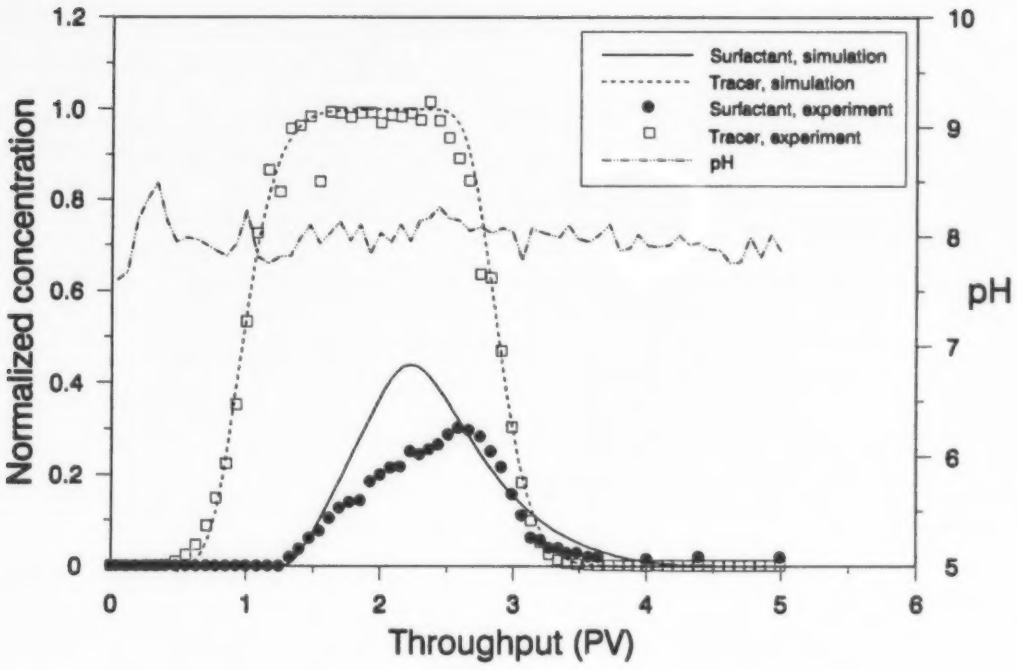

Figure 32.

Core CM-6 effluent profiles.
10 g/l Stepanflo 60 in 0.5% NaCl, 23 C.

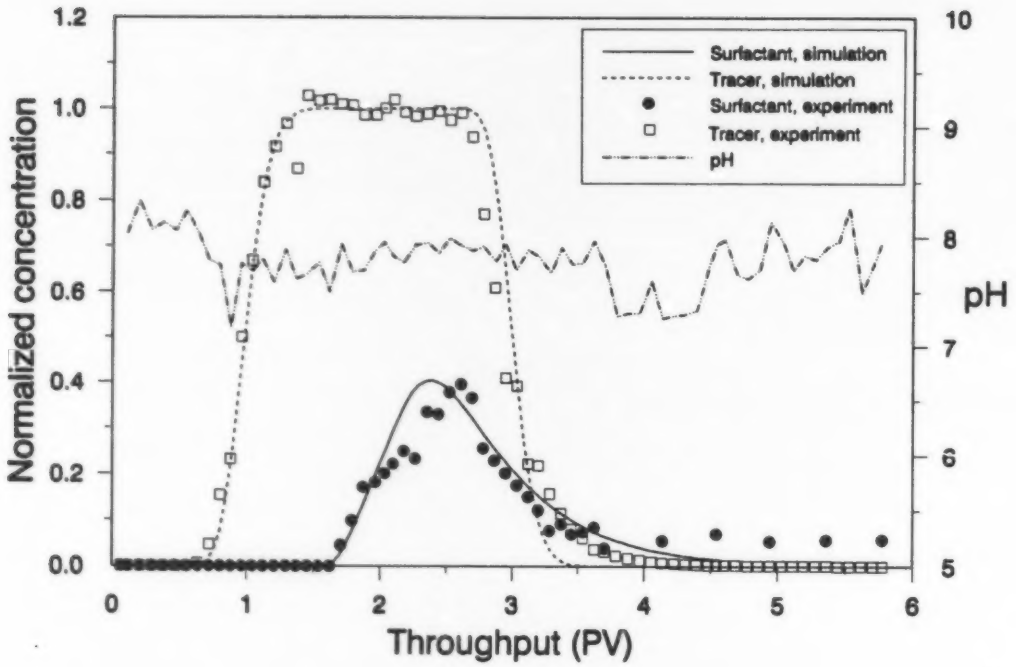

Figure 33.

Core CM-7 effluent profiles.
10 g/l Stepanflo 60 in 0.5% NaCl, 75 C.

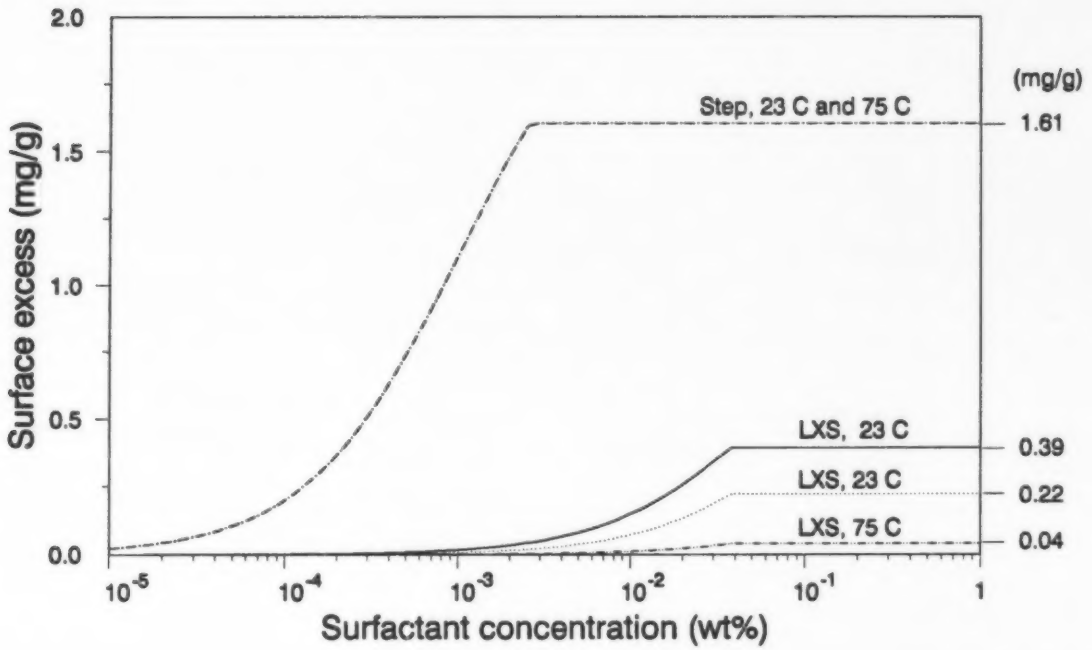

Figure 34.

Adsorption isotherms from flow model parameters, Enordet LXS 810 and Stepanflo 60 in 0.5% NaCl at different temperatures.

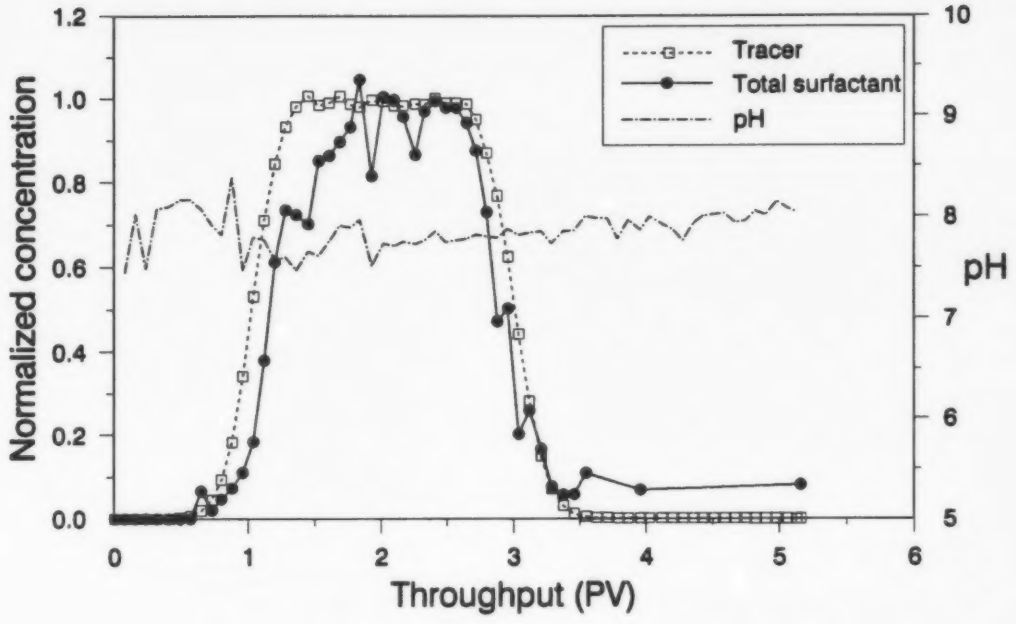

Figure 35.

Core CM-14 effluent profiles.
Surfactant Mixture in 0.5% NaCl, 23 C
(3 g/l Stepanflo 60 and 7 g/l Enordet IOS 1518).

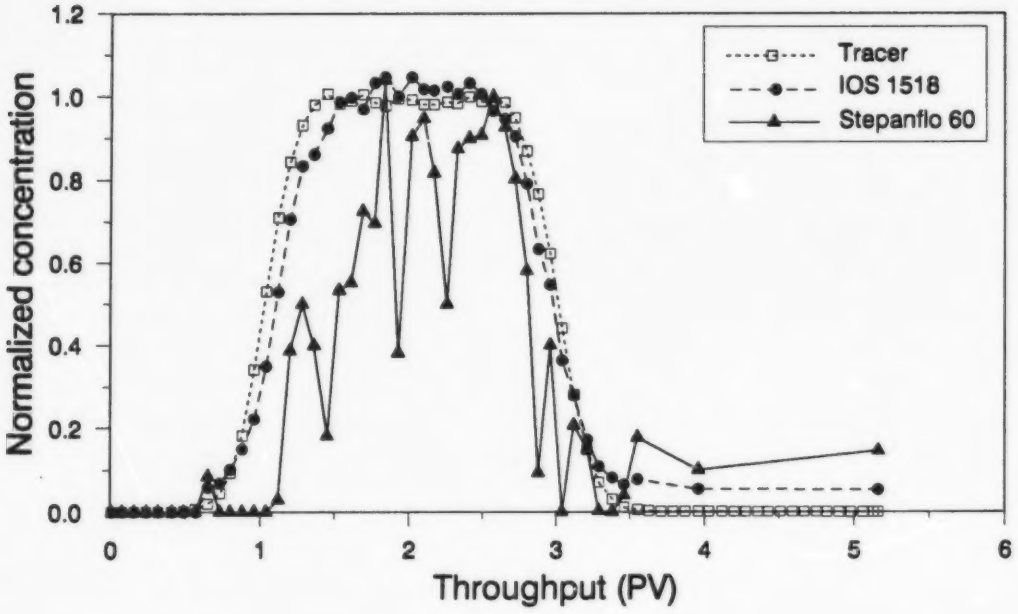

Figure 36.

Core CM-14 effluent profiles.
Surfactant Mixture in 0.5% NaCl, 23 C
(3 g/l Stepanflo 60 and 7 g/l Enordet IOS 1518).

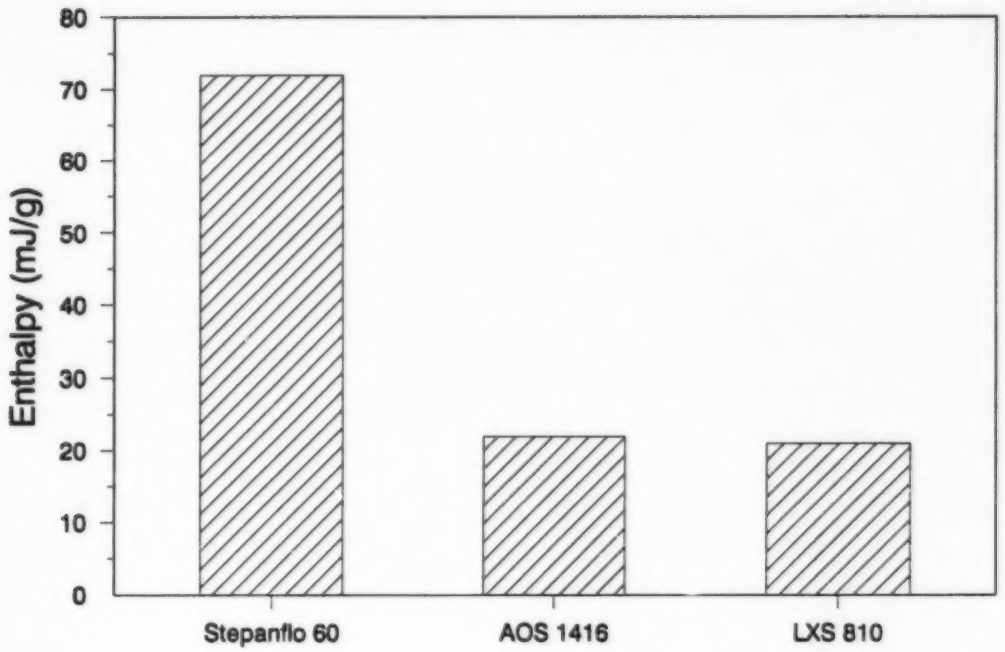

Figure 37.

Enthalpy of adsorption.
0.5% surfactant in 0.5% NaCl, Berea sandstone, 25 C.

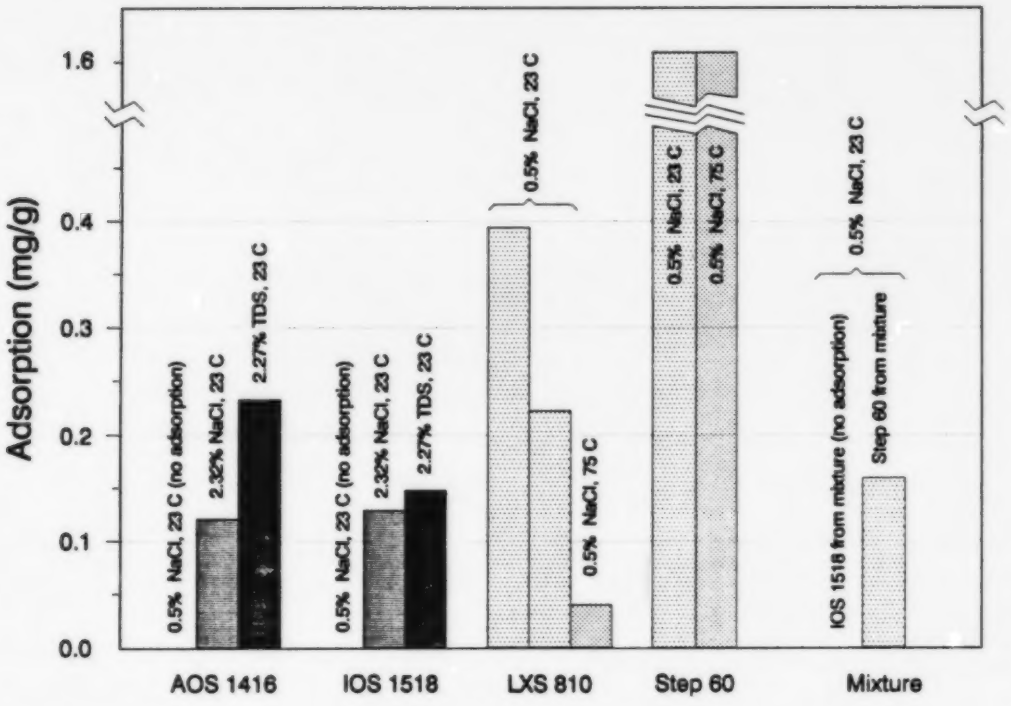

Figure 38.

Summary of adsorption data: Plotted are the maximum adsorption levels from the adsorption isotherms, except in the case of the mixture. Values for the mixture were obtained from material balance calculations.

APPENDIX A
Two-Phase Titration of an Anionic/Amphoteric Surfactant Mixture

The method used to analyze the concentrations of anionic (sulfonate) and amphoteric (carboxy-betaine) surfactant in an anionic/amphoteric surfactant mixture involved a combination of three different two-phase titrations in the system chloroform/water: anionic surfactant at pH 2 as described by Reid et al. (1967), amphoteric surfactant at pH 2 as described by Schramm et al. (1989), and anionic surfactant at pH 10. In all titrations, the mixed indicator suggested by Reid et al. (1967) was used. The principle of the procedure is as follows.

In the method described by Reid et al. (1967), an anionic (sulfonate) surfactant is titrated with Hyamine 1622 (cationic) at pH 2 using a mixed indicator. The same titration can also be carried out at pH 10, although this tends to be more difficult because an emulsion is more likely to form and obscure the end point.

A carboxy-betaine (such as Stepanflo 60) contains an anionic carboxyl group and a cationic quaternary amine group. At acidic pH, the carboxyl group will be neutralized to the undissociated carboxylic acid, and the molecule becomes a cation, which can be titrated with an anionic surfactant. In the method described by Schramm et al. (1989), sodium dodecyl sulfate (SDS) is used as titrant. Since the end point of this titration is difficult to detect, Schramm et al. (1989) suggest that excess SDS be added to the titration vessel and the excess SDS back-titrated with Hyamine 1622 in the same way as an anionic surfactant. The amount of amphoteric surfactant can be determined from the difference between the total amount of SDS added and the amount of Hyamine required to back-titrate the excess SDS that is not bound to the amphoteric surfactant. At basic pH, the amphoteric surfactant is zwitterionic and will not complex with either a cationic or an anionic titrant. It will therefore not titrate at this pH. (This was confirmed by attempting to titrate a Stepanflo 60 sample of known concentration at pH

10.)

In a mixture containing an anionic and an amphoteric surfactant at pH 2, the surfactants will complex with each other. At pH 10, the surfactants will not complex and will be present in solution as seperate entities. Since the anionic surfactant can be titrated at basic pH, but the amphoteric one cannot, titration of a mixed sample at pH 10 will yield the total concentration of anionic surfactant. At pH 2, anionic-amphoteric complexed surfactant will be present in the sample and, depending on the composition of the sample, excess free anionic or amphoteric. (The initial color of the indicator in the chloroform phase will indicate which surfactant is in excess, excess anionic - pink, excess amphoteric - blue.) If the anionic is in excess, it can be titrated with Hyamine using Reid's procedure. If the amphoteric is in excess, it is back-titrated with Hyamine using Schramm's procedure. Titrations at basic and acidic pH thus yield the total amount of anionic surfactant and the excess amount of one surfactant, respectively. The amount of complexed surfactant can then be found by difference, and this yields the total concentration of each surfactant in the mixture.

For the analysis of IOS 1518 and Stepanflo 60 used in this work, three calibration curves were required:

1. IOS standards titrated with Hyamine 1622 at pH 10. (The pH was adjusted by preparing the indicator solution in aqueous NaOH rather than in aqueous H_2SO_4 as in Reid's procedure.)
2. IOS standards titrated with Hyamine 1622 at pH 2.
3. Stepanflo standards titrated/back-titrated with a standard solution of IOS 1518 and Hyamine 1622. (Note that the SDS titrant used in Schramm's procedure has been replaced by IOS in this work.)

All three calibration curves were linear. The procedure for determining the components in the mixture was then as follows:

1. A sample was titrated at pH 10 with Hyamine 1622 to determine the total amount of anionic surfactant from calibration curve 1.

2. In our samples, IOS was always present in excess. Titration of the sample at pH 2 with Hyamine 1622 thus yielded the amount of free IOS from calibration curve 2.

3. The difference between the total IOS and the free IOS (from Steps 1 and 2) gave the amount of complexed IOS. The amount of complexed Stepanflo that this corresponded to could then be obtained from calibration curve 3. (The stoichiometry of complex formation is not clear (Schramm et al., 1989); a calibration curve is therefore required.) The amount of complexed Stepanflo was equal to the amount of total Stepanflo in the sample, since IOS was present in excess. This then completed the analysis for the case of excess IOS.

4. If Stepanflo was present in excess rather than IOS, then Step 2 would involve a titration/back-titration with IOS/Hyamine to determine the amount of free Stepanflo. The total IOS is known from Step 1, and, since Stepanflo is present in excess, it is also known that all of this IOS is complexed with Stepanflo. The amount of complexed Stepanflo can thus be determined from the total IOS and calibration curve 3, and is added to the free Stepanflo to obtain the total amount of Stepanflo. This completes the analysis for the case of excess Stepanflo.

In order to test this procedure, mixed samples containing Stepanflo 60 and IOS 1518 at known concentrations were prepared and titrated by the procedure described above. Since all our core flood samples contained more IOS than Stepanflo, these standard samples were prepared to contain excess IOS concentrations. The results are shown in Table A-1. The error in the total concentration of IOS is consistent with the reproducibility that we normally obtain in two-phase titration of anionic surfactants. The error in the concentration of amphoteric surfactant is somewhat larger. The determination of the amount of complexed (and therefore also of amphoteric) surfactant involves taking the difference between the results of two different titrations, and the error can therefore become quite large.

Some of the core flood samples for core CM-14 were titrated in duplicate in order to assess the reproducibility of the procedure. The results were within 10% of each other or better for the titration of total anionic

surfactant at basic pH and for the titration of excess surfactant at acidic pH, again consistent with the reproducibility usually obtained in two-phase titrations. However, in taking differences to obtain the concentration of complexed surfactant, a large error was sometimes introduced, the Stepanflo concentrations calculated on this basis differing by as much as a factor of 2 in some cases.

These errors should be kept in mind when evaluating the effluent data for core CM-14. It should also be kept in mind that, of the mixtures we have attempted to analyze, this particular type of surfactant mixture is the most difficult one to deal with. Further testing of the procedure is required, preferably with pure surfactants that would facilitate interpretation of the results.

Another point to note is that the procedure described here will work only if the anionic surfactant is a sulfonate or sulfate and the amphoteric is a carboxy- rather than a sulfo-betaine.

TABLE A-1: Results of two-phase titration of mixed standards containing IOS 1518 and Stepanflo 60.

IOS conc. (g/l)	IOS conc. from titration (g/l)	IOS conc. % Error
4.891	4.697	-4.0
3.115	3.324	+6.7
7.009	7.020	+0.2

Step conc. (g/l)	Step conc. from titration (g/l)	Step conc. % Error
2.145	1.630	-24.0
1.122	1.205	+ 7.4
3.015	3.345	+10.9

APPENDIX B
Surface Tension Data

All measurements were carried out with a Du Nouy ring tensiometer, unless otherwise noted, at 23°C.

(a) AOS 1416 in 0.5% NaCl

Concentration (g/l)	log(c)	Surface tension (dyne/cm)
9.99E-06	-5.00	70.7
9.99E-05	-4.00	69.2
9.99E-04	-3.00	67.5
5.00E-03	-2.30	50.1
9.99E-03	-2.00	43.3
9.99E-03	-2.00	43.3
2.00E-02	-1.70	37.7
3.00E-02	-1.52	34.6
5.00E-02	-1.30	31.7
5.00E-02	-1.30	33.4
9.99E-02	-1.00	29.9
9.99E-01	0.00	30.6
9.99E+00	1.00	30.7

(b) AOS 1416 in 2.32% NaCl

Concentration (g/l)	log(c)	Surface tension (dyne/cm)
1.01E-05	-5.00	70.8
1.01E-04	-4.00	70.7
1.01E-03	-3.00	63.3
5.06E-03	-2.30	43.9
1.01E-02	-2.00	40.0
2.03E-02	-1.69	32.2
3.04E-02	-1.52	31.0
5.06E-02	-1.30	29.0
1.01E-01	-1.00	28.4
1.01E+00	0.01	28.5
1.01E+01	1.01	28.4

(c) AOS 1416 in 2.27% TDS Brine

Concentration (g/l)	log(c)	Surface tension (dyne/cm)
1.02E-05	-4.99	71.6
1.02E-04	-3.99	71.8
1.02E-03	-2.99	65.5
2.03E-03	-2.69	58.5
3.05E-03	-2.52	54.3
5.08E-03	-2.29	45.8
1.02E-02	-1.99	40.3
2.03E-02	-1.69	34.1
3.05E-02	-1.52	31.4
5.08E-02	-1.29	29.6
1.02E+00	0.01	28.8

(d) IOS 1518 in 0.5% NaCl

Concentration (g/l)	log(c)	Surface tension (dyne/cm)
1.00E-05	-5.00	69.8
1.00E-04	-4.00	70.4
1.00E-03	-3.00	57.8
3.00E-03	-2.52	50.2
1.00E-02	-2.00	41.9
2.00E-02	-1.70	39.7
3.00E-02	-1.52	38.1
5.00E-02	-1.30	33.4
5.00E-02	-1.30	35.0
1.00E-01	-1.00	33.3
1.00E+00	0.00	29.8
1.00E+01	1.00	29.9

(e) IOS 1518 in 2.32% NaCl

Concentration (g/l)	log(c)	Surface tension (dyne/cm)
1.00E-05	-5.00	70.6
1.00E-04	-4.00	69.9
1.00E-03	-3.00	58.7
5.00E-03	-2.30	42.5
1.00E-02	-2.00	35.8
2.00E-02	-1.70	31.2
3.00E-02	-1.52	29.7
5.00E-02	-1.30	29.4
1.00E-01	-1.00	28.8
1.00E+00	0.00	28.7
1.00E+01	1.00	28.7

(f) IOS 1518 in 2.27% TDS Brine

Concentration (g/l)	log(c)	Surface tension (dyne/cm)
1.01E-05	-5.00	71.4
1.01E-04	-4.00	71.3
1.01E-03	-3.00	56.9
2.02E-03	-2.69	49.5
3.03E-03	-2.52	46.3
5.05E-03	-2.30	40.4
1.01E-02	-2.00	35.1
2.02E-02	-1.69	31.9
3.03E-02	-1.52	30.1
5.05E-02	-1.30	29.4
1.01E+00	0.00	28.3

(g) LXS 810 in 0.5% NaCl

Concentration (g/l)	log(c)	Surface tension (dyne/cm)
1.00E-05	-5.00	70.2
1.00E-04	-4.00	69.1
1.00E-03	-3.00	65.8
3.00E-03	-2.52	62.7
1.00E-02	-2.00	54.9
2.00E-02	-1.70	50.8
3.00E-02	-1.52	48.2
5.00E-02	-1.30	45.1
1.00E-01	-1.00	39.7
5.00E-01	-0.30	29.6
1.00E+00	0.00	28.8
1.00E+01	1.00	28.2

(h) Stepanflo 60 in 0.5% NaCl

Concentration (g/l)	log(c)	Surface tension (dyne/cm)
1.00E-05	-5.00	70.6
1.00E-04	-4.00	70.6
1.00E-03	-3.00	67.6
3.00E-03	-2.52	59.4
1.00E-02	-2.00	46.3
2.00E-02	-1.70	36.0
3.00E-02	-1.52	33.9
5.00E-02	-1.30	32.6
1.00E-01	-1.00	31.3
1.00E+00	0.00	31.3
1.00E+01	1.00	32.0

(i) Stepanflo 60 in 0.5% NaCl by spinning bubble

Concentration (g/l)	log(c)	Surface tension (dyne/cm)
1.06E-05	-4.975	49.7
1.06E-05	-4.975	53.7
1.06E-04	-3.975	61.3
1.06E-04	-3.975	55.8
1.06E-04	-3.975	76.7
1.06E-03	-2.975	51.6
1.06E-03	-2.975	66.6
4.24E-03	-2.373	36.5
4.24E-03	-2.373	44.1
4.24E-03	-2.373	33.3
1.06E-02	-1.975	30.4
1.06E-01	-0.975	29.4
1.06E-01	-0.975	28.8
1.06E+00	0.025	31.4

(j) Surfactant Mixture in 0.5% NaCl (0.72:0.30 w/w IOS 1518 : Stepanflo 60)

Concentration (g/l)	log(c)	Surface tension (dyne/cm)
1.02E-05	-4.99	70.7
1.02E-04	-3.99	70.6
1.02E-03	-2.99	65.2
2.04E-03	-2.69	61.4
3.06E-03	-2.51	56.3
5.10E-03	-2.29	54.1
1.02E-02	-1.99	49.8
2.04E-02	-1.69	36.1
2.04E-02	-1.69	39.2
3.06E-02	-1.51	36.3
5.10E-02	-1.29	34.4
1.02E-01	-0.99	32.2
1.02E+00	0.01	29.2
1.00E+01	1.00	29.2